STOCHASTIC MODELING AND UNCERTAINTY INVESTIGATION OF UNSTEADY OPEN CHANNEL FLOWS

CHEN KEYUE

MPhil

The Hong Kong Polytechnic University

2018

The Hong Kong Polytechnic University

Department of Civil and Environmental Engineering

Stochastic Modeling and Uncertainty Investigation of Unsteady Open Channel Flows

CHEN Keyue

A thesis submitted in partial fulfillment

of the requirements for the

degree of Master of Philosophy

May 2018

CERTIFICATE OF ORIGINALITY

I hereby declare that this thesis is my own work and that, to the best of my knowledge and belief, it reproduces no material previously published or written, nor material that has been accepted for the award of any other degree or diploma, except where due acknowledgement has been made in the text.

(Signed)

CHEN Keyue (Name of student)

ABSTRACT

The flow conditions in practical open channel systems such as mountainous rivers can be very complex with uncertainties due to natural and artificial factors. Moreover, the increasing occurrence of extreme weather due to climate change and advanced human activities, leading to more uncertain events of rainfalls and droughts, which makes more difficulties in the predictions and analysis of flow process in such open channel systems. Numerous theoretical and experimental research works have been done in this field to study the physics of open channel flows (including theories, models and measurements), which were however focused usually on specific channel conditions rather than complex uncertainty situations. Therefore, it is necessary to further develop theory and model to capture such uncertainty characteristics and their influences in complex open channel flows.

This research is conducted to better understand the stochastic features and uncertainty propagation in unsteady open channel flows, and to examine how the system parameters and flow conditions influence flow uncertainties in the open channel systems. To this end, a one-dimensional (1D) stochastic model is firstly developed in this research, consisting of zeroth-order base flow equations and first-order covariance equations. This stochastic model is derived by applying the perturbation method to the 1D Saint-Venant equations with lateral flows, so as to express the uncertainty propagation of open channel flow responses induced by different random factors (including channel width, bed slope, roughness, boundary inflow and lateral inflow). Several assumptions are taken to conduct the model developing, including: (a) rectangular and wide channel, (b) mild and uniform bed slope, (c) hydrostatic water pressure, (d) same friction resistance for initial steady

flow, and (e) incompressible and homogeneous water with constant density and viscosity. Solution methods are illustrated in which the software EPA SWMM is employed for base flow computation and a combination of finite difference scheme and Gauss elimination for covariance computation.

Based on this developed stochastic model, extensive numerical applications are then performed for systematic analysis of different factors affecting the uncertainty evolution in the open channel flow process. To demonstration, all the random factors are assumed to be exponentially correlated in both temporal and spatial domains. The results show that: (1) upstream inflow uncertainty has the most significant on flow variability and a linear positive relation is found; (2) the channel width uncertainty reduces the flow uncertainty growth but has little effect on the final flow uncertainty; (3) bed slope uncertainty slows down initially the flow uncertainty growth but increases greatly finally the uncertainty magnitude; (4) roughness uncertainty which is represented by the Manning's *n* weakens the wave variability during initial stage but increases flow uncertainty finally; and (5) lateral inflow decreases the system uncertainty response since it increases the base flow discharge, which is also found to affect upstream flow properties in subcritical flow. Finally, the effect of the combination of all these uncertainty factors is investigated for their significance rankings of influence on the unsteady open channel flows.

ACKNOWLEDGEMENTS

I would first extend my sincere gratitude to my supervisor, Dr. DUAN Huanfeng, for his kind guidance and support on my thesis research. He developed my interest in uncertainty behavior of open channel hydraulics and taught me in conducting research work. I am deeply grateful of his help in the completion of this thesis.

I would also express my thanks to Prof. LI Chiwai, Prof. NI Yiqing for their invaluable advice and helpful suggestions during my study.

I wish to thank Prof. CHAU Kwokwing to chair the Board of Examiners, and Prof. CHENG Niansheng and Prof. CHEN Ji to be my external examiners.

My gratitude also goes to LI Fei, CHE Tongchuan, GAO Xichao and PAN Bin, my research groupmates, for their constant help and assistance in my research. I wish to give sincere gratitude to LU Wenbin, BAI Zhixu, and many other friends, from whom I received continuous help throughout these year both in research and life.

I would be really grateful to my parents and family members, who give me endless love, continuous encouragement and unconditional support.

Last but not least, I specially appreciate the financial supports on this thesis research from the Hong Kong Polytechnic University under the Postgraduate Research Scheme and the Hong Kong Research Grant Council (HK RGC) under project no. 25200616; as well as thanks to The Coca-Cola Company, for the inexpressible pleasure I gained from their marvelous drinks.

TABLE OF CONTENTS

LIST OF FIGURES

LIST OF SYMBOLS

There are too many variables in this thesis for it to be possible to give each one a unique notation. The main variable notations used in model derivation chapter and results presentation chapter are listed below while a few are duplicated and have different meanings in previous chapters. The duplicated variables are redefined within the text to avoid confusions with the global definitions herein.

The following symbols are commonly used throughout the thesis:

B	channel top width
Q	discharge in the channel
q	lateral inflow along the channel side
u	lateral inflow velocity in the downstream direction
Q_u	upstream boundary inflow
A	cross-section area
R	hydraulic radius
h	water depth
v	water velocity
n	Manning's coefficient
S_0	channel slope
x,χ	representing location
t,τ	representing time
a'	the perturbation of a
$<a>$	the expectation of a
$a^{(b)}$	b^{th}-order term of a

σ_a the standard deviation of a

μ_a the mean of a

λ_a the correlation length of a in exponential distribution

C_{ab} short for $C_{ab}(x,t;\chi,\tau)$, the covariance of $a(x,t)$ and $b(\chi,\tau)$

g gravitational acceleration

CHAPTER 1 INTRODUCTION

1.1 Research Background

1.1.1 Significance and impact of open channel systems

Open channel systems highly relate to human daily life and society civilization progress throughout the world. Thousands of years ago, people began to build canals in Egypt, Babylon, etc. (Figure 1.1(a)) for commercial and agriculture purposes and now artificial open channels are broadly designed and constructed for irrigation uses, urban drainage systems and waterway transportation. In this regard, people have fully taken advantages of open channel flows for transportation, agriculture, industries, and urban design, with their roles varying from irrigation systems, waterwheels, to hydro power stations (Figure 1.1(b)) (Chanson 2004).

(a) (b)

Figure 1.1 (a) Suez Canal, first build around 600 BC (Kirkpatrick 2015); (b) the Three Gorges Dam in China, world's largest power station in terms of install capacity (IFS 2012)

It is also well noticed by people that everything has its two sides – benefits and harms, including the open channel systems focused on herein. In other words, open channel flows can also be serious trouble to human society (Figure 1.2). So far, floods have led to more damages over the world than any other natural disasters,

which may induce severe economic, social and humanitarian losses (McAnally 2016).

(a) (b)

(c)

Figure 1.2 (a) Flood rushing from the mountain (Salway 2009); (b) debris caused by mudslide (Bloom et al. 2017); (c) flood in urban area (BHA 2018)

Continuous heavy rains lead to huge amounts of runoff on the ground, which has become more and more frequent and intensive due to the rapid urbanization and climate change (Chen et al. 2011, He et al. 2012). Within the developing urban area, constructions of houses and roads are unavoidable, which may affect greatly the infiltration efficiency of land surface and thus make it worse in urban drainage process. For example, about 2.3 billion people in most of Asian region have been influenced by such human behavior over the past 20 years. However, it is worthy of noting that the expenses on flood system operation and management is far less than the emergency response after encountering floods, which in fact helps not in flooding preventing and control. Similarly, in other regions over the world, floods

lead to great losses in different aspects as well. In USA, it has been reported at least 176 people in the 26 states were killed by the only flood disaster event in 2015. In Germany, flood-related damage costs about 500 million euros per year; and it is expected to multiply in the future with more extreme events occurring under the influence of climate change (Hattermann et al. 2015). This situation becomes even worse in under developed or developing areas in the world. For example, in India, over 100 million people every year are exposed to flooding disasters (Bhatia and Riley 2016).

Due to climate change and geography conditions, about half of the cities in China are facing severe water shortage, while another half of the main cities are suffering the problems of flooding and waterlogging (Harris 2015). In July 2016, the flooding caused by an intense rainfall event has led to around 150 deaths in central and northern China. In recent years, the central government of China has launched "sponge cites" program to handle the adverse situation of urban flooding and pollution related disasters, with 16 cities selected as an attempt for implementing sustainable stormwater management and smart urban water supply (Leach 2016). By implementing this program, the government intends to achieve the purposes of decreasing urban flooding and solving urban water shortages. This program is also termed as Low-impact development (LID) in the US, which refers to systems and engineering practices approach that manage stormwater runoff to protect water quality as part of green infrastructure (EPA 2017). Various application practices in these schemes for urban water system management have demonstrated that design and analysis of open channel flows are one of key contents during this process, which is crucial to the implementation outcomes of such management policies.

Therefore, it is necessary and important to investigate the open channel systems for its flow conditions and hydraulic performance.

In addition to the flooding issues, water quality (pollution) is another problem that is crucial to the urban development and human health (Schneider et al. 1973). In urban area, especially under its rapid development stage, water environment is easily becoming serious for its water quality due to the discharge of domestic and industrial wastes. Furthermore, other inappropriate human activities including filling the lakes for farmland, deforestation and so on, may weaken the natural ability in adjusting the surface runoff and impoundment. Besides, as human activities affect environment more significantly, climate change has drawn many research interests. The strongest El Niño and La Niña events on record happened in last several decades, which disrupted normal weather patterns heavily, leading to extreme weather such as rainstorms and droughts all over the world. Open channel disasters including flooding, mudslide, and water shortage which are closely related to weather become more often and severe as well, with the fact that flooding accounts for 47% disasters related to weather (Nash 2017). In this regard, a reasonable design of artificial sewage channels, together with the advanced water quality analysis and treatment technologies applied to these open channels, may benefit very much for both water resource management and urban drainage quality. From this perspective, researches on open channel flows have become of great significance to help human better understand the physical process in the channel, therefore can shed useful lights on the design and management of such hydraulic structures.

1.1.2 Understanding and description of open channel flows

To understand the principle and physics of open channel flows, experimental tests and mathematical modeling are two common ways. Particularly, experimental observations are helpful to gain direct understanding of dynamic flow phenomena and processes in the open channels under specific system and flow conditions, while mathematical modeling may provide more general physical rules and principles to describe the results of open channel flows under any conditions. These two methods are useful to each other in terms of each method development. In this study, the model method is adopted for the investigation, since the aim of current research is to obtain an in-depth understanding and quantitative description of unsteady open channel flow evolution and process under various and general conditions.

Mathematically, open channel flow process can be commonly described by a set of hyperbolic partial differential equations (PDEs), called Saint-Venant equations or shallow water equations in the literature, which governs the mass balance and momentum variations in the channel system. Although the different forms including one dimensional (1D), 2D and 3D have been developed in the literature, the 1D form is commonly used due to its simplicity of expression and convenience of program implementation, with its detailed expressions shown in the Chapters 2 and 3 later in this thesis. In the early years for studying open channel flows, the main efforts were paid to developing analytical solution to 1D Saint-Venant equations by imposing necessary simplifications and approximations. Afterwards, with the development of computer facility and technology, intensive computation work becomes possible, and therefore, numerical model solutions to these equations are available by applying relevant numerical techniques such as finite difference, finite element, boundary integral, and methods of characteristics. With the modeling, a satisfying

understanding of unsteady open channel flows has been obtained for many applications in engineering practice. At the same time, field studies and physical model experiments were also carried out, in order to obtain direct measurement data of unsteady open channel flows for analysis and mathematical model validation.

Through experimental testes (laboratory or field), a limited number of spatial locations and time intervals of input data are available from the measurement (Willis et al. 1989), which are usually used as known conditions or benchmarks to the numerical modeling, so that the developed model and method can be validated and verified for its accuracy and validity. In spite of the progress and achievement of experimental tests and numerical modeling, these understanding and findings are mainly based on the different deterministic conditions (system and flow). That is, for each result obtained from test and model, it is usually not repeated in the reality, such that what we observed from the practical open channel flows are commonly different (with more or less extents) from the findings of previous tests and models. Such difference, or termed as error or bias, can actually be attributed to the uncertainties and randomness that are inevitable in realistic channel systems, including natural/inherent and artificial/external components. Therefore, understanding such uncertainty and randomness (i.e., stochastic characteristics) is an essential part of system and flow investigations by using the developed experimental test and modeling technologies.

In fact, unsteady open channel flow is a complex process which might be influenced by various natural (inherent) and artificial (external) factors in the channel system and surrounding conditions such as bed roughness, flow area, wetted perimeter and friction slope which are random in nature (Guganesharajah et al. 2006). Moreover, flow processes themselves under such natural and practical factors are

stochastic processes, especially for mountainous rivers with great variety in slopes, roughness and random inflows. In mountainous rivers, the natural hydraulic characteristics are much more complicated in comparison with lowland rivers due to the special geography features, where different variabilities commonly exist including channel platform, channel gradient, grain size, and bed forms, sediment dynamics and aquatic and riparian biota (Wohl 2013). Many previous studies have indicated that mountainous rivers can adjust channel geometry sufficiently to produce systematic downstream scaling of channel geometry, hydraulics and sediment transport (Comiti et al. 2006, Golden and Springer 2006, Wohl et al. 2004). All of these studies have confirmed again the existence of inevitable uncertainties and their substantial influences in the open channel systems.

Many previous researches in the literature have focused on the study of stochastic behavior of open channel flows, which demonstrates the importance and influence of system uncertainties from another point of view. For example, the numerical methods like the Monte Carlo simulation, the analytical methods like the first order reliability method (FORM), and the semi-analytical methods like perturbation methods, and so on (Tung et al. 2006). All these developed methods and obtained results have provided useful tools and insights for understanding the open channel flows. However, the limitations for each method and technology to the applications have confined our understanding and findings to limited ranges and under specific simplified conditions. In other words, it is necessary to further develop and extend the method and tool for better understanding the stochastic characteristics of open channel flows under more realistic system and flow conditions. This is the motivation and scope of current thesis research.

1.2 Scope, Objectives and Advancement of This Research Work

This research aims to study the stochastic characteristics of unsteady open channel flows under the conditions of different uncertainties. To this end, an extended stochastic analysis model based on the perturbation method is established in this study, which can be used to express the propagation of different uncertainty factors and their impacts on the system responses. The common uncertainty factors (as random variables in the model) including the random inflow (upstream and lateral inflows), random bottom roughness, random base flow and random cross-section area are considered in this study for the investigation of the stochastic characteristics of the unsteady open channel flows. The main objectives of this research are:

(a) To establish 1D stochastic open channel flow models, through the multiple-scale perturbation based analytical analysis;

(b) Based on the developed stochastic model, to conduct the uncertainty and sensitivity analysis of unsteady open channel flows for the different random inputs and parameters as well as system conditions (including upstream inflows, lateral flows, bottom roughness, complexities of river networks, hydrologic condition, etc.), and their correlations;

(c) To examine the influence range and relative importance of different uncertainty factors in (b) to the open channel flow responses (water depth and flowrate variation), under different system configurations and flow conditions, in order to understand statistically the stochastic characteristics of the unsteady open channel flows;

(d) With the understanding and findings of the stochastic analysis above, relevant discussions and recommendations on the risk analysis and

reliability design of open channel systems are provided, with perspective to better design and management of practical hydraulic engineering projects.

It is noted that the developed model and proposed method in this research is able to conduct uncertainty prediction for complex open channel flows by considering the spatial and temporal random variables with certain correlations in the flow process. Specifically, the stochastic moment equations are solved through implicit finite difference technique, so as to obtain the uncertainty of water depth and flowrate at any location and time. Furthermore, the developed model and method is extendable and flexible to any other conditions and systems where more uncertainty factors and general flow process can be considered and included. Finally, the results and analysis in this research is useful and applicable to general open channel flow process, since the normalized and dimensionless forms of the model and results are presented in the thesis.

1.3 Structure of the Thesis

This thesis consists of five chapters in total. Following this introduction Chapter 1, the literature relating to this research topic is briefly reviewed in Chapter 2. Specifically, the model development and progress of unsteady open channel flows are summarized, and the main stochastic analysis methods applied to open channel flows are also presented. Chapter 3 presents the research methodology and the key developed results of stochastic models that are used to uncertainty analysis later in this study. The governing equations used for analysis, the key assumptions imposed for the analytical derivations, the numerical scheme and implementation procedures,

as well as the stochastic analysis process are elaborated in this chapter. Based on the developed stochastic model, extensive cases are applied in Chapter 4 for the systematical stochastic analysis. The developed model in this study is firstly validated by well-established data from the literature (analytical and numerical data) to confirm its validity and accuracy. Afterwards, various cases with typical ranges of parameters and uncertainties are studied by the validated model, and the obtained results are used for the stochastic analysis of the unsteady open channel flows. Finally, the results are systematically analyzed and discussed for the stochastic features of complex unsteady open channel flows, especially for the influence and importance of different uncertainty factors on system responses. With the obtained results and analysis from the Chapter 4, key findings and conclusions are provided in the Chapter 5. Meanwhile, useful recommendations are also provided for the design and management of open channel systems form perspective of stochastic analysis in the end of the Chapter 5.

For clarity and convenience, the key content of each chapter and connections of different chapters are shown in the following flowchart (Figure 1.3).

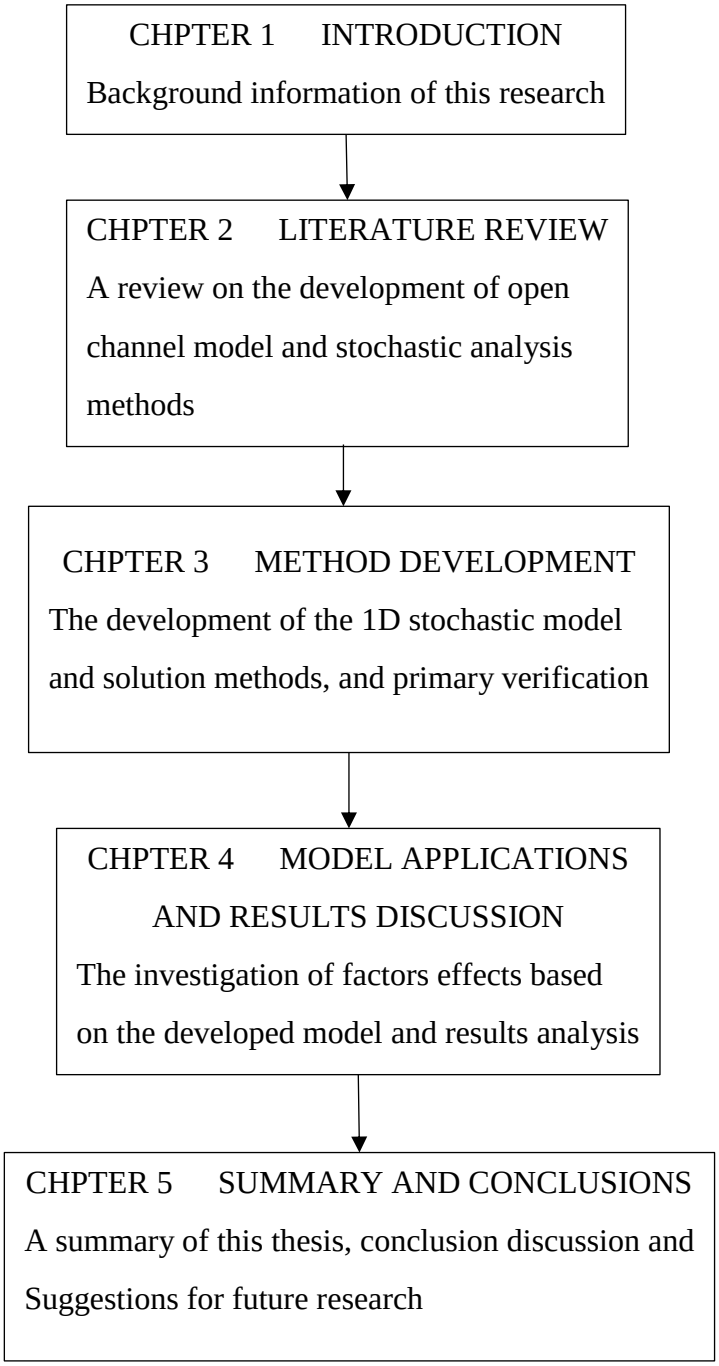

Figure 1.3 Framework of this thesis work

CHAPTER 2 LITERATURE REVIEW

2.1 Modeling and Analysis for Open Channel Flows

Open channel flows have been widely studied through theoretical analysis, modeling and experimental tests for their importance and impacts to the society nowadays. In early stage of these studies in this field, experiments are the main research method for a direct understanding and observation analysis of the phenomena and processes of open channel flow evolutions. Various scientists and engineers have conducted many classic experiments through laboratory, pilot or field tests, with aim to simulating the natural open channel flows so as to learn the characteristics of the flow process. With these efforts, many important theories or empirical formulas such as Manning's equation that was developed for estimating average velocity in an open channel flow have been obtained in this field, which formed as the important basis on the development and progress of the study. Later, more experimental studies on open channel flows have mainly focused on boundary shear stress distribution, momentum transfer, energy loss, and resistance in channels with complex topography (e.g., compound channels, various slope), although some of them were difficult to be described in mathematical forms, which provided fundamental understanding and scientific perspective of the physics and mechanisms during open channel flow process (Knight and Demetriou 1983, Lin and Soong 1979, Myers 1978, Myers and Brennan 1990). Till now in this field, the experimental test method is still important and necessary to the further and specific study of open channel flows.

Different from experimental studies, modeling analysis is another important but more general way to understand the open channel flow behaviors. As the

computation technology has greatly developed during past several decades, and the widespread of high-performance computers, modeling analysis based on extensive numerical simulations has played, and will continue to play, a more and more important role in open channel flow research. In the early stage of modeling analysis, when the computational facilities were not well developed, many researchers in this field have taken their great efforts to propose, improve and implement mathematical models to solve some relatively simple open channel flow problems. For example, Yen (1971) re-examined the compatibility of the open channel flow equations for unsteady spatially varied flow problems to suit new numerical techniques and higher computer performance. The mass, momentum and energy equations for unsteady non-uniform flows with incompressible viscous nonhomogeneous fluid with lateral flow in cross-section of any shape were derived. By integrating the 3D equations in vertical and cross channel direction (assuming no vertical acceleration and small bed slope) and replacing viscous terms with friction slope, these equations are reduced to 1D form (Liggett 1993), which is the well-known Saint-Venant equations (also known as 1D shallow water equations), as follows:

$$\frac{\partial Q}{\partial x} + \frac{\partial A}{\partial t} - q = 0 \qquad [2.1]$$

$$\frac{\partial Q}{\partial t} + \frac{\partial (Q^2/A)}{\partial x} + gA\frac{\partial h}{\partial x} - g\left(S_0 - S_f\right) - qu = 0 \qquad [2.2]$$

where Q is flowrate in the channel, x is distance along flow direction, A is cross-section area, t is time, q is the flowrate of side inflow, u is the side inflow velocity in main flow direction, g is gravity acceleration, h is water depth, S_0 is channel bed slope and S_f represents the friction slope.

For practical problem applications, equations for special cases were formulated by deducing the general equations (kinematic and diffusion wave models for flood routing), and hence computation effort can be saved. On this point, Heggen (1991) studied several definitions of critical depth and their applicability for different channel shapes and velocity profiles. Meanwhile, research focuses were also given to the resistance terms in the channel due to cross-section shape, boundary nonuniformity, flow unsteadiness, and compound channel resistances (Rouse 1965, Yen 2002). Further research on flow resistance estimation and formulating is conducted for more precise representation and large-scale roughness (Cheng 2014, Cheng et al. 2010). Thereafter, Alias et al. (2011) presented a Godunov-type alternative for solving the 1D inhomogeneous shallow water equations with complex source terms which has the capability of dealing with highly dynamic and complex flood flow. The 1D equations were also developed for storage cell inundation models which cost very low computation effort compare to full 2D models (Bates et al. 2010). Recently, Vila et al. (2017) conducted a 1D width averaged model from 2D shallow water equations for constrained flow. These 1D models have showed good capability to be coupled with 2D models for hydrodynamic investigation. To examine and improve this capability, (Bates and De Roo 2000) combined 2D diffusion wave of floodplain flow with 1D kinematic wave for channel flow to model floodplain inundation in low land rivers. Furthermore, (Liu et al. 2015a) presented a model linking the channel and flood detention basin with complex topography and irregular boundary, applying 1D Saint-Venant equations governing channel flow and 2D shallow equations simulating floods in flood detention basin. To solve these developed 1D or 2D or coupled 1D-2D models, many numerical solutions have been proposed and improved during the development process of these

models. Among these numerical methods, the finite-difference scheme is one of the commonly used and mostly employed for practical applications due to their convenience of implementations in the program codes. In this regard, the discretization schemes of governing equations can be rather explicit or implicit depending on how the terms in these models are evaluated for their influence on the modeling results. Another common method is the method of characteristics (MOC), in which the partial differential equations (PDEs) of the developed models (1D or 2D) are transformed to ordinary differential equations (ODEs) along the characteristic curves and thus the solutions are obtained easily from the ODEs. Among these methods, the implicit method presents unconditional stability with no limitation on computation timestep for variable spatial steps, therefore, it has become very popular in 1D model computation (Sturm 2010). Finite element methods and finite volume methods are also available for 1D shallow water equations solutions, which are commonly adopted for complex systems where the boundary conditions are complicated and/or dynamic and thus are usually influential to the flows (Hicks and Steffler 1995, Ying et al. 2004).

Since the wide existence of compound channels for their practicality of flow conveyance function, 2D models have become essential for such applications on flood inundation researches and appeal the most research interest in past decades for its capability to represent 2D flood plain flows. In 2D models, the water depth is assumed to be shallow as well, and the equations are depth-averaged. For instance, (Keller and Rodi 1988) exploited a depth-averaged form of the k-ε turbulence model and conducted a 2D model for compound channel cross-section flow characteristic calculation. Limitations of the 2D surface flow equations for overland flows with irregular topography and rapidly varying surface were investigated by Tayfur et al.

(1993). Afterwards, Liang (2010) developed a second-order accurate 2D model extended from 1D shallow water model for flood simulations, which is capable of simulating slow-varying inundations to extreme rapid floods in complex domains both for natural terrains and urban areas. The differences in capability of 1D and 2D models for flood simulation were tested, and the different responses to friction parameterizations were captured (Horritt and Bates 2002). Discontinuities in open channel were also under investigation by a well-balanced 2D model based on shallow water equations (Amiri et al. 2013). For 2D models, finite difference, finite volume, and finite element methods have been commonly employed for numerical discretizations. Different from 1D numerical technics, finite volume and finite element methods are more popular in solving 2D shallow water equations due to the complex boundary conditions encountered commonly in 2D geometric systems (Alcrudo and Garcia‐Navarro 1993, Anastasiou and Chan 1997, Bermúdez et al. 1991, Bradford and Sanders 2002, Liu et al. 2015b, Pironneau 1989). For Riemann problems arose in the finite volume scheme based applications, the Godunov-type scheme has been widely used, which is first-order accurate in both space and time and developable for higher-order methods (Fujihara and Borthwick 2000, Liu 2014). Apart from the Godunov's scheme, other approximate Riemann solvers were also commonly developed and employed such as Roe's solver (Roe 1981), HLL solver (Harten et al. 1983) for the two-dimensional model solutions. Particularly, for open channel equations where Riemann problems are difficult to solve, Benkhaldoun and Seaïd (2010) developed a new finite volume method avoiding Riemann solution during the time integration process.

Usually, a 3D model is required if it is necessary to capture the flow properties in vertical direction. Fischer-Antze et al. (2001) conducted a 3D model for

vegetation covered channel which is able to consider vegetation over the whole water depth rather than just apply large roughness to the model. However, 3D models usually demand higher computation effort and therefore become more time consuming and lower efficiency in practical applications, and as a result, they are usually adopted for theoretical research purposes so far. To put forward with the progress of 3D modeling for open channel flows, Audusse (2005) introduced a new approximation of the Navier-Stokes equations consisting of a set of coupled Saint-Venant system, which describes vertical profile of the horizontal velocity precisely and preserves the efficiency of 1D models. Many commercial or open source software/models are currently available and widely used in engineering practice for 3D open channel computation, such as Fluent, Pheonics (commercial), and OpenFOAM, Delft3D (open source) (Teng et al. 2017). These software/models are well developed and also validated substantially for complex open channel with relatively good computation efficiency for their used advanced programming techniques and thus can offer various applications for research works and small-scale practical systems.

Through various applications, these relatively well-developed models and solution methods in previous researches still have different limitations and disadvantages. For example, they are usually theoretically formulated and developed within the assumed computation domain with essential simplifications and hypothesizes, which however might become inaccurate/invalid to other practical systems, which has been evidenced by the profound discrepancies (or termed as errors) between model results and experimental data. It has been known that the incapability of numerical schemes might be one of the reasons, while the model and data errors can be more significant to such incapability in practical applications,

since uncertainty and randomness are always unavoidable in our real-world open channel systems (including both natural and artificial systems), especially when the knowledge about the studied open channel system is limited (Merz and Thieken 2005) (see more elaborations in the next section). Herein, the study focused on uncertainty and stochastic characteristics of the open channel flows is of strong significance in hydraulic research and engineering. Moreover, it would be helpful in better modeling and interpret real-world observations to understand and quantify stochastic characteristics of open channel flows, which is then also useful to facilitate the theory and practice of open channel flows under complex uncertainty conditions. Consequently, this becomes the motivation and purpose of current thesis research.

2.2 Uncertainty Studies for Open Channel Flows

Uncertainty in unsteady open channel flows has been studied for decades, with the effects of spatially varying friction resistance, cross-section area and other dependent variables on the flow processes investigated widely in the literature. The uncertainty factors in hydraulic engineering systems may include: (1) nature variability associated with the inherent randomness of natural geophysical processes; (2) model formulation uncertainty reflects the inability of the model to precisely describe the process in the system; (3) parameter uncertainty from the inability to accurately quantify model inputs; (4) data uncertainty; (5) operational uncertainty include those associated with construction, manufacture, and other human activities (Tung et al. 2006).

The studies emphasizing on the uncertainties of open channels have benefited greatly the design and maintenance of hydraulic structures since hydraulic structures are inherently subject to potential risks in design and operation associated with not only hydrologic events but also many other natural and artificial factors (Yen and Tung 1993). Researches on flooding risk analysis, flood management have been conducted for the design of hydraulic structures such as flood levees and sewers, with models systematically analyzing the various types of uncertainties in the hydrologic aspect and hydraulic aspect as well of design, and analysis defining the risk and reliability of overtopping. In these studies, the levees were regarded as random variable with a particular distribution to obtain the probability (or risk) of failure and the expected flood benefits due to the uncertainty of flood levees (Tung and Mays 1981, Wood 1977). Thereafter, Chau and Yang (1992) built an expert system on hydrodynamics for assisting engineering in unsteady open channel flow for river networks. Recently, the artificial intelligence (AI) technology based hybrid models have also been popular and used for flood forecasting (Chau et al. 2005).

In addition to these researches focused on the effects of uncertainties on hydraulic structures in open channel, the uncertainties models of open channel have also been further examined and widely investigated with stochastic processes. For example, Wood and Rodríguez-Iturbe (1975) proposed a Bayesian probability model accounts for all sources of statistical uncertainty including parameter and model uncertainty to analyze the uncertainty among flood frequency models. Gates and Al-Zahrani (1996) presented the Saint-Venant model as a set of stochastic PDEs with parameters of spatiotemporal random fields, and alternative solution methods are discussed and compared based on the consideration of the stochastic governing equations and the parameters statistical characteristics. Afterwards, Numerical

simulations were conducted by Di Liberto and Ciofalo (2011) which has shown the effects of periodic unsteadiness on the structure of main flow and turbulence. At the same time, it is worthy of noting that the vegetation effects under random waves of flows in the channel systems were also investigated by many researchers where the uncertainties were proved to pose substantial influences on the system flows and hydraulic performance (Li and Zeng 2009, Li and Zhang 2010).

Despite of these various studies with regard to uncertainties in open channel flows, there has so far not yet a systematical study on the comprehensive understanding and analysis for the quantitative impact and relative importance of different uncertainty factors in the open channel flow system, with providing exact expressions and formulations for such impact description. As presented in the introduction chapter, this is the motivation and scope of current thesis research.

2.3 Stochastic Analysis Methods for Open Channel Flows

Stochastic analysis in engineering has been investigated for many years due to the significance and inescapability of the stochastic process occurrence in engineering practice. In the literature, it can be summarized that there are two main categories of methods employed for stochastic analysis for physical problems: simulation methods and non-simulation methods. On the basis of these two categories of methods, a combination of simulation methods (such as Monte Carlo simulation) and non-simulation method has also been developed and applied afterwards to overcome the disadvantages (or part of them) of each method. Overall speaking, the simulation method can represent the stochastic processes fairly well though it may be computationally intensive, and therefore, it is commonly used to

validate and confirm the accuracy and reliability of the relevant non-simulation method. In this section, the main representatives of these two categories of methods and their combined form developed in the literature are briefly reviewed and summarized as follows.

2.3.1 Simulation methods

Simulation methods are commonly employed for the analysis of stochastic process in engineering practice due to their advantages of accuracy and reliability for representing different system complexities. In principle, this sort of method deals with the random data directly, and therefore it has main advantage in flexibility and generality of application since it can deal with any kind of stochastic factors in the system if only they can be treated/described appropriately in mathematical or numerical forms. In the regard, stochastic simulation methods can incorporate complicated features of these systems, allow calculation of any desired set of reliability measures, and thus can provide a realistic analysis. Though it is applicable to any circumstance in principle, the generation and operation of sample realizations for complex systems could be numerous, which leads to the need for great efforts in computation. Even for nowadays development of computational capacity, it is still impossible to accomplish such stochastic numerical simulation for many practical problems.

Basically, the simulation program of stochastic numerical methods for analyzing system reliability consists of two following parts (Wagner et al. 1988):

(1) The simulation section, which generates realizations of system input according to specified probability distributions;

(2) The solution section, which gives the solution samples for all realizations generated in (1), and obtain the statistics of these samples for probability distribution analysis.

It is also noted that for different open channel systems, e.g., with different complexities of flows and structures, the requirements of computational capacity and program skills will be greatly different. So far, there still not exists a general criterion that can govern such numerical requirements and process for all systems. Amongst these numerical methods, the Monte Carlo simulation is the commonly used one, and has been proved to be robust and reliable, in principle, to model the hydrosystems (Tung et al. 2006), which is taken as example herein for illustrating this type of numerical methods.

In a parametrically nonlinear system with a sufficiently large number of simulations, the Monte Carlo method is much superior in accuracy to perturbation or first-order methods. The use of Monte Carlo simulation and random field generators have played an important role in solving nonlinear stochastic problems that cannot be solved by other types of methods such as analytical or semi-analytical techniques. (Mantoglou and Wilson 1982). On this point, the Monte Carlo Simulation is the most common simulation method used for nonlinear stochastic process modeling and analysis.

In principle, the Monte Carlo simulation method is a broad class of computational algorithms relying on repeated random sampling to obtain numerical results and can deal with any problem with probability distribution function in principle. In more details, the Monte Carlo methods aim to solve two problems (MacKay 1998): (a) to generate samples from a given probability distribution; and (b)

to estimate expectations of functions under this distribution. In the application of this method, the latter problem is very based on the solution of former one (sampling), which is used to test the reliability of the samples.

Regarding the sample generation (the first problem) in the Monte Carlo simulation, various sampling methods have been developed in the literature, such as simple random sampling which is just an ensemble of random numbers, e.g., the Latin Hypercube sampling (LHS) ensuring samples to represent the real variability (McKay et al. 2000); and the Orthogonal sampling guaranteeing better representative of the real variability (Garcia 2000). However, in complex stochastic processes, the input variables are usually correlated to each other, such that difficulty may occur in the generation process for accurately representing input random functions. To this end, different data generation approaches have been developed, including the linear Gaussian state-space model coupled with the well-known and widespread Kalman filter; the hidden Markov model HMM filter with a finite state-space Markov chain (Doucet et al. 2001); and the Sequential Monte Carlo (SMC) model for more flexible and general to provide a convenient and attractive approach for computing the posterior distributions. Furthermore, the developed Sequential Gaussian simulation (SGs) can model the spatial uncertainty through generation of several equally probable stochastic realizations, which are useful and applicable to generate spatial variables in open channel flows (Delbari et al. 2009).

With its various advantages, the Monte Carlo Simulation has been widely applied for different purposes in hydraulic engineering problems. For instance, Smith and Freeze (1979) conducted a stochastic analysis of 1-D steady state groundwater flow through a bounded domain which is divided into a finite set of discrete block, and the spatial variations in conductivity are assumed to be presented as a first-order

nearest-neighbor stochastic process model. Fai (1987) then employed this method to explore the effect of input uncertainty on output variability for the formulation developed for the synthesis of random fields in which groundwater flows. Recently, it has been used to sample uncertain variables including channel roughness and friction slope in the flood water level estimation (Guganesharajah et al. 2006).

2.3.2 Non-simulation methods

Non-simulation methods of stochastic modeling deal with the partial differential equations (PDEs) analytically for describing the hydraulic evolution process of open channel flows. In this type of methods, the variables in the governing equations are treated as random functions. As a result, the governing equations can be transformed into stochastic PDEs with necessary mathematical operations, and the solution to which becomes also stochastic functions. Compared with former simulation methods, the non-simulation methods are convenient and efficient in calculation, but difficulties may occur in the analytical derivation process of governing equations because of complicated mathematical work.

Probability distribution function method

Probability density function (PDF) method is conducted by deriving probability density functions from the stochastic PDEs with particular methods. Pope (1985) introduced a method whose principle is to solve a modelled transport equation for the velocity-composition joint PDF for calculating the properties of turbulent reactive flow fields. Later, this method was further developed with the help

of Monte Carlo Simulation to calculate the properties of inhomogeneous turbulence flows (Pope 1994), and the accuracy of PDF model calculations with different models was examined later by others (Cao et al. 2007). Yoon (2003) also proposed a method with Fokker-Planck equation (FPE) describing the evolution of the PDF of overland flow depth at the downstream section of a hill slope. Under particular conditions, this method can produce a good comparison between the predicted evolution of the PDF for overland flow depth and the corresponding prediction from the Monte Carlo method. Thereafter, A new modeling approach—multiple mapping conditioning (MMC) which combines the advantages of PDF and moment equation methods is developed for treating turbulent reactive flows (Klimenko and Pope 2003). More recently, Sett (2007) presented a solution for the evolution of the PDF of elastic-plastic stress-strain relationship in 1D form.

The PDF methods have emerged as one of the most promising and powerful approaches for accommodating the effects of turbulent fluctuations in velocity and chemical composition in CFD-based modeling of turbulent reacting flows (Haworth 2010). However, these solution methods are based on the approximation imposed on the original system equations, with the accuracy highly dependent on the pre-understanding of the system. Moreover, in many general and complex cases, it will be hardly to obtain the solutions of stochastic PDEs for nonlinear complex systems.

Moment equation method

The moment equations method investigates not a single case but the statistical moments of the stochastic processes, which leads to less consideration of objects and enhances the efficiency of computation. The moment equations can be derived from the stochastic PDEs and the solution of moment equations presents the statistical characteristics of the stochastic process. Several commonly used moment equation methods are introduced herein.

Spectral method

The spectral method is accomplished by employing spectral representations of the uncertain variables of the PDEs. These uncertain random inputs are expressed in the spectral representation with the treatment process of Fourier-Stieltjes integral (Gelhar et al. 1979). As a result, the moment equations can be established and solved with a series of derivations. This method has been widely applied to solve perturbed forms of the stochastic differential equation which describes flow through porous media with random variety in hydraulic conductivity (Bakr et al. 1978). Dikow (1988) studied a saturated flow problem with spatially varying conductivity in a rectangular domain, using discrete spectra to calculate the expected flux across the outflow boundary and its variability. Li and McLaughlin (1991) further combined the classical Fourier transform with numerical solution techniques, extending its application to nonstationary processes. In the study of Si (2008), the spectral analysis was applied to study soil hydraulic conductivity, which has significant meaning in natural resources management and environment protecting. Furthermore, Ni et al. (2011) presented an unconditional approximate spectral method for delineating well

capture zones in nonstationary groundwater systems. Thereafter, Ghanbari and Bravo (2011) applied spectral methods to study the phase lag between precipitation and groundwater-level response. At the same time, Ge and Cheung (2010) extended the spectral method for long-wave runup calculation, which is able to minimize truncation errors and provide an accurate and robust solution for forecasting of flood events. More recently, this method has been further developed with backward particle tracking algorithm to delineate stochastic well capture zones in Choushui River in Taiwan (Lin et al. 2015). Moreover, the spectral analysis has also been used to obtain the design hydrographs based on historical floods (Fuentes-Mariles et al. 2015).

On the other hand, the polynomial chaos based spectral method has also attracted many studies in different research fields. Xiu et al. (2002) developed a generalized polynomial chaos algorithm for modeling the input uncertainty and its propagation in flow-structure interactions, in which the random inputs are represented spectrally by the use of orthogonal polynomial functions. Polynomial chaos was also employed in modeling the input uncertainty and propagation in incompressible flow simulations (Xiu and Karniadakis 2003), model problems involving simplified dynamic system and Rayleigh-Benard instability (Le Maıtre et al. 2004) with Wiener-Haar representation, uncertain representation and propagation in CFD computations (Knio and Le Maitre 2006), and for the "non-intrusive" analysis of parametric uncertainty in reacting-flow systems (Reagana et al. 2003). Afterwards, Marzouk et al. (2007) developed an efficient reformulation of the Bayesian approach to inverse problems based on polynomial chaos expansions representing random variables. In practical applications of these spectral methods, the unknown or a simple basic distribution of the process can be represented by

conducting a numerical projection procedure with a set of Wiener-Askey polynomial chaos expansion (Xiu and Karniadakis 2002). Therefore, different forms of the polynomial methods have been widely developed and successfully applied in different fields.

In these previous studies, the spectral method has been proved to have the attractive feature that can provide a response continuous in time (Gambolati 1993). It is demonstrated in the literature that, when applied in solving 1D shallow water wave problems, this method may have infinite-order accuracy in space and first-order accurate in time, and have better performance when the time-stepping errors are relatively low (Sinha et al. 1995). When it is applied to groundwater problems, the spectral method has the advance of high-order accuracy and fast convergence for calculating the flow field in porous media (Fagherazzi et al. 2004, Li and Liu 2015). However, it is also shown from various applications that the random processes in this type of methods are represented by truncated spectral expansions, which may lead to non-exponential convergence of the expansion, therefore induce potential inefficiency in computation.

Perturbation method

The perturbation method is relatively a simple approach in mathematics so that is it efficient in practical applications compared to other methods such as the spectral method with complicated derivation processes and results. Therefore, the perturbation method has become the most popular one among various non-sampling methods, in which the random functions are essentially expanded via Taylor series around their mean and truncated to a certain order as desired (Xiu 2009). In practical

applications, the analysis up to second-order expansion is fairly enough to obtain the expected accuracy, while it has to be extended to high-order (>2) analysis for some very particular and complex problems.

For the use of this method, Dettinger and Wilson (1981) conducted the first- and second-order analysis of uncertainty for the numerical model of groundwater flows. This state-space method utilized a compact matrix calculus notation to derive Taylor series expansions of the model for estimating the mean and variance-covariance properties of piezometric head predictions. Graham and McLaughlin (1989) then applied perturbation techniques to the governing transport equation for a conservative solute to deriving PDEs for a statistical moment for the analysis and prediction of solute transport in heterogeneous saturated porous media, and a solution procedure relying on a Galerkin finite element algorithm is also illustrated.

In an extended application in Andersson and Shapiro (1983), an analytical derivation from a first-order perturbation solution was employed with the assistance of Monte Carlo simulation to the investigation of stochastic nature of moisture content in a soil profile where the saturated hydraulic conductivity was taken as a stationary stochastic process. In that study, the link of the perturbation expressions with Monte Carlo simulation method has indicated an accurate representation of the nature stochastic process, and the result showed that the analytic nature of the perturbation solution could represent very well the nature stochastic properties.

Based on the original perturbation method, Willis et al. (1989) presented a new methodology for solving the stochastic hydraulic equations that characterize the steady 1D estuarine flow. This method was developed based on the combination of quasi-linearization and perturbation methods, and the finite difference approximation

of the stochastic differential operators, which assumed Manning's roughness coefficient to be the governing uncertainty source in the model so as to derive the stochastic equations. The results of moment equations can include the mean and variance of water depth, which were examined and analyzed for a comparison with the results of Monte Carlo simulation, in order to understand and investigate the effects of random channel roughness on flow process.

In the study of Horritt (2002), a second-order perturbation approach was developed and used to investigate the effects of topographic uncertainty on a numerical model of shallow water flow. Finite difference techniques were employed to discretize the partial differential governing equations, and the resulted nonlinear system was expanded in Taylor series to a second-order performance. The Fourier analysis technique was then employed for estimation of the first- and second-order approximations, and the results showed that the second-order terms could be very significant even for small perturbations. In that study, the Monte Carlo simulation was also conducted to verify the developed second-order perturbation model.

In order to solve particularly complex system, a higher-order analysis is necessary to better understand the relationships between variables (inputs and outputs) and the system dynamic processes. To this end, the higher-order solutions of the means and covariance of hydraulic head for saturated flows in randomly heterogeneous porous media were conducted in Zhang and Lu (2004) and Liu et al. (2006). This new high-order stochastic approach, termed the Karhunen-Loeve decomposition-based moment equation (KLME) in their studies, was actually developed on the basis of a combination of Karhunen-Loeve decomposition, polynomial expansion and perturbation methods. A series of numerical tests were conducted, in comparison with Monte Carlo simulation results, and the results

indicated that the KLME approach was more efficient in estimating the covariance and means of stochastic variables than the Monte Carlo simulation under the condition of same accuracy settings.

In addition, Chen et al. (2005) proposed a new solution based on the KLME approach to the stochastic multi-phase flows. In this problem, the perturbation of the two soil properties is firstly decomposed into an infinite series with the help of orthogonal normal random variables, and other dependent variables are expanded by polynomial expansions and the perturbation method to formulate differential equations of different orders. The moments of the dependent variables are then constructed from the solutions of these equations. The obtained results have also been validated by the Monte Carlo simulations using the finite element heat and mass (FEHM) transfer code (Chen et al. 2006), indicating that a better computational efficiency has been obtained by the newly proposed method for transient two-phase flow problems.

Recently, Lu (2008) further developed the perturbation method, in which a stochastic model was derived for describing the spatial varied roughness and random initial boundary conditions in open channel flows, in order to investigate the influence range of these two stochastic parameters. But other parameters, such as lateral flows, initial flow conditions and channel scales, which were widely observed to also have great influence on the unsteady open channel flow process in the literature, were not considered and included in that developed method. It is a reminder that the current thesis research aims to develop a more general stochastic model so as to include and examine these common and important factors in the open channel systems.

2.4 Summary on Research Gap and Needs

Despite that the development and progress of different methods (numerical and non-numerical methods) in the literature, it is also noted that these existing approaches are either computational expensive for applications (e.g. numerical methods) or inaccurate/invalid due to many different assumptions/simplifications in the method (non-numerical methods), especially for complex and practical hydrosystems (Vereecken et al. 2007). However, all these previous studies and their results have demonstrated the clear advantages of perturbation methods with regard to compromise the computational cost and efficiency of the applications and the description/representation of system complexities, compared with other numerical and non-numerical methods. From this perspective, it is necessary to further develop and extend such effective method to more practical and complex situations so as to capture accurately and efficiently the complete stochastic feathers of hydro-systems including open channel flow system. For this reason, the perturbation method will be adopted as the main tool and method for the further extension and development in this thesis research for the stochastic analysis of unsteady open channel flows, with the aims to investigate systematically the common and different parameters (system and flow) for their influences and relative importance on the unsteady open channel flow evolution and process.

CHAPTER 3 METHOD DEVELOPMENT AND VERIFICATION

3.1 Governing Equations of 1D Unsteady Open Channel Flow

As introduced in Chapter 2, the one-dimensional (1D) unsteady open channel flow can be modelled by two hyperbolic partial-differential equations (PDEs) including the mass equation (continuity equation) and the momentum equation over the channel cross-section. The full form of these governing equations, which are also known as shallow water equations or St.Venant equations in the literature (Schaffranek 1987), can be written as follows:

$$\begin{cases} B\dfrac{\partial h}{\partial t}+\dfrac{\partial Q}{\partial x}-q=0 \\ \dfrac{\partial Q}{\partial t}+\dfrac{\partial\left(\beta Q^2/A\right)}{\partial x}+gA\dfrac{\partial h}{\partial x}+\dfrac{gn^2}{AR^{4/3}}Q|Q|-qu-gS_0A+\xi B_C U_a^2\cos\alpha=0 \end{cases} \quad [3.1]$$

where x is horizontal spatial coordinate along the channel, t is time coordinate, $B = B(x)$ is the top width of the channel flow at location x, $h = h(x, t)$ is the water depth normal to the horizontal coordinate, $Q = Q(x, t)$ is the flowrate averaged for the cross-sectional area, β is the momentum coefficient, $q = q(x, t)$ is the lateral inflow per unit length of channel, $u = u(x, t)$ is the x-component of lateral flow velocity, g is the gravitational acceleration, R is the hydraulics radius, n is the roughness representation since Manning's formula is applied for friction slope expression, ξ is the wind-resistance coefficient, B_c is the top width of conveyance part of cross section, U_c is the wind velocity and α is wind direction measured from positive x-axis.

It is noted that the full form of governing equations in Eq. [3.1] is relatively complicated for analysis due to the difficulties of the complex mathematical expressions of system configurations (e.g., channel shape), flow processes (e.g., turbulence dynamics) and external factor characteristics (e.g., wind and friction). For the solvability and feasibility to the development of stochastic model in this study, several key assumptions are made as follows:

(a) The water is incompressible and homogeneous, and the density and viscosity of water are constant.

(b) The water pressure distribution is hydrostatic.

(c) The channel bed slope is relatively mild and constant.

(d) The channel cross section is rectangular and wide, so the area of cross section can be $A = Bh$, and the hydraulic radius could be illustrated as $R = h$.

(e) Frictional resistance is the same as steady flow, so the Manning's formula can be used to describe the friction loss.

(f) Wind resistance is negligible.

With these assumptions, the governing equations of 1D unsteady open channel flow with lateral flow in wide rectangular open channels can be transformed into:

$$\begin{cases} B\dfrac{\partial h}{\partial t} + B\dfrac{\partial hv}{\partial x} + hv\dfrac{\partial B}{\partial x} - q = 0 \\ B\dfrac{\partial hv}{\partial t} + 2\beta Bhv\dfrac{\partial v}{\partial x} + \beta v^2 h\dfrac{\partial B}{\partial x} + \beta v^2 B\dfrac{\partial h}{\partial x} + gBh\dfrac{\partial h}{\partial x} + gn^2v^2Bh^{-1/3} - gS_0Bh - qu = 0 \end{cases} \quad [3.2]$$

Within this simplified form, the unknown variables are only the water depth h and velocity v, which would be more concise and efficient in later perturbation treatment and computation. Therefore, the governing equations of Eq. [3.2] are a set

of partial differential equations expressing the mass and momentum conservations in a relatively simplified open channel. The initial and boundary conditions describing the initial state of flow and boundaries of the computation flow region are required to obtain the solution of a designated flow problem.

Initial conditions

The steady state flow water surface and velocity distribution are taken as the initial condition for solving the governing equations, which are described by:

$$h(x,0) = h_I(x), v(x,0) = v_I(x) \qquad [3.3]$$

where $h_I(x)$ and $v_I(x)$ are the initial water surface profile of the channel flow and the cross-sectional average velocity. For simplicity, the steady uniform flow is used as initial conditions for theoretical analysis, in which the water surface profile and velocity distribution can be analytically obtained, i.e., the normal depth and velocity of a particular open channel system.

Boundary conditions

Boundary conditions of open channel flow problems usually include the variations of water surface, velocity or flow rate, and the relation between velocity and water depth and the boundaries of the solution domain. For subcritical flow, both the upstream and downstream boundaries are required since the perturbed wave in the flow may propagate to both ends. For the supercritical flow, two upstream conditions would be necessary since the wave only propagates downstream under this condition. In this study, focus is given only to the subcritical flow, while similar

analysis method and process can be performed to the supercritical flow situation. For this purpose, an upstream boundary condition and a downstream boundary condition are needed to specify in a mathematical form to obtain the solution.

For the upstream boundary, an inflow profile is specified and given by:

$$h(0,t)v(0,t) = q_u(t) \quad [3.4]$$

in which $q_u(t)$ is the flow rate of inflow at the upstream boundary of the channel.

In this study, a water level time series at downstream boundary is taken for the consideration, so as to eliminate the potential influence from downstream end to the wave behavior from upstream under analysis (Napiorkowski and Dooge 1988). That is:

$$h(L_e,t) = h_e(t) \quad [3.5]$$

where L_e represents the location of the end of the channel, and h_e represents the water level at the end node.

3.2 Moment Equations for 1D Unsteady Open Channel Flows

The input parameters of the governing equations for describing realistic channel flows are usually accompanied by uncertainties with randomness, therefore, the solution to the governing equations is also subject to stochastic characteristics. The random parameters concerned in the model of current study include: the channel width B, lateral flow per channel length q, the lateral flow velocity in x-component u, Manning's n for roughness, bed slope S_0, initial water depth h_I, initial velocity v_I, and inflow rate at upstream boundary q_u.

To express and understand the probability distribution functions of these stochastic input parameters, experimental tests or field measurement can be one option for research, which is actually impossible or impractical for most of cases because of the unrealistic sample sizes and resolutions for measurement. In this regard, the statistical method might be another feasible way to obtain the stochastic moments of these parameters. Similarly, it is also difficult to obtain or solve directly the probability distribution functions of the unknown variables, i.e., water depth $h(x,t)$ and velocity $v(x,t)$ in the governing equations so as to understand the stochastic properties of flow processes. However, if the statistical moments of water depth and velocity are of interest and can be dealt by moment equations method instead (where equations with stochastic variables can be greatly simplified), the investigation for the flow characteristics becomes possible and more practical (Lu 2008). For this purpose, the means of the variables water depth and velocity, denoted by $<h(x,t)>$ and $<v(x,t)>$ respectively, and their covariance $C_{hh}(x,t;\chi,\tau)$, $C_{hv}(x,t;\chi,\tau)$ and $C_{vv}(x,t;\chi,\tau)$ are the main concerns to solve and analyze, where the covariance here is defined as $C_{hh}(x,t;\chi,\tau) = <h'(x,t)h'(x,t)>$, in which h' represents the fluctuation of water depth, with independent variables (x,t) from the sample space and (χ,τ) being a probability measure. In principle, the covariance of these variables reflects the tendency of the changes for the corresponding variables at (x,t), when the variables are changing and other parameters are measured at different location and time (χ,τ).

The moment equations governing the means and covariance of water depth and velocity of unsteady open channel flow can be derived from the 1D unsteady channel flow model. In this study, the perturbation expansion based moment equation method is adopted for its efficiency and accuracy of computation, which is described in detail later in the next section. As stated above, the random parameters

for the stochastic analysis include the channel width, lateral flowrate and flow velocity, channel bed slope, initial conditions, and boundary conditions.

Perturbation expansion of 1D model

To solve the 1D model, the unknown variables of water depth and flow velocity are firstly expanded into infinite series as represented by follows (Lu, 2008):

$$\begin{aligned} h &= h^{(0)} + h^{(1)} + h^{(2)} + \cdots + h^{(k)} \\ v &= v^{(0)} + v^{(1)} + v^{(2)} + \cdots + v^{(k)} \end{aligned} \qquad [3.6]$$

in which $h^{(k)}$ represents the k th-order in the perturbation parameter scale factor δ which will be explained later, namely $h^{(k)} = O(\delta^k)$. In physics, different orders of the series represent the influences or results from the system dynamic responses of different scales. For example, usually the zero order terms refer to the results of mean flow scales, while the first order ones for the results of system boundary variation induced scales such as channel bank width changes or bottom slope changes, which have relatively smaller scale than whole system domain (mean flow). A further smaller scale might be resulted from the friction of the channel bottom roughness, and so on. As a result, the overall/total response of the system dynamic flows becomes the superposition of all these different scale responses or influence results (Afzal et al. 2009, Lambrechtsen 2013, Smith and McLean 1984).

To examine the impacts of the uncertainties of different system and input parameters, the following perturbation factors are considered and applied to this study regarding the stochastic characteristics of unsteady channel flows (i.e., each random parameter is composed of the mean part with "<>" and perturbed part with " ′ " respectively):

$$
\begin{aligned}
q &= \langle q \rangle + q' \\
u &= \langle u \rangle + u' \\
B &= \langle B \rangle + B' \\
n &= \langle n \rangle + n' \\
h_I &= \langle h_I \rangle + h_I' \\
v_I &= \langle v_I \rangle + v_I' \\
q_u &= \langle q_u \rangle + q_u'
\end{aligned}
\qquad [3.7]
$$

Here we take a variable A to explain the perturbation parameter scale factor δ. This factor δ is assumed to be very small, and the variable A can thus be approximated into a series as follows:

$$A = A_0 + \delta A_1 + \delta^2 A_2 + \delta^3 A_3 + \cdots$$

Since the perturbation parameter scale factor δ is small (in order to distinguish and highlight the difference of different scales), the high order terms in the series become successively small compared to the lower order terms. Therefore, by truncating this series we could obtain an approximate perturbation solution for the variable A.

As a result of these assumptions and approximations, the k^{th}-other variable $h^{(k)}$ in this study equals $\delta^k h_k$ and $v^{(k)}$ in this study equals $\delta^k v_k$. Similarly for the known or input parameters, q' is of the same order as δ_q, which is defined by $\delta_q = \sigma_q / \langle q \rangle$ and σ_q is the standard deviation of q. Since $\delta_q \ll 1$, the convergence of the perturbation expansion of h and v as well as other perturbation parameters δ_n, δ_B, δ_{qu}… are guaranteed from the perspective of mathematical operations, with the minimum of which providing the best convergence.

Furthermore, to apply the above perturbation method, additional treatments for some special terms in the governing equations are necessary. Particularly, the term $h^{-1/3}$ in equation [3.2] is expanded with binomial expansion as

$$h^{-1/3} = \left(h^{(0)}\right)^{-1/3}\left[1+\frac{h^{(1)}}{h^{(0)}}+\frac{h^{(2)}}{h^{(0)}}+\cdots\right]^{-1/3}$$

$$= \left(h^{(0)}\right)^{-1/3}\left[1-\frac{1}{3}\frac{h^{(1)}}{h^{(0)}}-\frac{1}{3}\frac{h^{(2)}}{h^{(0)}}+\frac{2}{9}\left(\frac{h^{(1)}}{h^{(0)}}\right)^{2}+\cdots\right]$$

This expansion converges under the condition $\delta \ll 1$, since $h^{(1)}/h^{(0)}$ and $h^{(2)}/h^{(0)}$ are order of δ and δ^2 respectively.

Substituting these variable expansions into the governing mass and momentum equations [3.1] & [3.2], yields

$$\begin{aligned}
&\left(\langle B\rangle + B'\right)\frac{\partial\left(h^{(0)}+h^{(1)}+h^{(2)}\right)}{\partial t}+\left(\langle B\rangle + B'\right)\frac{\partial\left(h^{(0)}+h^{(1)}+h^{(2)}\right)\left(v^{(0)}+v^{(1)}+v^{(2)}\right)}{\partial x}\\
&+\left(h^{(0)}+h^{(1)}+h^{(2)}\right)\left(v^{(0)}+v^{(1)}+v^{(2)}\right)\frac{\partial\left(\langle B\rangle + B'\right)}{\partial x}-\left(\langle q\rangle + q'\right)=0\\
&\left(\langle B\rangle + B'\right)\frac{\partial\left(h^{(0)}+h^{(1)}+h^{(2)}\right)\left(v^{(0)}+v^{(1)}+v^{(2)}\right)}{\partial t}+2\beta\left(\langle B\rangle + B'\right)\left(h^{(0)}+h^{(1)}+h^{(2)}\right)\left(v^{(0)}+v^{(1)}+v^{(2)}\right)\frac{\partial\left(v^{(0)}+v^{(1)}+v^{(2)}\right)}{\partial x}\\
&+\beta\left(v^{(0)}+v^{(1)}+v^{(2)}\right)^{2}\left(h^{(0)}+h^{(1)}+h^{(2)}\right)\frac{\partial\left(\langle B\rangle + B'\right)}{\partial x}+\beta\left(v^{(0)}+v^{(1)}+v^{(2)}\right)^{2}\left(\langle B\rangle + B'\right)\frac{\partial\left(h^{(0)}+h^{(1)}+h^{(2)}\right)}{\partial x}\\
&+g\left(\langle B\rangle + B'\right)\left(h^{(0)}+h^{(1)}+h^{(2)}\right)\frac{\partial\left(h^{(0)}+h^{(1)}+h^{(2)}\right)}{\partial x}+g\left(\langle n\rangle + n'\right)^{2}\left(v^{(0)}+v^{(1)}+v^{(2)}\right)^{2}\left(\langle B\rangle + B'\right)\left(h^{(0)}+h^{(1)}+h^{(2)}\right)^{-1/3}\\
&-g\left(\langle S\rangle + S'\right)\left(\langle B\rangle + B'\right)\left(h^{(0)}+h^{(1)}+h^{(2)}\right)-\left(\langle q\rangle + q'\right)\left(\langle u\rangle + u'\right)=0
\end{aligned}$$

[3.8]

Consequently, the results of any order representative from the governing equations can be expressed through extracting and collecting the relevant terms in that order/scale (i.e., with the same order of factor δ). Specifically, the zeroth-order equations and the corresponding initial and boundary conditions can be obtained as,

$$
\begin{cases}
\langle B\rangle \dfrac{\partial h^{(0)}}{\partial t} + \langle B\rangle \dfrac{\partial h^{(0)} v^{(0)}}{\partial x} + h^{(0)} v^{(0)} \dfrac{\partial \langle B\rangle}{\partial x} - \langle q\rangle = 0 \\
\langle B\rangle \dfrac{\partial h^{(0)} v^{(0)}}{\partial t} + 2\beta \langle B\rangle h^{(0)} v^{(0)} \dfrac{\partial v^{(0)}}{\partial x} + \beta \left(v^{(0)}\right)^2 h^{(0)} \dfrac{\partial \langle B\rangle}{\partial x} + \beta \left(v^{(0)}\right)^2 \langle B\rangle \dfrac{\partial h^{(0)}}{\partial x} \\
+ g \langle B\rangle h^{(0)} \dfrac{\partial h^{(0)}}{\partial x} + g \langle n\rangle^2 \left(v^{(0)}\right)^2 \langle B\rangle \left(h^{(0)}\right)^{-1/3} - g \langle S_0\rangle \langle B\rangle h^{(0)} - \langle q\rangle \langle u\rangle = 0 \\
h^{(0)}(x,0) = \langle h_I(x)\rangle \\
v^{(0)}(x,0) = \langle v_I(x)\rangle \\
h^{(0)}(0,t) v^{(0)}(0,t) = \langle q_u(t)\rangle \\
h^{(0)}(L_e,t) = \langle h_e(t)\rangle
\end{cases}
\qquad [3.9]
$$

which has exactly the same format as the original governing equation, and thus can be solved by the well-developed numerical schemes and tools for the 1D unsteady channel flow model in this field.

Accordingly, all the perturbation equations can be obtained from the derived equation [3.8] above. For example, the first-order perturbation equation with the corresponding initial and boundary conditions is shown in following equation [3.10]. All other different order perturbation equations can also be extracted and obtained easily from the derived equation [3.8] above by following this similar procedure, which are omitted in this study.

$$
\begin{cases}
B'\dfrac{\partial h^{(0)}}{\partial t}+\langle B\rangle\dfrac{\partial h^{(1)}}{\partial t}+\langle B\rangle\dfrac{\partial h^{(1)}v^{(0)}}{\partial x}+\langle B\rangle\dfrac{\partial h^{(0)}v^{(1)}}{\partial x}+B'\dfrac{\partial h^{(0)}v^{(0)}}{\partial x}+h^{(0)}v^{(0)}\dfrac{\partial B'}{\partial x}+h^{(1)}v^{(0)}\dfrac{\partial\langle B\rangle}{\partial x} \\
+h^{(0)}v^{(1)}\dfrac{\partial\langle B\rangle}{\partial x}-q'=0 \\
B'\dfrac{\partial h^{(0)}v^{(0)}}{\partial t}+\langle B\rangle\dfrac{\partial h^{(1)}v^{(0)}}{\partial t}+\langle B\rangle\dfrac{\partial h^{(0)}v^{(1)}}{\partial t}++2\beta B'h^{(0)}v^{(0)}\dfrac{\partial v^{(0)}}{\partial x}+2\beta\langle B\rangle h^{(1)}v^{(0)}\dfrac{\partial v^{(0)}}{\partial x} \\
+2\beta\langle B\rangle h^{(0)}v^{(1)}\dfrac{\partial v^{(0)}}{\partial x}+2\beta\langle B\rangle h^{(0)}v^{(0)}\dfrac{\partial v^{(1)}}{\partial x}+2\beta v^{(0)}v^{(1)}\langle B\rangle\dfrac{\partial h^{(0)}}{\partial x}+\beta v^{(0)^2}B'\dfrac{\partial h^{(0)}}{\partial x} \\
+\beta v^{(0)^2}\langle B\rangle\dfrac{\partial h^{(1)}}{\partial x}+2\beta v^{(0)}v^{(1)}h^{(0)}\dfrac{\partial\langle B\rangle}{\partial x}+\beta v^{(0)^2}h^{(1)}\dfrac{\partial\langle B\rangle}{\partial x}+\beta v^{(0)^2}h^{(0)}\dfrac{\partial B'}{\partial x}+gB'h^{(0)}\dfrac{\partial h^{(0)}}{\partial x} \\
+g\langle B\rangle h^{(1)}\dfrac{\partial h^{(0)}}{\partial x}+g\langle B\rangle h^{(0)}\dfrac{\partial h^{(1)}}{\partial x}+2g\langle n\rangle n'v^{(0)^2}\langle B\rangle\left(h^{(0)}\right)^{-\frac{1}{3}}+2g\langle n\rangle^2v^{(0)}v^{(1)}\langle B\rangle\left(h^{(0)}\right)^{-\frac{1}{3}} \\
+g\langle n\rangle^2v^{(0)^2}B'\left(h^{(0)}\right)^{-\frac{1}{3}}+g\langle n\rangle^2v^{(0)^2}\langle B\rangle\left(h^{(0)}\right)^{-\frac{1}{3}}\left(-\dfrac{1}{3}\dfrac{h^{(1)}}{h^{(0)}}\right)-gS_0'\langle B\rangle h^{(0)}-g\langle S_0\rangle B'h^{(0)} \\
-g\langle S_0\rangle\langle B\rangle h^{(1)}-\langle q\rangle u'-q'\langle u\rangle=0 \\
h^{(1)}(x,0)=h_I'(x) \\
v^{(1)}(x,0)=v_I'(x) \\
h^{(1)}(0,t)v^{(0)}(0,t)+h^{(0)}(0,t)v^{(1)}(0,t)=q_u'(t) \\
h^{(1)}(L_e,t)=h_e'(t)
\end{cases}
\qquad [3.10]
$$

It is noted that the formats of the perturbation equations (even for the 1st order equation) are much more complicated than the zero[th]-order or original governing equations, which are very difficult to solve directly and accurately by so-far available numerical methods. Particularly, the complexity of these perturbation equations increases rapidly as the order grows and the number of unknown parameters required for a solution also increases progressively. As illustrated formerly in this study, only the first two statistical moments are of interest and used to understand and investigate the stochastic characteristics of unsteady channel flows in this preliminary research, and therefore, these complex perturbation equations are truncated to the first-order approximations only in the following moment analysis.

Moment representation

As shown in equation [3.9], the zeroth-order equations are identical to the original governing equations with representing the mean flow state with all potential random inputs, which are used to solve the mean water depth and velocity of the uncertain unsteady open channel flow. For convenience, the flow with mean water depth and mean velocity of the open channel system is termed mean flow or base flow hereafter. Since the stochastic characteristics are the objective of this study (but not the mean flow), the available free solution tool (i.e., software platform of Storm Water Management Model, SWMM) is adopted in this study to compute the mean flow results so as to provide the basis for the analysis of the statistical moments (i.e., stochastics).

On the other hand, the solutions of first-order equation [3.10] represent the perturbations (variations) of the unknown water depth and velocity on the basic of the mean flow. Instead of solving directly the perturbation equations, the covariance or cross-covariance is used to express the variation and stochastic properties of the unsteady open channel flows. To this end, the obtained perturbation equations are converted into the corresponding covariance equations so that the statistical moments can be analyzed explicitly.

To obtain the covariance equations, multiplying the perturbation of unknowns water depth and velocity at different location and time $h'(\chi,\tau)$, $v'(\chi,\tau)$ with the first-order equation [3.10] respectively and then taking expectation for the whole equation, yields two sets of following equations [3.11, 3.12], with the solutions to which are the cross-covariance $C_{hh}(x,t;\chi,\tau)$, $C_{hv}(x,t;\chi,\tau)$ and

$C_{vv}(x,t;\chi,\tau)$. Noting that the covariance terms are denoted as C_{hh}, C_{vv} and C_{hv} for simplification and readability in the covariance functions.

(1) Covariance equations for C_{hh} and C_{hv}:

$$
\begin{cases}
C_{bh}\dfrac{\partial h^{(0)}}{\partial t}+\langle B\rangle\dfrac{\partial C_{hh}}{\partial t}+\langle B\rangle\dfrac{\partial C_{hh}v^{(0)}}{\partial x}+\langle B\rangle\dfrac{\partial h^{(0)}C_{vh}}{\partial x}+C_{bh}\dfrac{\partial h^{(0)}v^{(0)}}{\partial x}+h^{(0)}v^{(0)}\dfrac{\partial C_{bh}}{\partial x} \\
+C_{hh}v^{(0)}\dfrac{\partial\langle B\rangle}{\partial x}+h^{(0)}C_{vh}\dfrac{\partial\langle B\rangle}{\partial x}-C_{qh}=0 \\
C_{bh}\dfrac{\partial h^{(0)}v^{(0)}}{\partial t}+\langle B\rangle\dfrac{\partial C_{hh}v^{(0)}}{\partial t}+\langle B\rangle\dfrac{\partial h^{(0)}C_{vh}}{\partial t}++2\beta C_{bh}h^{(0)}v^{(0)}\dfrac{\partial v^{(0)}}{\partial x}+2\beta\langle B\rangle C_{hh}v^{(0)}\dfrac{\partial v^{(0)}}{\partial x} \\
+2\beta\langle B\rangle h^{(0)}C_{vh}\dfrac{\partial v^{(0)}}{\partial x}+2\beta\langle B\rangle h^{(0)}v^{(0)}\dfrac{\partial C_{vh}}{\partial x}+2\beta v^{(0)}C_{vh}\langle B\rangle\dfrac{\partial h^{(0)}}{\partial x}+\beta v^{(0)^2}C_{bh}\dfrac{\partial h^{(0)}}{\partial x} \\
+\beta v^{(0)^2}\langle B\rangle\dfrac{\partial C_{hh}}{\partial x}+2\beta v^{(0)}C_{vh}h^{(0)}\dfrac{\partial\langle B\rangle}{\partial x}+\beta v^{(0)^2}C_{hh}\dfrac{\partial\langle B\rangle}{\partial x}+\beta v^{(0)^2}h^{(0)}\dfrac{\partial C_{bh}}{\partial x} \\
+gC_{bh}h^{(0)}\dfrac{\partial h^{(0)}}{\partial x}+g\langle B\rangle C_{hh}\dfrac{\partial h^{(0)}}{\partial x}+g\langle B\rangle h^{(0)}\dfrac{\partial C_{hh}}{\partial x}+2g\langle n\rangle C_{nh}v^{(0)^2}\langle B\rangle\left(h^{(0)}\right)^{-\frac{1}{3}} \\
+2g\langle n\rangle^2 v^{(0)}C_{vh}\langle B\rangle\left(h^{(0)}\right)^{-\frac{1}{3}}+g\langle n\rangle^2 v^{(0)^2}C_{bh}\left(h^{(0)}\right)^{-\frac{1}{3}}+g\langle n\rangle^2 v^{(0)^2}\langle B\rangle\left(h^{(0)}\right)^{-\frac{1}{3}}\left(-\dfrac{1}{3}\dfrac{C_{hh}}{h^{(0)}}\right) \\
-gC_{sh}\langle B\rangle h^{(0)}-g\langle S_0\rangle C_{bh}h^{(0)}-g\langle S_0\rangle\langle B\rangle C_{hh}-\langle q\rangle C_{uh}-C_{qh}\langle u\rangle=0 \\
C_{hh}(x,0)=C_{hIh}(x) \\
C_{vh}(x,0)=C_{vIh}(x) \\
C_{hh}(0,t)v^{(0)}(0,t)+h^{(0)}(0,t)C_{vh}(0,t)=C_{quh}(t) \\
C_{hh}(L_e,t)=C_{heh}(t)
\end{cases}
\qquad [3.11]
$$

(2) Covariance equations for C_{vh} and C_{vv}:

$$
\begin{cases}
C_{bv}\dfrac{\partial h^{(0)}}{\partial t}+\langle B\rangle\dfrac{\partial C_{hv}}{\partial t}+\langle B\rangle\dfrac{\partial C_{hv}v^{(0)}}{\partial x}+\langle B\rangle\dfrac{\partial h^{(0)}C_{vv}}{\partial x}+C_{bv}\dfrac{\partial h^{(0)}v^{(0)}}{\partial x}+h^{(0)}v^{(0)}\dfrac{\partial C_{bv}}{\partial x} \\
+C_{hv}v^{(0)}\dfrac{\partial\langle B\rangle}{\partial x}+h^{(0)}C_{vv}\dfrac{\partial\langle B\rangle}{\partial x}-C_{qv}=0 \\
C_{bv}\dfrac{\partial h^{(0)}v^{(0)}}{\partial t}+\langle B\rangle\dfrac{\partial C_{hv}v^{(0)}}{\partial t}+\langle B\rangle\dfrac{\partial h^{(0)}C_{vv}}{\partial t}++2\beta C_{bv}h^{(0)}v^{(0)}\dfrac{\partial v^{(0)}}{\partial x}+2\beta\langle B\rangle C_{hv}v^{(0)}\dfrac{\partial v^{(0)}}{\partial x} \\
+2\beta\langle B\rangle h^{(0)}C_{vv}\dfrac{\partial v^{(0)}}{\partial x}+2\beta\langle B\rangle h^{(0)}v^{(0)}\dfrac{\partial C_{vv}}{\partial x}+2\beta v^{(0)}C_{vv}\langle B\rangle\dfrac{\partial h^{(0)}}{\partial x}+\beta v^{(0)^2}C_{bv}\dfrac{\partial h^{(0)}}{\partial x} \\
+\beta v^{(0)^2}\langle B\rangle\dfrac{\partial C_{hv}}{\partial x}+2\beta v^{(0)}C_{vv}h^{(0)}\dfrac{\partial\langle B\rangle}{\partial x}+\beta v^{(0)^2}C_{hv}\dfrac{\partial\langle B\rangle}{\partial x}+\beta v^{(0)^2}h^{(0)}\dfrac{\partial C_{bv}}{\partial x} \\
+gC_{bv}h^{(0)}\dfrac{\partial h^{(0)}}{\partial x}+g\langle B\rangle C_{hv}\dfrac{\partial h^{(0)}}{\partial x}+g\langle B\rangle h^{(0)}\dfrac{\partial C_{hv}}{\partial x}+2g\langle n\rangle C_{nv}v^{(0)^2}\langle B\rangle\left(h^{(0)}\right)^{-\frac{1}{3}} \\
+2g\langle n\rangle^2 v^{(0)}C_{vv}\langle B\rangle\left(h^{(0)}\right)^{-\frac{1}{3}}+g\langle n\rangle^2 v^{(0)^2}C_{bv}\left(h^{(0)}\right)^{-\frac{1}{3}}+g\langle n\rangle^2 v^{(0)^2}\langle B\rangle\left(h^{(0)}\right)^{-\frac{1}{3}}\left(-\dfrac{1}{3}\dfrac{C_{hv}}{h^{(0)}}\right) \\
-gC_{sv}\langle B\rangle h^{(0)}-g\langle S_0\rangle C_{bv}h^{(0)}-g\langle S_0\rangle\langle B\rangle C_{hv}-\langle q\rangle C_{uv}-C_{qv}\langle u\rangle=0 \\
C_{hv}(x,0)=C_{hIv}(x) \\
C_{vv}(x,0)=C_{vIv}(x) \\
C_{hv}(0,t)v^{(0)}(0,t)+h^{(0)}(0,t)C_{vv}(0,t)=C_{quv}(t) \\
C_{hv}(L_e,t)=C_{hev}(t)
\end{cases}
$$

[3.12]

However, to solve these two sets of equations, a series of model input parameters with unknown covariance expressions, including $C_{bh}, C_{qh}. C_{uh}, C_{hih}, C_{vih}, C_{quh}, C_{nh}$ and $C_{bv}, C_{qv}. C_{uv}, C_{hiv}, C_{viv}, C_{quv}, C_{nv}$, are necessary. For this purpose, the similar mathematical operations are imposed to the perturbation equation in terms of each input parameters. That is, multiplying the first-order equation with the perturbations of all these required random input parameters (namely $B, q, u, h_i, v_i, q_u,$ and n) respectively and taking expectations, yields the following equations for expressing the covariance of the uncertain input parameters.

(3) Covariance equations for C_{bh} and C_{bv}:

$$
\begin{cases}
C_{bb}\dfrac{\partial h^{(0)}}{\partial t}+\langle B\rangle\dfrac{\partial C_{hb}}{\partial t}+\langle B\rangle\dfrac{\partial C_{hb}v^{(0)}}{\partial x}+\langle B\rangle\dfrac{\partial h^{(0)}C_{vb}}{\partial x}+C_{bb}\dfrac{\partial h^{(0)}v^{(0)}}{\partial x}+h^{(0)}v^{(0)}\dfrac{\partial C_{bb}}{\partial x} \\
+C_{hb}v^{(0)}\dfrac{\partial\langle B\rangle}{\partial x}+h^{(0)}C_{vb}\dfrac{\partial\langle B\rangle}{\partial x}-C_{qb}=0 \\
C_{bb}\dfrac{\partial h^{(0)}v^{(0)}}{\partial t}+\langle B\rangle\dfrac{\partial C_{hb}v^{(0)}}{\partial t}+\langle B\rangle\dfrac{\partial h^{(0)}C_{vb}}{\partial t}++2\beta C_{bb}h^{(0)}v^{(0)}\dfrac{\partial v^{(0)}}{\partial x}+2\beta\langle B\rangle C_{hb}v^{(0)}\dfrac{\partial v^{(0)}}{\partial x} \\
+2\beta\langle B\rangle h^{(0)}C_{vb}\dfrac{\partial v^{(0)}}{\partial x}+2\beta\langle B\rangle h^{(0)}v^{(0)}\dfrac{\partial C_{vb}}{\partial x}+2\beta v^{(0)}C_{vb}\langle B\rangle\dfrac{\partial h^{(0)}}{\partial x}+\beta v^{(0)^2}C_{bb}\dfrac{\partial h^{(0)}}{\partial x} \\
+\beta v^{(0)^2}\langle B\rangle\dfrac{\partial C_{hb}}{\partial x}+2\beta v^{(0)}C_{vb}h^{(0)}\dfrac{\partial\langle B\rangle}{\partial x}+\beta v^{(0)^2}C_{hb}\dfrac{\partial\langle B\rangle}{\partial x}+\beta v^{(0)^2}h^{(0)}\dfrac{\partial C_{bb}}{\partial x} \\
+gC_{bb}h^{(0)}\dfrac{\partial h^{(0)}}{\partial x}+g\langle B\rangle C_{hb}\dfrac{\partial h^{(0)}}{\partial x}+g\langle B\rangle h^{(0)}\dfrac{\partial C_{hb}}{\partial x}+2g\langle n\rangle C_{nb}v^{(0)^2}\langle B\rangle\left(h^{(0)}\right)^{-\frac{1}{3}} \\
+2g\langle n\rangle^2 v^{(0)}C_{vb}\langle B\rangle\left(h^{(0)}\right)^{-\frac{1}{3}}+g\langle n\rangle^2 v^{(0)^2}C_{bb}\left(h^{(0)}\right)^{-\frac{1}{3}}+g\langle n\rangle^2 v^{(0)^2}\langle B\rangle\left(h^{(0)}\right)^{-\frac{1}{3}}\left(-\dfrac{1}{3}\dfrac{C_{hb}}{h^{(0)}}\right) \\
-gC_{sb}\langle B\rangle h^{(0)}-g\langle S_0\rangle C_{bb}h^{(0)}-g\langle S_0\rangle\langle B\rangle C_{hb}-\langle q\rangle C_{ub}-C_{qb}\langle u\rangle=0 \\
C_{hb}(x,0)=C_{hIb}(x) \\
C_{vb}(x,0)=C_{vIb}(x) \\
C_{hb}(0,t)v^{(0)}(0,t)+h^{(0)}(0,t)C_{vb}(0,t)=C_{qub}(t) \\
C_{hb}(L_e,t)=C_{heb}(t)
\end{cases}
\qquad [3.13]
$$

(4) Covariance equations for C_{qh} and C_{qv}:

$$
\begin{cases}
C_{bq}\dfrac{\partial h^{(0)}}{\partial t}+\langle B\rangle\dfrac{\partial C_{hq}}{\partial t}+\langle B\rangle\dfrac{\partial C_{hq}v^{(0)}}{\partial x}+\langle B\rangle\dfrac{\partial h^{(0)}C_{vq}}{\partial x}+C_{bq}\dfrac{\partial h^{(0)}v^{(0)}}{\partial x}+h^{(0)}v^{(0)}\dfrac{\partial C_{bq}}{\partial x} \\
+C_{hq}v^{(0)}\dfrac{\partial\langle B\rangle}{\partial x}+h^{(0)}C_{vq}\dfrac{\partial\langle B\rangle}{\partial x}-C_{qq}=0 \\
C_{bq}\dfrac{\partial h^{(0)}v^{(0)}}{\partial t}+\langle B\rangle\dfrac{\partial C_{hq}v^{(0)}}{\partial t}+\langle B\rangle\dfrac{\partial h^{(0)}C_{vq}}{\partial t}++2\beta C_{bq}h^{(0)}v^{(0)}\dfrac{\partial v^{(0)}}{\partial x}+2\beta\langle B\rangle C_{hq}v^{(0)}\dfrac{\partial v^{(0)}}{\partial x} \\
+2\beta\langle B\rangle h^{(0)}C_{vq}\dfrac{\partial v^{(0)}}{\partial x}+2\beta\langle B\rangle h^{(0)}v^{(0)}\dfrac{\partial C_{vq}}{\partial x}+2\beta v^{(0)}C_{vq}\langle B\rangle\dfrac{\partial h^{(0)}}{\partial x}+\beta v^{(0)^2}C_{bq}\dfrac{\partial h^{(0)}}{\partial x} \\
+\beta v^{(0)^2}\langle B\rangle\dfrac{\partial C_{hq}}{\partial x}+2\beta v^{(0)}C_{vq}h^{(0)}\dfrac{\partial\langle B\rangle}{\partial x}+\beta v^{(0)^2}C_{hq}\dfrac{\partial\langle B\rangle}{\partial x}+\beta v^{(0)^2}h^{(0)}\dfrac{\partial C_{bq}}{\partial x} \\
+gC_{bq}h^{(0)}\dfrac{\partial h^{(0)}}{\partial x}+g\langle B\rangle C_{hq}\dfrac{\partial h^{(0)}}{\partial x}+g\langle B\rangle h^{(0)}\dfrac{\partial C_{hq}}{\partial x}+2g\langle n\rangle C_{nq}v^{(0)^2}\langle B\rangle\left(h^{(0)}\right)^{-\frac{1}{3}} \\
+2g\langle n\rangle^2 v^{(0)}C_{vq}\langle B\rangle\left(h^{(0)}\right)^{-\frac{1}{3}}+g\langle n\rangle^2 v^{(0)^2}C_{bq}\left(h^{(0)}\right)^{-\frac{1}{3}}+g\langle n\rangle^2 v^{(0)^2}\langle B\rangle\left(h^{(0)}\right)^{-\frac{1}{3}}\left(-\dfrac{1}{3}\dfrac{C_{hq}}{h^{(0)}}\right) \\
-gC_{sq}\langle B\rangle h^{(0)}-g\langle S_0\rangle C_{bq}h^{(0)}-g\langle S_0\rangle\langle B\rangle C_{hq}-\langle q\rangle C_{uq}-C_{qq}\langle u\rangle=0 \\
C_{hq}(x,0)=C_{hIq}(x) \\
C_{vq}(x,0)=C_{vIq}(x) \\
C_{hq}(0,t)v^{(0)}(0,t)+h^{(0)}(0,t)C_{vq}(0,t)=C_{quq}(t) \\
C_{hq}(L_e,t)=C_{heq}(t)
\end{cases}
\qquad [3.14]
$$

(5) Covariance equations for C_{uh} and C_{uv}:

$$
\begin{cases}
C_{bu}\dfrac{\partial h^{(0)}}{\partial t}+\langle B\rangle\dfrac{\partial C_{hu}}{\partial t}+\langle B\rangle\dfrac{\partial C_{hu}v^{(0)}}{\partial x}+\langle B\rangle\dfrac{\partial h^{(0)}C_{vu}}{\partial x}+C_{bu}\dfrac{\partial h^{(0)}v^{(0)}}{\partial x}+h^{(0)}v^{(0)}\dfrac{\partial C_{bu}}{\partial x} \\
+C_{hu}v^{(0)}\dfrac{\partial\langle B\rangle}{\partial x}+h^{(0)}C_{vu}\dfrac{\partial\langle B\rangle}{\partial x}-C_{qu}=0 \\
C_{bu}\dfrac{\partial h^{(0)}v^{(0)}}{\partial t}+\langle B\rangle\dfrac{\partial C_{hu}v^{(0)}}{\partial t}+\langle B\rangle\dfrac{\partial h^{(0)}C_{vu}}{\partial t}++2\beta C_{bu}h^{(0)}v^{(0)}\dfrac{\partial v^{(0)}}{\partial x}+2\beta\langle B\rangle C_{hu}v^{(0)}\dfrac{\partial v^{(0)}}{\partial x} \\
+2\beta\langle B\rangle h^{(0)}C_{vu}\dfrac{\partial v^{(0)}}{\partial x}+2\beta\langle B\rangle h^{(0)}v^{(0)}\dfrac{\partial C_{vu}}{\partial x}+2\beta v^{(0)}C_{vu}\langle B\rangle\dfrac{\partial h^{(0)}}{\partial x}+\beta v^{(0)^2}C_{bu}\dfrac{\partial h^{(0)}}{\partial x} \\
+\beta v^{(0)^2}\langle B\rangle\dfrac{\partial C_{hu}}{\partial x}+2\beta v^{(0)}C_{vu}h^{(0)}\dfrac{\partial\langle B\rangle}{\partial x}+\beta v^{(0)^2}C_{hu}\dfrac{\partial\langle B\rangle}{\partial x}+\beta v^{(0)^2}h^{(0)}\dfrac{\partial C_{bu}}{\partial x} \\
+gC_{bu}h^{(0)}\dfrac{\partial h^{(0)}}{\partial x}+g\langle B\rangle C_{hu}\dfrac{\partial h^{(0)}}{\partial x}+g\langle B\rangle h^{(0)}\dfrac{\partial C_{hu}}{\partial x}+2g\langle n\rangle C_{nu}v^{(0)^2}\langle B\rangle\left(h^{(0)}\right)^{-\frac{1}{3}} \\
+2g\langle n\rangle^2 v^{(0)}C_{vu}\langle B\rangle\left(h^{(0)}\right)^{-\frac{1}{3}}+g\langle n\rangle^2 v^{(0)^2}C_{bu}\left(h^{(0)}\right)^{-\frac{1}{3}}+g\langle n\rangle^2 v^{(0)^2}\langle B\rangle\left(h^{(0)}\right)^{-\frac{1}{3}}\left(-\dfrac{1}{3}\dfrac{C_{hu}}{h^{(0)}}\right) \\
-gC_{su}\langle B\rangle h^{(0)}-g\langle S_0\rangle C_{bu}h^{(0)}-g\langle S_0\rangle\langle B\rangle C_{hu}-\langle q\rangle C_{uu}-C_{qu}\langle u\rangle=0 \\
C_{hu}(x,0)=C_{hIu}(x) \\
C_{vu}(x,0)=C_{vIu}(x) \\
C_{hu}(0,t)v^{(0)}(0,t)+h^{(0)}(0,t)C_{vu}(0,t)=C_{quu}(t) \\
C_{hu}(L_e,t)=C_{heu}(t)
\end{cases}
\qquad [3.15]
$$

(6) Covariance equations for C_{hIh} and C_{hIv}:

$$
\begin{cases}
C_{bhI}\dfrac{\partial h^{(0)}}{\partial t}+\langle B\rangle\dfrac{\partial C_{hhI}}{\partial t}+\langle B\rangle\dfrac{\partial C_{hhI}v^{(0)}}{\partial x}+\langle B\rangle\dfrac{\partial h^{(0)}C_{vhI}}{\partial x}+C_{bhI}\dfrac{\partial h^{(0)}v^{(0)}}{\partial x}+h^{(0)}v^{(0)}\dfrac{\partial C_{bhI}}{\partial x} \\
+C_{hhI}v^{(0)}\dfrac{\partial\langle B\rangle}{\partial x}+h^{(0)}C_{vhI}\dfrac{\partial\langle B\rangle}{\partial x}-C_{qhI}=0 \\
C_{bhI}\dfrac{\partial h^{(0)}v^{(0)}}{\partial t}+\langle B\rangle\dfrac{\partial C_{hhI}v^{(0)}}{\partial t}+\langle B\rangle\dfrac{\partial h^{(0)}C_{vhI}}{\partial t}++2\beta C_{bhI}h^{(0)}v^{(0)}\dfrac{\partial v^{(0)}}{\partial x}+2\beta\langle B\rangle C_{hhI}v^{(0)}\dfrac{\partial v^{(0)}}{\partial x} \\
+2\beta\langle B\rangle h^{(0)}C_{vhI}\dfrac{\partial v^{(0)}}{\partial x}+2\beta\langle B\rangle h^{(0)}v^{(0)}\dfrac{\partial C_{vhI}}{\partial x}+2\beta v^{(0)}C_{vhI}\langle B\rangle\dfrac{\partial h^{(0)}}{\partial x}+\beta v^{(0)^2}C_{bhI}\dfrac{\partial h^{(0)}}{\partial x} \\
+\beta v^{(0)^2}\langle B\rangle\dfrac{\partial C_{hhI}}{\partial x}+2\beta v^{(0)}C_{vhI}h^{(0)}\dfrac{\partial\langle B\rangle}{\partial x}+\beta v^{(0)^2}C_{hhI}\dfrac{\partial\langle B\rangle}{\partial x}+\beta v^{(0)^2}h^{(0)}\dfrac{\partial C_{bhI}}{\partial x} \\
+gC_{bhI}h^{(0)}\dfrac{\partial h^{(0)}}{\partial x}+g\langle B\rangle C_{hhI}\dfrac{\partial h^{(0)}}{\partial x}+g\langle B\rangle h^{(0)}\dfrac{\partial C_{hhI}}{\partial x}+2g\langle n\rangle C_{nhI}v^{(0)^2}\langle B\rangle\left(h^{(0)}\right)^{-\frac{1}{3}} \\
+2g\langle n\rangle^2 v^{(0)}C_{vhI}\langle B\rangle\left(h^{(0)}\right)^{-\frac{1}{3}}+g\langle n\rangle^2 v^{(0)^2}C_{bhI}\left(h^{(0)}\right)^{-\frac{1}{3}}+g\langle n\rangle^2 v^{(0)^2}\langle B\rangle\left(h^{(0)}\right)^{-\frac{1}{3}}\left(-\dfrac{1}{3}\dfrac{C_{hhI}}{h^{(0)}}\right) \\
-gC_{shI}\langle B\rangle h^{(0)}-g\langle S_0\rangle C_{bhI}h^{(0)}-g\langle S_0\rangle\langle B\rangle C_{hhI}-\langle q\rangle C_{uhI}-C_{qhI}\langle u\rangle=0 \\
C_{hhI}(x,0)=C_{hIhI}(x) \\
C_{vhI}(x,0)=C_{vIhI}(x) \\
C_{hhI}(0,t)v^{(0)}(0,t)+h^{(0)}(0,t)C_{vhI}(0,t)=C_{quhI}(t) \\
C_{hhI}(L_e,t)=C_{hehI}(t)
\end{cases}
\qquad [3.16]
$$

(7) Covariance equations for C_{vIh} and C_{vIv}:

$$
\begin{cases}
C_{bvI}\dfrac{\partial h^{(0)}}{\partial t}+\langle B\rangle\dfrac{\partial C_{hvI}}{\partial t}+\langle B\rangle\dfrac{\partial C_{hvI}v^{(0)}}{\partial x}+\langle B\rangle\dfrac{\partial h^{(0)}C_{vvI}}{\partial x}+C_{bvI}\dfrac{\partial h^{(0)}v^{(0)}}{\partial x}+h^{(0)}v^{(0)}\dfrac{\partial C_{bvI}}{\partial x} \\
+C_{hvI}v^{(0)}\dfrac{\partial\langle B\rangle}{\partial x}+h^{(0)}C_{vvI}\dfrac{\partial\langle B\rangle}{\partial x}-C_{qvI}=0 \\
C_{bvI}\dfrac{\partial h^{(0)}v^{(0)}}{\partial t}+\langle B\rangle\dfrac{\partial C_{hvI}v^{(0)}}{\partial t}+\langle B\rangle\dfrac{\partial h^{(0)}C_{vvI}}{\partial t}++2\beta C_{bvI}h^{(0)}v^{(0)}\dfrac{\partial v^{(0)}}{\partial x}+2\beta\langle B\rangle C_{hvI}v^{(0)}\dfrac{\partial v^{(0)}}{\partial x} \\
+2\beta\langle B\rangle h^{(0)}C_{vvI}\dfrac{\partial v^{(0)}}{\partial x}+2\beta\langle B\rangle h^{(0)}v^{(0)}\dfrac{\partial C_{vvI}}{\partial x}+2\beta v^{(0)}C_{vvI}\langle B\rangle\dfrac{\partial h^{(0)}}{\partial x}+\beta v^{(0)^2}C_{bvI}\dfrac{\partial h^{(0)}}{\partial x} \\
+\beta v^{(0)^2}\langle B\rangle\dfrac{\partial C_{hvI}}{\partial x}+2\beta v^{(0)}C_{vvI}h^{(0)}\dfrac{\partial\langle B\rangle}{\partial x}+\beta v^{(0)^2}C_{hvI}\dfrac{\partial\langle B\rangle}{\partial x}+\beta v^{(0)^2}h^{(0)}\dfrac{\partial C_{bvI}}{\partial x} \\
+gC_{bvI}h^{(0)}\dfrac{\partial h^{(0)}}{\partial x}+g\langle B\rangle C_{hvI}\dfrac{\partial h^{(0)}}{\partial x}+g\langle B\rangle h^{(0)}\dfrac{\partial C_{hvI}}{\partial x}+2g\langle n\rangle C_{nvI}v^{(0)^2}\langle B\rangle\left(h^{(0)}\right)^{-\frac{1}{3}} \\
+2g\langle n\rangle^2 v^{(0)}C_{vvI}\langle B\rangle\left(h^{(0)}\right)^{-\frac{1}{3}}+g\langle n\rangle^2 v^{(0)^2}C_{bvI}\left(h^{(0)}\right)^{-\frac{1}{3}}+g\langle n\rangle^2 v^{(0)^2}\langle B\rangle\left(h^{(0)}\right)^{-\frac{1}{3}}\left(-\frac{1}{3}\frac{C_{hvI}}{h^{(0)}}\right) \\
-gC_{svI}\langle B\rangle h^{(0)}-g\langle S_0\rangle C_{bvI}h^{(0)}-g\langle S_0\rangle\langle B\rangle C_{hvI}-\langle q\rangle C_{uvI}-C_{qvI}\langle u\rangle=0 \\
C_{hvI}(x,0)=C_{hIvI}(x) \\
C_{vvI}(x,0)=C_{vIvI}(x) \\
C_{hvI}(0,t)v^{(0)}(0,t)+h^{(0)}(0,t)C_{vvI}(0,t)=C_{quvI}(t) \\
C_{hvI}(L_e,t)=C_{hevI}(t)
\end{cases}
\qquad [3.17]
$$

(8) Covariance equations for C_{quh} and C_{quv}:

$$
\begin{cases}
C_{bqu}\dfrac{\partial h^{(0)}}{\partial t}+\langle B\rangle\dfrac{\partial C_{hqu}}{\partial t}+\langle B\rangle\dfrac{\partial C_{hqu}v^{(0)}}{\partial x}+\langle B\rangle\dfrac{\partial h^{(0)}C_{vqu}}{\partial x}+C_{bqu}\dfrac{\partial h^{(0)}v^{(0)}}{\partial x}+h^{(0)}v^{(0)}\dfrac{\partial C_{bqu}}{\partial x} \\
+C_{hqu}v^{(0)}\dfrac{\partial\langle B\rangle}{\partial x}+h^{(0)}C_{vqu}\dfrac{\partial\langle B\rangle}{\partial x}-C_{qqu}=0 \\
C_{bqu}\dfrac{\partial h^{(0)}v^{(0)}}{\partial t}+\langle B\rangle\dfrac{\partial C_{hqu}v^{(0)}}{\partial t}+\langle B\rangle\dfrac{\partial h^{(0)}C_{vqu}}{\partial t}++2\beta C_{bqu}h^{(0)}v^{(0)}\dfrac{\partial v^{(0)}}{\partial x}+2\beta\langle B\rangle C_{hqu}v^{(0)}\dfrac{\partial v^{(0)}}{\partial x} \\
+2\beta\langle B\rangle h^{(0)}C_{vqu}\dfrac{\partial v^{(0)}}{\partial x}+2\beta\langle B\rangle h^{(0)}v^{(0)}\dfrac{\partial C_{vqu}}{\partial x}+2\beta v^{(0)}C_{vqu}\langle B\rangle\dfrac{\partial h^{(0)}}{\partial x}+\beta v^{(0)^2}C_{bqu}\dfrac{\partial h^{(0)}}{\partial x} \\
+\beta v^{(0)^2}\langle B\rangle\dfrac{\partial C_{hqu}}{\partial x}+2\beta v^{(0)}C_{vqu}h^{(0)}\dfrac{\partial\langle B\rangle}{\partial x}+\beta v^{(0)^2}C_{hqu}\dfrac{\partial\langle B\rangle}{\partial x}+\beta v^{(0)^2}h^{(0)}\dfrac{\partial C_{bqu}}{\partial x} \\
+gC_{bqu}h^{(0)}\dfrac{\partial h^{(0)}}{\partial x}+g\langle B\rangle C_{hqu}\dfrac{\partial h^{(0)}}{\partial x}+g\langle B\rangle h^{(0)}\dfrac{\partial C_{hqu}}{\partial x}+2g\langle n\rangle C_{nqu}v^{(0)^2}\langle B\rangle\left(h^{(0)}\right)^{-\frac{1}{3}} \\
+2g\langle n\rangle^2 v^{(0)}C_{vqu}\langle B\rangle\left(h^{(0)}\right)^{-\frac{1}{3}}+g\langle n\rangle^2 v^{(0)^2}C_{bqu}\left(h^{(0)}\right)^{-\frac{1}{3}}+g\langle n\rangle^2 v^{(0)^2}\langle B\rangle\left(h^{(0)}\right)^{-\frac{1}{3}}\left(-\frac{1}{3}\frac{C_{hqu}}{h^{(0)}}\right) \\
-gC_{squ}\langle B\rangle h^{(0)}-g\langle S_0\rangle C_{bqu}h^{(0)}-g\langle S_0\rangle\langle B\rangle C_{hqu}-\langle q\rangle C_{uqu}-C_{qqu}\langle u\rangle=0 \\
C_{hqu}(x,0)=C_{hIqu}(x) \\
C_{vqu}(x,0)=C_{vIqu}(x) \\
C_{hqu}(0,t)v^{(0)}(0,t)+h^{(0)}(0,t)C_{vqu}(0,t)=C_{ququ}(t) \\
C_{hqu}(L_e,t)=C_{hequ}(t)
\end{cases}
\qquad [3.18]
$$

(9) Covariance equations for C_{nh} and C_{nv}:

$$
\begin{cases}
C_{bn}\dfrac{\partial h^{(0)}}{\partial t}+\langle B\rangle\dfrac{\partial C_{hn}}{\partial t}+\langle B\rangle\dfrac{\partial C_{hn}v^{(0)}}{\partial x}+\langle B\rangle\dfrac{\partial h^{(0)}C_{vn}}{\partial x}+C_{bn}\dfrac{\partial h^{(0)}v^{(0)}}{\partial x}+h^{(0)}v^{(0)}\dfrac{\partial C_{bn}}{\partial x} \\
+C_{hn}v^{(0)}\dfrac{\partial\langle B\rangle}{\partial x}+h^{(0)}C_{vn}\dfrac{\partial\langle B\rangle}{\partial x}-C_{qn}=0 \\
C_{bn}\dfrac{\partial h^{(0)}v^{(0)}}{\partial t}+\langle B\rangle\dfrac{\partial C_{hn}v^{(0)}}{\partial t}+\langle B\rangle\dfrac{\partial h^{(0)}C_{vn}}{\partial t}++2\beta C_{bn}h^{(0)}v^{(0)}\dfrac{\partial v^{(0)}}{\partial x}+2\beta\langle B\rangle C_{hn}v^{(0)}\dfrac{\partial v^{(0)}}{\partial x} \\
+2\beta\langle B\rangle h^{(0)}C_{vn}\dfrac{\partial v^{(0)}}{\partial x}+2\beta\langle B\rangle h^{(0)}v^{(0)}\dfrac{\partial C_{vn}}{\partial x}+2\beta v^{(0)}C_{vn}\langle B\rangle\dfrac{\partial h^{(0)}}{\partial x}+\beta v^{(0)^2}C_{bn}\dfrac{\partial h^{(0)}}{\partial x} \\
+\beta v^{(0)^2}\langle B\rangle\dfrac{\partial C_{hn}}{\partial x}+2\beta v^{(0)}C_{vn}h^{(0)}\dfrac{\partial\langle B\rangle}{\partial x}+\beta v^{(0)^2}C_{hn}\dfrac{\partial\langle B\rangle}{\partial x}+\beta v^{(0)^2}h^{(0)}\dfrac{\partial C_{bn}}{\partial x} \\
+gC_{bn}h^{(0)}\dfrac{\partial h^{(0)}}{\partial x}+g\langle B\rangle C_{hn}\dfrac{\partial h^{(0)}}{\partial x}+g\langle B\rangle h^{(0)}\dfrac{\partial C_{hn}}{\partial x}+2g\langle n\rangle C_{nn}v^{(0)^2}\langle B\rangle\left(h^{(0)}\right)^{-\frac{1}{3}} \\
+2g\langle n\rangle^2 v^{(0)}C_{vn}\langle B\rangle\left(h^{(0)}\right)^{-\frac{1}{3}}+g\langle n\rangle^2 v^{(0)^2}C_{bn}\left(h^{(0)}\right)^{-\frac{1}{3}}+g\langle n\rangle^2 v^{(0)^2}\langle B\rangle\left(h^{(0)}\right)^{-\frac{1}{3}}\left(-\dfrac{1}{3}\dfrac{C_{hn}}{h^{(0)}}\right) \\
-gC_{sn}\langle B\rangle h^{(0)}-g\langle S_0\rangle C_{bn}h^{(0)}-g\langle S_0\rangle\langle B\rangle C_{hn}-\langle q\rangle C_{un}-C_{qn}\langle u\rangle=0 \\
C_{hn}(x,0)=C_{hIn}(x) \\
C_{vn}(x,0)=C_{vIn}(x) \\
C_{hn}(0,t)v^{(0)}(0,t)+h^{(0)}(0,t)C_{vn}(0,t)=C_{qun}(t) \\
C_{hn}(L_e,t)=C_{hen}(t)
\end{cases}
\qquad [3.19]
$$

(10) Covariance equations for C_{sh} and C_{sv}:

$$
\begin{cases}
C_{bs}\dfrac{\partial h^{(0)}}{\partial t}+\langle B\rangle\dfrac{\partial C_{hs}}{\partial t}+\langle B\rangle\dfrac{\partial C_{hs}v^{(0)}}{\partial x}+\langle B\rangle\dfrac{\partial h^{(0)}C_{vs}}{\partial x}+C_{bs}\dfrac{\partial h^{(0)}v^{(0)}}{\partial x}+h^{(0)}v^{(0)}\dfrac{\partial C_{bs}}{\partial x} \\
+C_{hs}v^{(0)}\dfrac{\partial\langle B\rangle}{\partial x}+h^{(0)}C_{vs}\dfrac{\partial\langle B\rangle}{\partial x}-C_{qs}=0 \\
C_{bs}\dfrac{\partial h^{(0)}v^{(0)}}{\partial t}+\langle B\rangle\dfrac{\partial C_{hs}v^{(0)}}{\partial t}+\langle B\rangle\dfrac{\partial h^{(0)}C_{vs}}{\partial t}++2\beta C_{bs}h^{(0)}v^{(0)}\dfrac{\partial v^{(0)}}{\partial x}+2\beta\langle B\rangle C_{hs}v^{(0)}\dfrac{\partial v^{(0)}}{\partial x} \\
+2\beta\langle B\rangle h^{(0)}C_{vs}\dfrac{\partial v^{(0)}}{\partial x}+2\beta\langle B\rangle h^{(0)}v^{(0)}\dfrac{\partial C_{vs}}{\partial x}+2\beta v^{(0)}C_{vs}\langle B\rangle\dfrac{\partial h^{(0)}}{\partial x}+\beta v^{(0)^2}C_{bs}\dfrac{\partial h^{(0)}}{\partial x} \\
+\beta v^{(0)^2}\langle B\rangle\dfrac{\partial C_{hs}}{\partial x}+2\beta v^{(0)}C_{vs}h^{(0)}\dfrac{\partial\langle B\rangle}{\partial x}+\beta v^{(0)^2}C_{hs}\dfrac{\partial\langle B\rangle}{\partial x}+\beta v^{(0)^2}h^{(0)}\dfrac{\partial C_{bs}}{\partial x} \\
+gC_{bs}h^{(0)}\dfrac{\partial h^{(0)}}{\partial x}+g\langle B\rangle C_{hs}\dfrac{\partial h^{(0)}}{\partial x}+g\langle B\rangle h^{(0)}\dfrac{\partial C_{hs}}{\partial x}+2g\langle n\rangle C_{ns}v^{(0)^2}\langle B\rangle\left(h^{(0)}\right)^{-\frac{1}{3}} \\
+2g\langle n\rangle^2 v^{(0)}C_{vs}\langle B\rangle\left(h^{(0)}\right)^{-\frac{1}{3}}+g\langle n\rangle^2 v^{(0)^2}C_{bs}\left(h^{(0)}\right)^{-\frac{1}{3}}+g\langle n\rangle^2 v^{(0)^2}\langle B\rangle\left(h^{(0)}\right)^{-\frac{1}{3}}\left(-\dfrac{1}{3}\dfrac{C_{hs}}{h^{(0)}}\right) \\
-gC_{ss}\langle B\rangle h^{(0)}-g\langle S_0\rangle C_{bs}h^{(0)}-g\langle S_0\rangle\langle B\rangle C_{hs}-\langle q\rangle C_{us}-C_{qs}\langle u\rangle=0 \\
C_{hs}(x,0)=C_{hIs}(x) \\
C_{vs}(x,0)=C_{vIs}(x) \\
C_{hs}(0,t)v^{(0)}(0,t)+h^{(0)}(0,t)C_{vs}(0,t)=C_{qus}(t) \\
C_{hs}(L_e,t)=C_{hes}(t)
\end{cases}
$$

[3.20]

Consequently, the solution of statistical moments (covariance or cross-covariance) to the first-order perturbation equation can be obtained by combining equations [3.11] to [3.20]. All the input parameters of equations [3.13-3.20] are zeroth-order based results that are deterministic and available in advance. With obtained $C_{bh}, C_{qh}. C_{uh}, C_{hih}, C_{vih}, C_{quh}, C_{nh}$ and $C_{bv}, C_{qv}. C_{uv}, C_{hiv}, C_{viv}, C_{quv}, C_{nv}$ from equations [3.13] through [3.20], equations [3.11] and [3.12] can be solved and the statistical moments of decision variables (water depth and flow velocity) , C_{hh}, C_{vv} and C_{hv} , are then obtained.

Stochastic flowrate

Based on the perturbation method illustrated above, the statistical moments of two decision variables (water depth h and flow velocity v) are obtained for the analysis of stochastic characteristics of unsteady open channel flows. In addition to the water depth and flow velocity, however, the flowrate is another quantity/variable that is of great interest in engineering field. In deterministic theory and definition, the variable flowrate (usually denoted as Q) is actually dependent on those two obtained variables – water depth h and flow velocity v. To obtain the stochastic result of this additional variable in this study, the following operations are performed on the basis of the two formerly obtained variables.

Since $Q(x,t) = h(x,t)v(x,t)$, the perturbation expansion for $Q(x,t)$ can be expressed as:

$$Q^{(0)} + Q^{(1)} + Q^{(2)} + \cdots = \left(h^{(0)} + h^{(1)} + h^{(2)} + \cdots\right)\left(v^{(0)} + v^{(1)} + v^{(2)} + \cdots\right)$$

Therefore, the following results can be obtained:

Zeroth-order: $Q^{(0)}(x,t) = h^{(0)}(x,t)v^{(0)}(x,t)$

First-order: $Q^{(1)}(x,t) = h^{(1)}(x,t)v^{(0)}(x,t) + h^{(0)}(x,t)v^{(1)}(x,t)$

Accordingly, the mean and covariance of the flowrate Q are:

$$\langle Q(x,t)\rangle = h^{(0)}(x,t)v^{(0)}(x,t)$$

$$\begin{aligned} C_{QQ}(x,t;\chi,\tau) = {} & h^{(0)}(x,t)h^{(0)}(\chi,\tau)C_{vv}(x,t;\chi,\tau) \\ & + h^{(0)}(x,t)v^{(0)}(\chi,\tau)C_{vh}(x,t;\chi,\tau) \\ & + h^{(0)}(\chi,\tau)v^{(0)}(x,t)C_{hv}(x,t;\chi,\tau) \\ & + v^{(0)}(x,t)v^{(0)}(\chi,\tau)C_{hh}(x,t;\chi,\tau) \end{aligned}$$

Based on the solved variables $h^{(0)}(x,t)$, $v^{(0)}(\chi,\tau)$, $C_{vv}(x,t;\chi,\tau)$, $C_{vh}(x,t;\chi,\tau)$, $C_{hv}(x,t;\chi,\tau)$, $C_{hh}(x,t;\chi,\tau)$ from the previous perturbation method, the mean and covariance of the variable flowrate can thus be obtained from these expressions.

To summarize, the procedure of the perturbation method to solve the 1D unsteady open channel flows is shown in the flowchart of Figure 3.1. The details on the numerical scheme and method for each solution step in this procedure are presented in the next section.

3.3 Numerical Scheme and Method

Both the obtained zeroth-order and first-order moment equations are partial differential equations (PDEs), and thus it is usually difficult to obtain the analytical solutions, especially under complex system and flow conditions. Therefore, numerical methods such as finite difference or finite volume are usually employed to solve these equations. It is also noted that all the moment equations from [3.11] to [3.20] are linear PDEs, which are easily solved by using many well-established numerical schemes. In this study, the Preissmann four-point implicit difference scheme, which is widely used scheme in open channel flow modeling, is adopted in this study (Fread 1974b). As shown in Figure 3.2, the whole system/solution range/domain is discretized into small domains with grids, with axes of x and t for spatial and temporal coordinates, respectively. As a result, each partial differential term could be approximated by

$$\begin{cases} \dfrac{\partial f}{\partial t} = \dfrac{\left(f_i^{j+1} + f_{i+1}^{j+1}\right) - \left(f_i^{j} + f_{i+1}^{j}\right)}{2\Delta t} \\ \dfrac{\partial f}{\partial x} = \dfrac{\theta\left(f_{i+1}^{j+1} - f_i^{j+1}\right)}{\Delta x} + \dfrac{(1-\theta)\left(f_{i+1}^{j} - f_i^{j}\right)}{\Delta x} \\ f = \dfrac{1}{2}\theta\left(f_{i+1}^{j+1} + f_i^{j+1}\right) + \dfrac{1}{2}(1-\theta)\left(f_{i+1}^{j} + f_i^{j}\right) \end{cases} \quad [3.21]$$

where θ is a weighting coefficient, f represents the variables involved in the equations, and f_i^j refers to the value of variable at the time-space grid point (i, j).

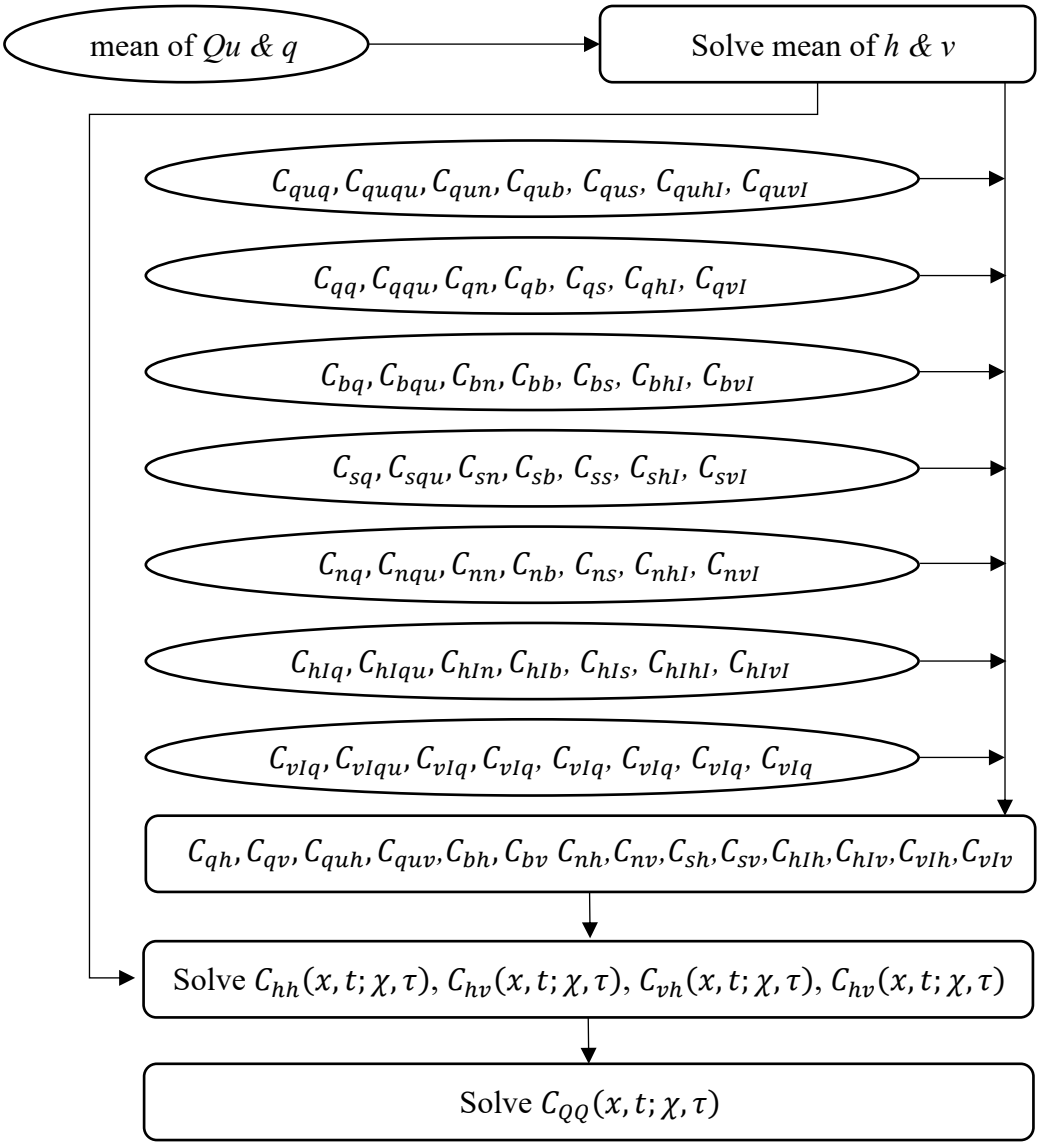

Figure 3.1 Flow chart of the model solution process

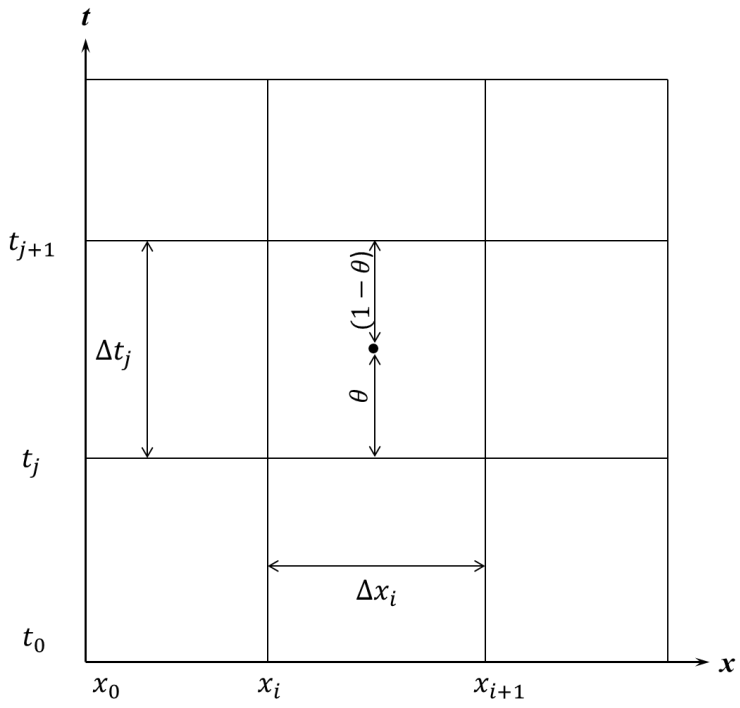

Figure 3.2 Discretization grids for computation

Based on the Preissmann four-point implicit difference scheme, this difference form is unconditionally stable if $0.5 \leq \theta \leq 1$ and the accuracy order decreases from second to first as the value of θ grows from 0.5 to 1. In this study, the value of $\theta = 0.55$ is taken to minimize the loss of accuracy order with the growing value of θ, and at the same time to avoid the possibility of pseudo-instability (Fread 1974a).

With this numerical scheme, all the partial differential equations [3.11-3.20] are thus discretized. For n grids of the whole channel domain, $2n$ equations and 2 boundary equations are obtained, and therefore, the solution of $(2n + 2)$ unknowns become possible. It is noted again that these moment equations are linear PDEs, and thus the following linear matrix equation can be obtained:

$$JX_{j+1} = B$$

where J stands for the Jacobian matrix and X_{j+1} represents the $(2n + 2)$ unknowns at timestep $j + 1$. Since J and B are both formed by knowns for the current computation step, the Gaussian elimination is then applied here to provide an efficient solution process with fast convergence speed (Hougardy and Vygen 2016).

This numerical scheme and procedure are successfully implemented in the MatLab based program (named "Stopch"), which allows a flexible input and output definitions, and thus may provide an integrated platform for simulating and analyzing the stochastic process of unsteady open channel flows.

3.4 Base Flow Computation

As mentioned in section 3.2, the software package of Storm Water Management Model (SWMM) is employed in this study to compute the base flow condition because of its wide recognitions with regard to accuracy and efficiency in this field. Moreover, this software is freely available and open source based tool, which can be easily integrated into the developed stochastic framework in this study (the MatLab platform "Stopch").

In this research, the whole designed channel system under computation is a rectangular shaped channel with the width of $20m$ and length of $60km$. The average/mean channel bottom (bed) slope is set as $0.5m$ decrease in elevation per kilometer (i.e., 0.5‰). For numerical simulation, the channel is divided into 100 sections (i.e., $n = 101$). An inflow time series profile is given at the upstream boundary, a water level control with negligible wave reflection is set at the end of the channel. In the study of lateral flows, the inflow is given at the first 10 nodes from nodes 2 to 11 as shown in Figure 3.3(a) (or the second 10 nodes from nodes 12 to 21

in Figure 3.3(b)). Once the base flow conditions are obtained from the SWMM tool, the results are then sent to the stochastic analysis framework (Figure 3.1) as input/known conditions.

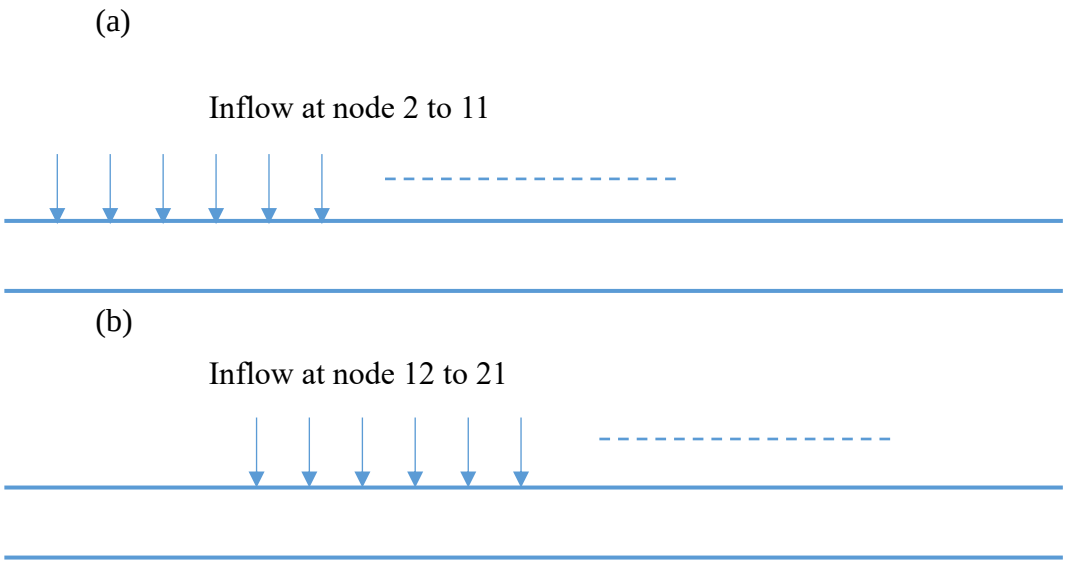

Figure 3.3 (a) inflow at upstream nodes; (b) inflow at middle channel nodes

Despite that these specific channel system conditions and settings are adopted throughout this thesis research, the obtained results for stochastic analysis are basically converted into appropriate forms of normalization, so as to provide general views/findings and conclusions to this research field.

3.5 Primary Verification for the Model

This model and solution methods are employed to compute a simple case, with the results compared with the solutions obtained in a previous research which were presented by both numerical and the analytical approach (Chen et al. 2017).

The following initial and system conditions are taken to conduct this computation: (1) cross-covariance functions C_{uqu}, C_{qqu} are zero; (2) the mean velocity and water depth in the channel are steady and uniform; (3) the channel is semi-infinite so that the downstream boundary effect is negligible.

Therefore, the hypothetical channel in this case is set to be semi-infinite with a constant bed slope S_0 = 0.0005, channel width $B = 20m$, Manning coefficient is set to be n = 0.03, and the uniform steady mean flow is assumed as F_r = 0.25, Q = $20m^3/s$. The results are analyzed in terms of the dimensionless independent variables defined with the help of bottom slope, mean water depth and velocity as

$$L_0 = h^{(0)} / s; T_0 = L_0 / v^{(0)} \qquad [3.22]$$

The upstream boundary which is the stochastic process of the upstream inflow is generated by an exponential covariance function as

$$C_{ququ}(t;\tau) = \sigma_{qu}^2 \exp\left(-|t-\tau| / \lambda_{qu} T_0\right) \qquad [3.23]$$

where σ_{qu}^2 is the variance of inflow discharge, and t, τ are independent time positions, λ_{qu} is the correlation length of the exponential distribution which is set to be 0.27.

Under these conditions, the results of the uncertainty of unsteady open channel flows based on the developed method and procedure in this research are obtained and shown in Figure 3.1, in which the results from the literature (Dooge et al. 1983, Lu 2008) are also plotted in the figure for comparison. For illustration, only the temporal variation of the uncertainty covariance C_{quQ} at the location $x = 5L_0$ along the channel are extracted and shown here for the comparative analysis.

Figure 3.4 shows clearly the good agreement at early stage of the results by different methods (numerical in this study and both numerical & analytical results from literature), which confirms the validity and accuracy of the derived stochastic model and the developed computation methods in this research. The lower covariance value after the crest resulted mainly from the rather small grid density while at present stage this study cannot afford the computation effort for larger grid system. Afterwards, the developed model and methods are further applied to analyze more complicated variable influences on the stochastic process of the complex unsteady open channel flows in this research.

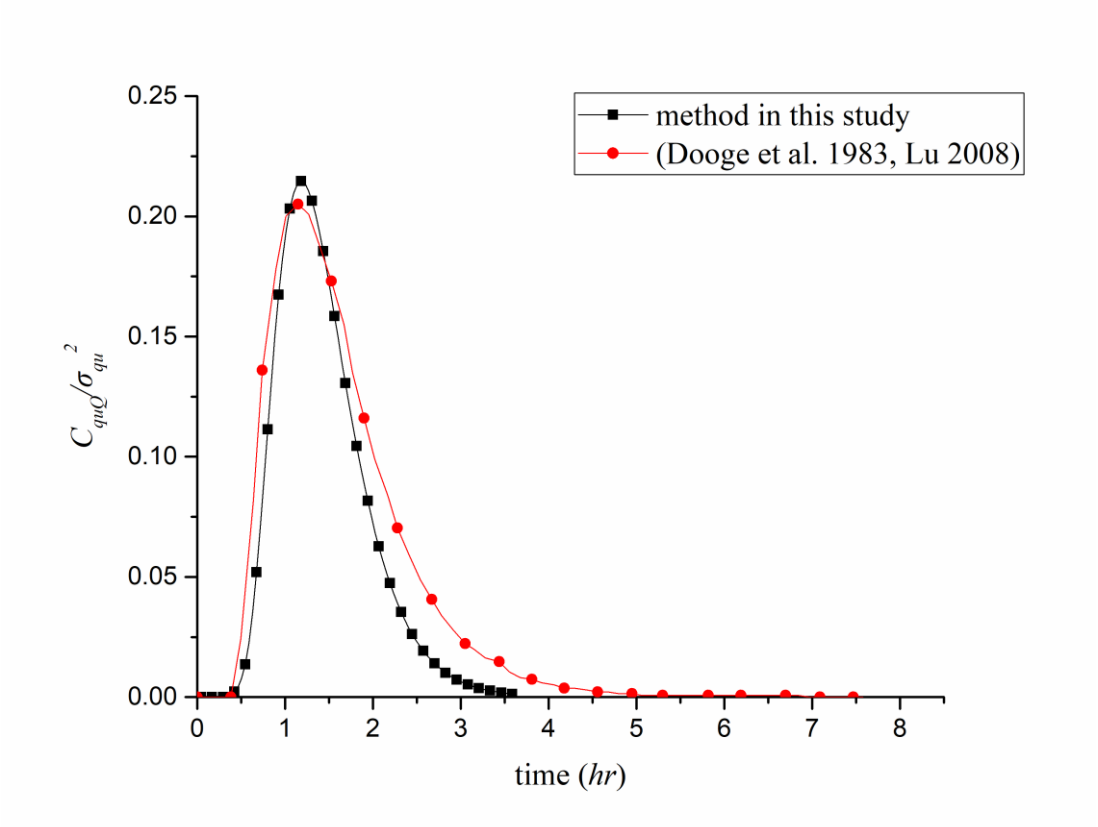

Figure 3.4 Comparison between results from this model and the literature

3.6 Summary

In this chapter, a 1D stochastic open channel flow model is developed based on the 1D St.Venant equations with the help of the perturbation method for solution to the first two statistical moments (mean and variance) of flow properties. The original St.Venant equations are simplified with several assumptions at first, and then equations of different orders are derived, in which zeroth-order equations governs the mean flow condition, and first-order equations represents the fluctuations of flow properties. Afterwards, the covariance equations are derived based on the first-order equations. The software EPA SWMM is employed to obtain the solutions to mean flow, and the covariance equations, which are linear partial differential equations, are discretized in Preissmann four-point scheme and solved by Gaussian Elimination Algorithm (also known as row reduction). The whole solution process is introduced then, and the detailed setup in EPA SWMM is also described.

This stochastic model and solution methods are then primarily verified by comparison of model computation results for a simple case and the results from the literature. It is found that the covariance data computed from this model and the literature match good in magnitude and tendency despite there is still little disparity possibly due to subtle differences in initial setup. In next chapter, this model will be applied in more complicated conditions and more variables are to be considered for a general understanding of the stochastic behavior in complex open channels.

CHAPTER 4 MODEL APPLICATIONS AND RESULTS DISCUSSION

4.1 Introduction

As presented in the former chapter, the 1D stochastic model has been developed and validated in this research for capturing the first two statistic moments of the unsteady flow process in complex open channels with different uncertainties, namely the mean and variance of water depth and flow velocity (or flowrate). In this chapter, this developed stochastic flow model is applied for the analysis of stochastic characteristics in unsteady open channel flows under different conditions, with aim to understand and analyze the influences of such different conditions/factors on the variability of unsteady flow responses in the open channel. In this research, the considered factors affecting the uncertainty propagation in the open channel flows include: channel top width B, bed slope S, channel roughness (Manning's roughness coefficient n), upstream boundary inflow Q_u, and lateral inflow q along the channel. In particular, the random features of these factors are considered to be both spatially and temporally correlated, so as to mimic the common situations in the realistic open channel flow process. As a result, this stochastic model may provide spatial-temporal solutions for the unsteady flow process including the mean water depth h and flow velocity v, and their standard deviations σ_h and σ_v for better analysis of uncertainty propagation of the system responses. Meanwhile, from these results, the probability distribution function of flow velocity v (and also flowrate) and water depth h could be effectively estimated with the assumption that these quantities are in Gaussian distribution.

4.2 Numerical Experiment

In this research, a hypothetical open channel system (as shown in Figure 4.1 below) is employed to conduct extensive numerical applications, in order to analyze the stochastic characteristics of unsteady open channel flows. In this numerical experimental system, the channel is assumed to be prismatic and rectangular, with deterministic parameters (i.e., mean values) as follows: total channel length L = 48km, channel width B = 20m, channel bed slope S = 0.0005, and the Manning's roughness coefficient n = 0.03. For simplicity and illustration purposes, the initial state of the flow in the channel is set to be a uniform steady flow with a flowrate Q = 20m^3/s, water depth h = 1.25m and average velocity v = 0.8m/s. Under this condition, the Froude number for the initial flow Fr = 0.23. For unsteady flow state, the inflow from upstream boundary (i.e., left hand side end of the channel in Figure 4.1) is given by a time-dependent variation function of flowrate in each application case, and a settled surface height h = 1.25m (downstream control has little effects on location far from channel end) (Napiorkowski and Dooge 1988) is given to the downstream discharge end of the channel (i.e., right hand side end of the channel in Figure 4.1). The total simulation duration for the unsteady flow process of this open channel system is about 10 hours (i.e., before the flooding wave reflection from the downstream end to avoid the analysis complexity). After the grid dependence tests for the deterministic flow condition, the temporal and spatial grid numbers are set to be 100 and 80, to obtain an effective trade-off the efficiency and accuracy for the computation.

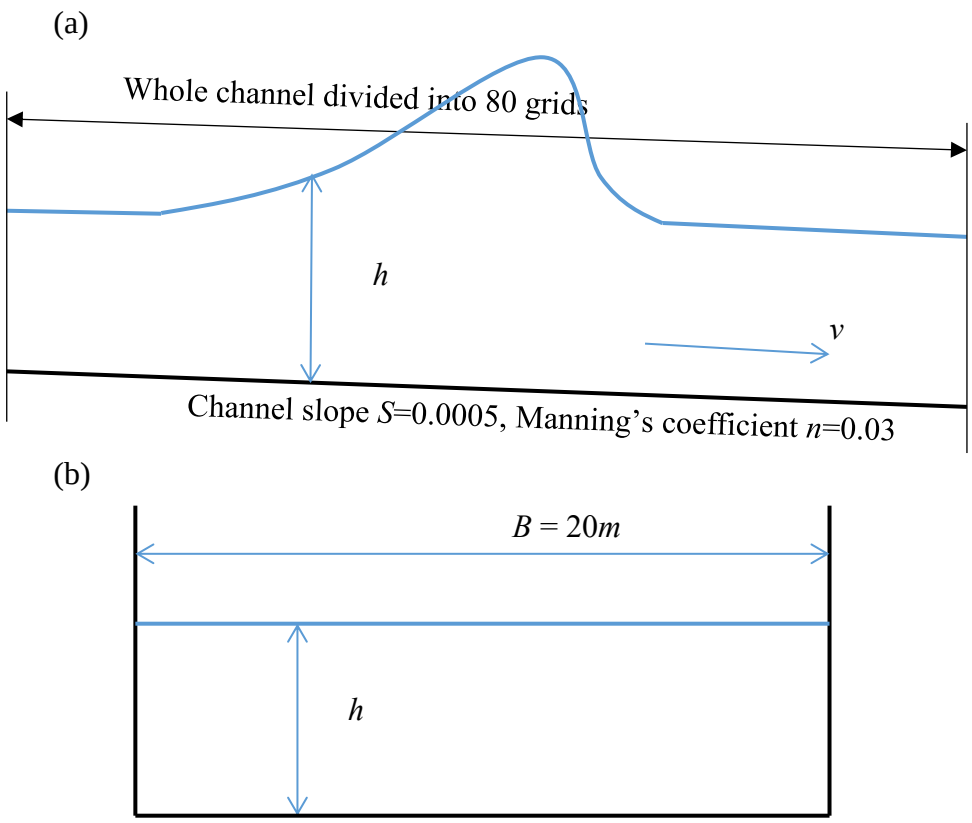

Figure 4.1 (a) schematic diagram for wave propagation in the hypothesis channel; (b) cross-section shape of the channel at $x = 1km$

With the consideration that parameters at closer location (time/space) usually have stronger relation, the random parameters for stochastic flow process in this study are assumed to be distributed in an exponential manner (convenient in changing magnitude and correlation strenth) with correlation in either space or time or both (though the real world scenario can be more complex), and for illustration in this research, these parameters are supposed to be second-order stationary in the application cases, with following expression:

$$C_{nn}(x;\chi) = \sigma_n^2 * \exp(-|x-\chi|/\lambda_n L_0) \qquad [4.1]$$

As a result, the covariance $C_{nn}(x;\chi)$ only depends on the distance or time lag between points ($|t-\tau|$ or $|x-\chi|$), where (t, x) and (τ, χ) are two sets of variables for different times and locations. Specifically, the standard deviation σ_n governs the

magnitude of uncertainty/randomness of each parameter and the coefficient λ_n shapes the level of variation in space (or time for other variables). All the parameters are considered in such similar way, and the detailed exponential distribution functions of these model input parameters are to be presented in each study case study later.

4.3 Stochastic Influence of Random Upstream Inflows

In this section, the influence of random upstream inflows on the stochastic response and uncertainty propagation of the open channel flows is firstly investigated, with followed by other factors in the next sections. It is noted that the other factors are assumed to be deterministic (i.e., without uncertainties) when one of these factors is examined for its stochastic influence. Meanwhile, it is good to start the inspection from the stationary inflow state (i.e., in the section 4.3.1 below) so as for comparative study of further complex conditions (non-stationary). Under this condition, the influences of different uncertainty features of the random upstream inflows (including the deviation σ_n and correlation length λ_n) are examined respectively in the subsequent sections (i.e., sections 4.3.2 and 4.3.3). Thereafter, the more general situation of non-stationary inflows is investigated in the section 4.3.4.

4.3.1 Stationary mean-uniform inflow

In this case, the upstream inflow is set to be stochastic with relevant mean and standard deviation process, but the mean flow is assumed to be time-independent (stationary) and the uncertainty feature can be time-dependent. For numerical tests,

the mean inflow discharge is fixed as q = 20m^3/s, and the covariance distribution function is given by:

$$C_{ququ}(t;\tau) = \sigma_{qu}^2 * \exp(-|t-\tau|/\lambda_{qu}T_0) \quad [4.2]$$

where σ_{qu} is the standard deviation of the upstream inflow discharge and λ_{qu} is the correlation length in time, t and τ are two independent moments considered in the specific case. It is indicated by this second-order stationary exponential distribution that the covariance of random inflows at two any time moments depends only on the distance between them rather than the exact time location. Herein, the standard deviation of upstream inflow is set to be σ_{qu} = 0.1Q_u, with the correlation length λ_n = 0.27, with aim to study the uncertainty propagation and stochastic response of the open channel flow. The influences of these two stochastic parameters are to be examined in detail later in the next sections.

Based on the developed stochastic model and numerical procedure in Chapter 3, the results are obtained and plotted in Figures 4.2(a) and 4.2(b) for the temporal and spatial variations of stochastic responses of the open channel flow. The system response of water depth is taken here for demonstration, and similar variation trends have also been obtained for other responses (velocity or flowrate).

Figure 4.2(a) shows the temporal profile of σ_h (standard deviation of water depth variation) at nodes 11 (6*km* to upstream) and 31 (18*km* to upstream) for example. These results show clearly that the uncertainty of the flow response from the upstream inflows arrives at each node after certain time period, with the propagation time actually determined by the wave speed of the zeroth-other equation (i.e., mean flow). Thereafter, the uncertainty of the water depth (σ_{qu}) starts to increase with time, and finally achieves a relatively constant and maximum value

(i.e., steady variation speed for the stochastic response of water depth). Furthermore, the comparative results of these two nodes imply that the increasing speed of uncertainty is slower with distance from upstream inflow location, e.g., the gradient of the increasing curve is smaller (flatter) at node 31 than that at node 11. Moreover, the achieved steady and maximum value of the uncertainty of system response is also decreasing with the flowing distance along the channel. For example, the achieved steady uncertainty is decreasing from about 0.028 at node 11 to about 0.022 at node 31, which reveals over 21% damping of the maximum uncertainty value. This is mainly due to the gravity (flooding) wave dispersion and dissipation during the propagation process along the open channel, which simultaneously results in the decrease of uncertainty level propagating from upstream to downstream in the channel.

The spatial uncertainty distribution results at different time moments shown in Figure 4.2(b) demonstrate clearly the uncertainty propagation of system response induced from the upstream inflows with time. Meanwhile, at the same location, e.g., at distance of 10 km for example, the uncertainty level is increasing with time after the arrival of the upstream inflow wave, which is actually consistent with the results of Figure 4.2(a). Moreover, after a relatively long period, e.g., before the distance of 3 km in Figure 4.2(b), the uncertainty level achieves a relatively steady state (i.e., maximum value), which again confirms the results and analysis in Figure 4.2(a). Consequently, the results in Figures 4.2 demonstrate the propagation and change (damping) of stochastic features of random upstream inflows in the open channel system.

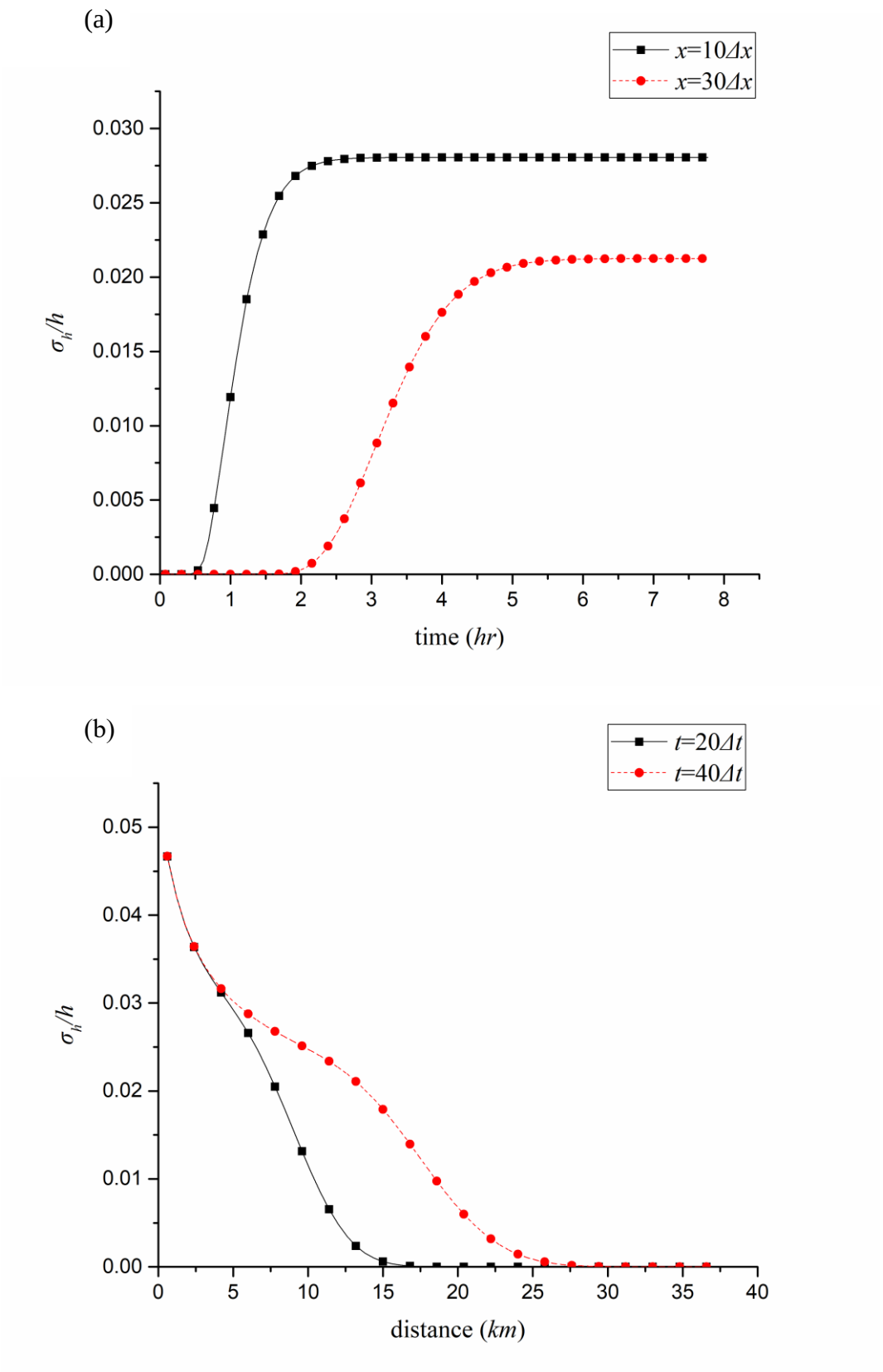

Figure 4.2 (a) Time variation of σ_h at node 11 and 31; (b) spatial profile of σ_h at time 20 and 40

4.3.2 Effect of standard deviation σ_{qu} of random upstream inflows

To study the effect of the stochastic features of random upstream inflows on the uncertainty propagation, the same channel flow system in Figure 4.1 is adopted and the flow conditions are assumed to be the same, but with different standard deviations of the random inflows. For illustration, the temporal and spatial variations of uncertainty propagation for different standard deviations of random inflows ($\sigma_{qu} = 0.1Q_u$ and $\sigma_{qu} = 0.2Q_u$) are shown in Figure 4.4. Specifically, Figure 4.3(a) shows the comparison of uncertainty propagation with time at the two nodes (11 and 31) for different standard deviations, and Figure 4.3(b) reveals that of uncertainty distribution at different time moments under different standard deviations. Both results indicate clearly the significant influence of the standard deviation of random upstream inflows on the uncertainty level and propagation. In particular, both the increasing speed and the achieved maximum steady uncertainty level are increasing with the standard deviation of the random inflows. A numerical estimation for the results comparison implies that the resulted uncertainty level and increasing speed are directly proportional to the initial uncertainty level (standard deviation) of the random upstream inflows. For example, for both the uncertainty level and changing speed in Figure 4.3, the results of the case $\sigma_{qu} = 0.2Q_u$ are almost as twice as those of the case $\sigma_{qu} = 0.1Q_u$. This is reasonable according to the derived analytical results of first-order equations in Chapter 3, which are exactly in linear forms from the perturbation analysis.

However, both results also indicate clearly that the standard deviation of random upstream inflows has little impact on the propagation speed of system response uncertainty in the open channel. That is, the arrival time moments of the resulted uncertainty of system responses are exactly same for different cases in

Figure 4.3. From the perspective, the uncertainty propagation speed is governed mainly by the zeroth-order flows (base/mean flows), while the uncertainty level and variation are dependent largely on the randomness level of the upstream inflows.

4.3.3 Effect of correlation length λ_{qu} of random upstream inflows

In addition to the influence of standard deviation of random inflows, the correlation length λ_{qu} in Eq. [4.1] is another important factor that may affect the stochastic characteristics of system responses. Under the other same conditions ($\sigma_{qu} = 0.1Q_u$), the results for different correlation lengths are obtained and shown in Figure 4.4, which presents the significant influence of this factor. Specifically, the uncertainty level and changing speed are increasing with the correlation length in time domain. This is mainly because the correlation length can affect average covariance of system responses based on Eq. [4.1]. In other words, a larger time-domain correlation length may lead to higher average covariance of Q_u, and result in larger uncertainty of system response. Meanwhile, a larger correlation length in time domain indicates a stronger correlation of the results at different time steps, which therefore provides a potential influence on the variation speed (increasing gradient of the results in Figure 4.4) of the uncertainty in the open channel flows. However, similar to the above stander deviation of random upstream inflows, the correlation length factor has little impact on the propagation speed of uncertainty in the open channel.

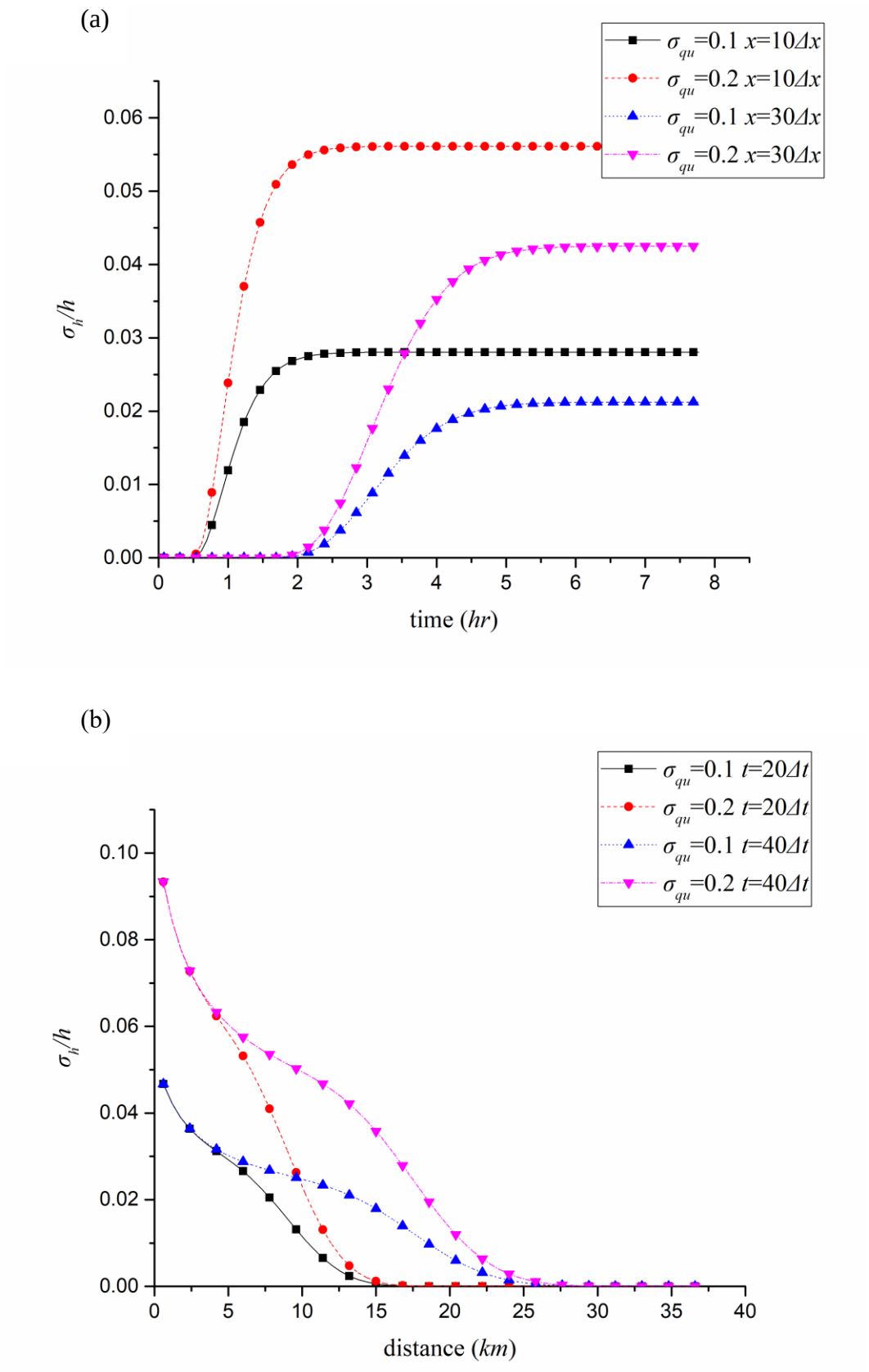

Figure 4.3 (a) Time variation of σ_h at node 11 and 31; (b) spatial profile of σ_h at time 20 and 40 under different σ_{qu}

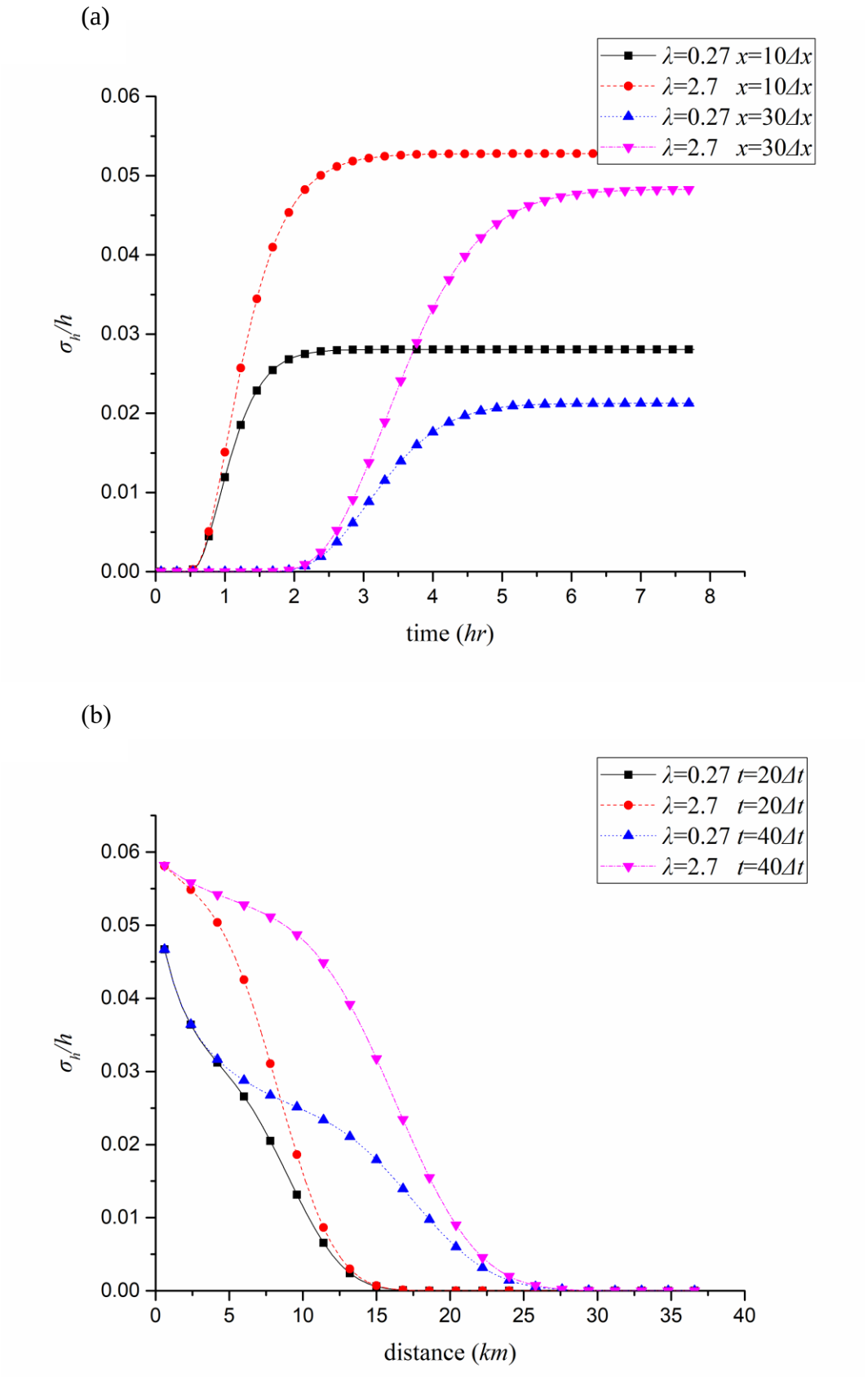

Figure 4.4 (a) Time variation of σ_h at node 11 and 31; (b) spatial profile of σ_h at time 20 and 40 under different λ_{qu}

4.3.4 Effect of non-uniform non-stationary boundary inflows

All the above results and analysis are based on simple situations of uniform base flows and stationary inflows with uncertainty. In this section, a base flow with non-uniform boundary inflow is considered for the investigation. For tests, the mean inflow discharge is set to be: (with unit m^3/s)

$$\begin{cases} Q_u(t) = 20 + 10(1 - \cos(2\pi t/T)) & t < T \\ 20 & t \geq T \end{cases} \quad [4.3]$$

and the covariance function is the same to section 4.3.2, which is defined by:

$$C_{ququ}(t;\tau) = \sigma_{qu}(t) * \sigma_{qu}(\tau) * \exp(-|t-\tau|/\lambda_{qu}T_0) \quad [4.4]$$

Firstly, the standard deviation of upstream inflows is set to be $\sigma_{qu}(t) = 0.1Q_u(t)$, and the correlation length is $\lambda_{qu} = 0.27$. Since the mean inflow discharge is no longer steady but a function of time, this exponential distribution function is therefore a non-stationary updating process in which different time and location results will affect the covariance rather than only the time interval between two locations.

Based on the results from the developed model and numerical method, Figure 4.5(a) presents the water depth variation in time at node points 11 and 31, and Figure 4.5(b) shows the water surface profile along the channel at time points 20 and 40. It is found that the flow in the channel is steady at the beginning, and as time goes, an unsteady wave propagates from upstream to downstream, giving fluctuation to the mean flow in the channel. After the wave passed, the flow in the channel returns to the steady-state that is same as the initial condition. It is also noticed that the wave crest attenuates and wave length grows as the wave propagates toward downstream in the force of gravity and pressure.

As for the standard deviation considered in this case, Figure 4.6 presents the time variation at node point 11 and 31, and the horizontal profile along the channel at time 20 and 40. It is again confirmed that the uncertainty propagation speed in the channel is only dependent on wave speed of mean flows since the first-order and zeroth-order equations have the same characteristic curves according to the previously derived results in Chapter 3. It is also noticed that the crest of standard deviation appears slightly later than the flood wave, which means at the same location, the peak of uncertainty occurs after the crest of flood wave, indicating that the uncertainty level still accumulates (increases) for a while after the flood wave passed. This is mainly because of the non-stationary characteristics of the base flow, which is different from the former stationary case. After that the non-stationary upstream discharge passed, the system finally returns to a steady state same as plotted in Figure 4.2, since the base flow conditions are identical again and the effects of non-stationary σ_{qu} become negligible.

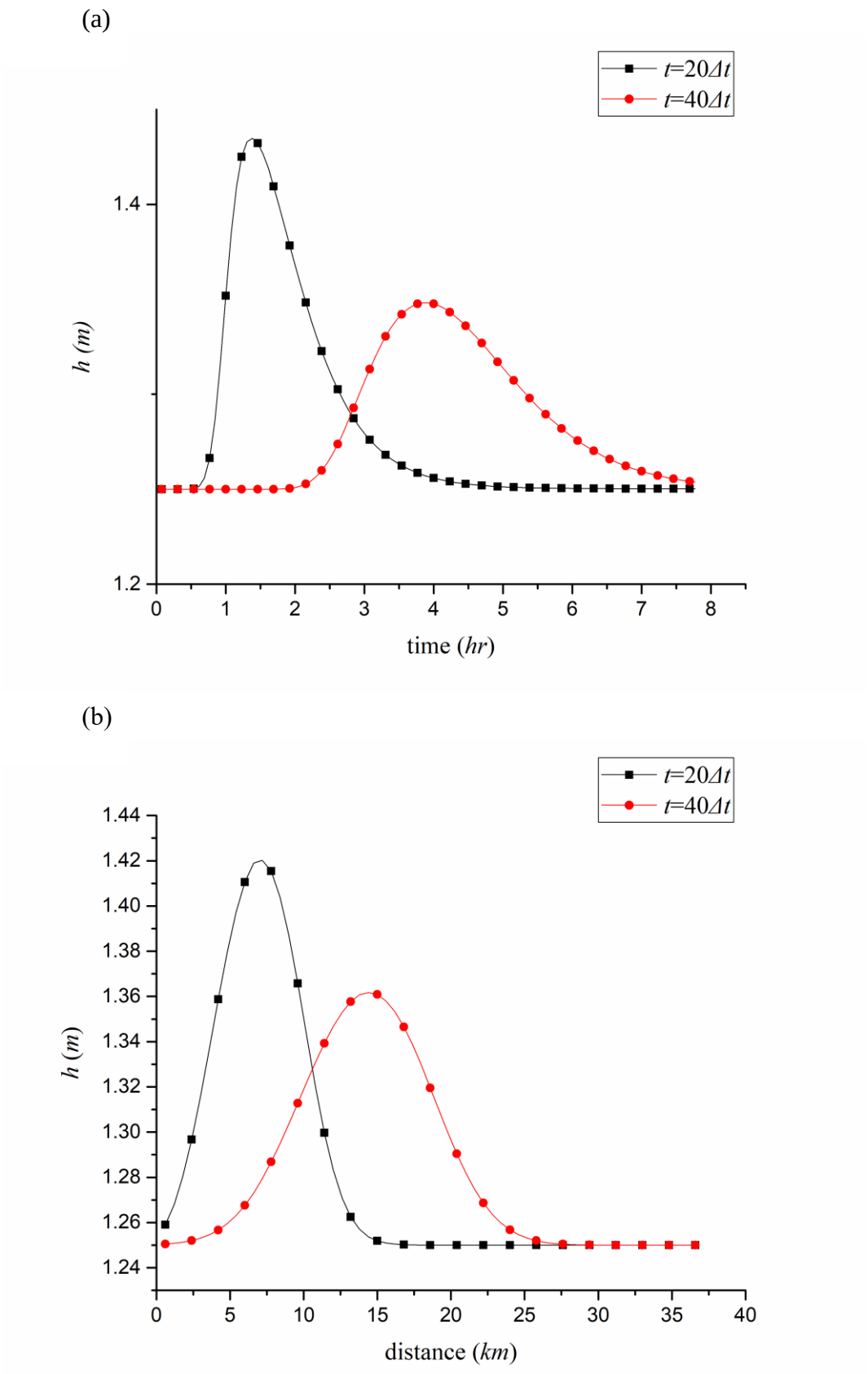

Figure 4.5 (a) Temporal variation of water depth at node 11 and 31; (b) spatial profile of water depth at time 20 and 40 under non-uniform boundary inflow

(a)

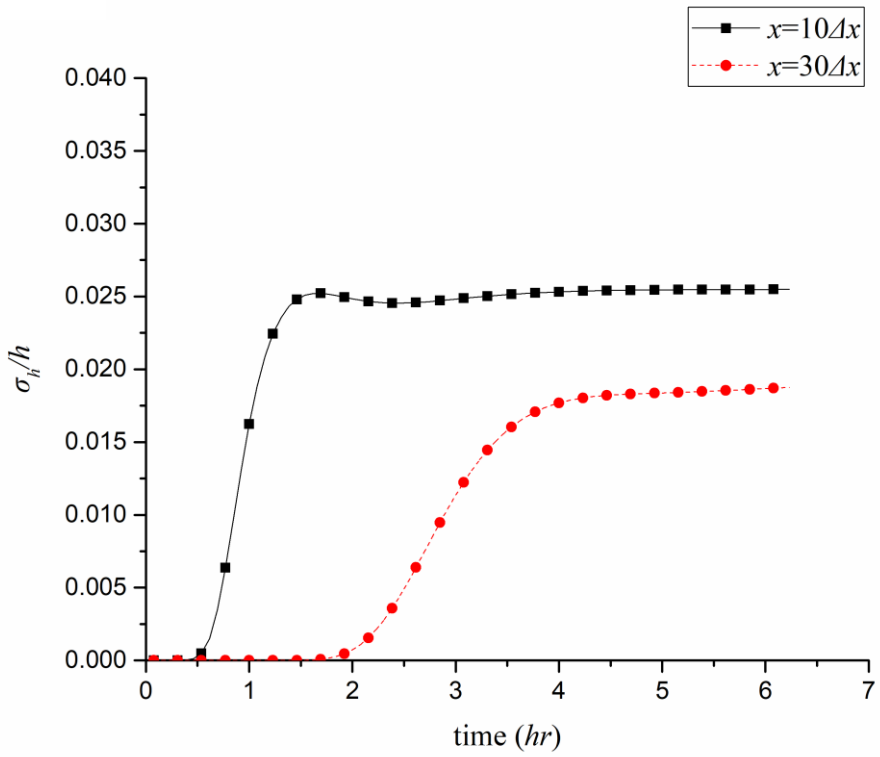

(b)

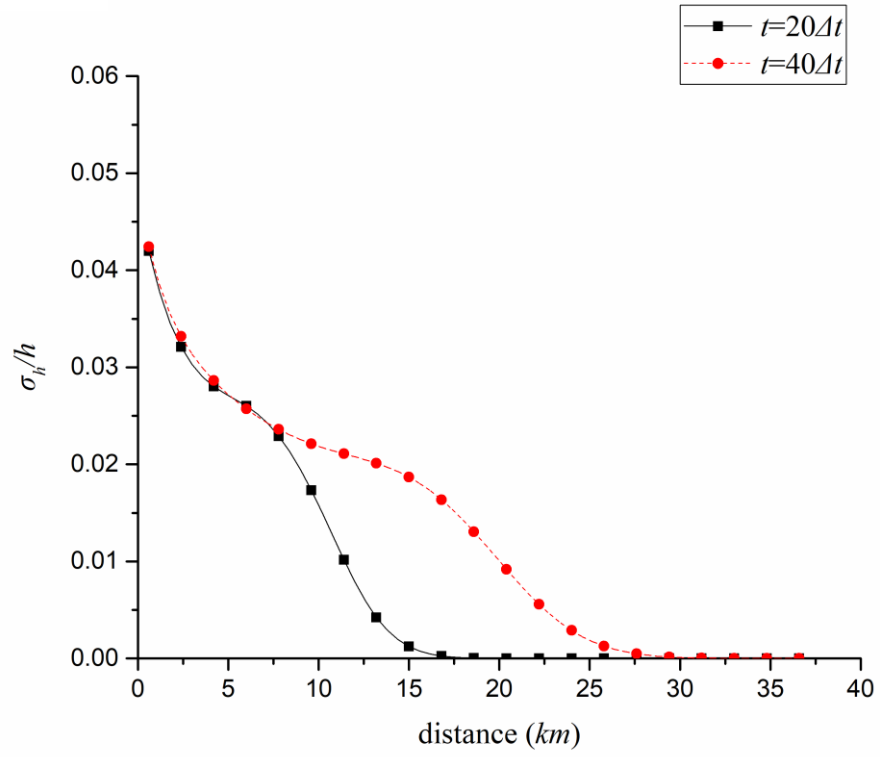

Figure 4.6 (a) Time variation of σ_h at node 11 and 31; (b) spatial profile of σ_h at time 20 and 40 under non-stationary boundary inflow

4.4 Stochastic Influence of Random Channel Width *B*

It is easily understood from the zero[th]-order equations that the channel width B has significant influence on flow properties in the channel. However, it is difficult to analyze directly the influence of channel width uncertainty on the flow stochastic behaviors from the governing equations because of its relatively complicated differential forms. In this section, the channel width is examined by the developed stochastic model for its influence on the flow uncertainty properties, under the non-uniform mean inflow conditions as conducted in section 4.3.4. Due to the prismatic rectangular assumption of channel cross-section shape, the channel width along the channel is supposed to vary in the same pattern (otherwise the governing equation will fail for the analysis). To this end, the stochastic distribution of channel width B is assumed as:

$$C_{BB}(x,\chi) = \sigma_B^2 \qquad [4.5]$$

Note that the values of $\sigma_B = 0.1\mu_B$ and $\sigma_B = 0.1\mu_B$ are taken in the numerical experiments for illustration in this thesis research work, where μ_B is the mean of channel width.

By applying the developed stochastic model and numerical scheme in Chapter 3, the simulation results under different uncertainty conditions (σ_h) of the channel width are plotted in Figure 4.7 for comparison. Firstly, it is found that the growth curves of different σ_h at same location (e.g., herein node 11 in Fig. 4.7(a) or node 31 in Fig. 4.7(b)) are almost on the top of each other during the beginning stage of the upstream flooding wave arrival. Thereafter, the σ_h values for stochastic channel width situations become gradually smaller than that for the deterministic width situation (i.e., $\sigma_B = 0$). As the whole upstream wave with uncertainty passed

through, however, these curves in the figures start to become close to each other again, which means the final σ_h values are kept the same for all cases with different uncertainties of channel width. This result indicates that the existence of channel width uncertainty can slow down the growth of flow uncertainties at the downstream but cannot decrease the total and final uncertainty magnitudes of the uncertainty propagation process. This can actually be explained through the covariance equations derived in Chapter 3. In Eq.[3.12], it can be found that C_{bb} (the covariance of channel width B) terms are mostly multiplied with spatial and temporal partial differential terms of $h^{(0)}$ and $v^{(0)}$ which results in the initially small difference of the different results in the figures (i.e., the separation of curves in the figures). Specifically, the flow properties vary relatively smoothly first on arrival of the flood wave, so that C_{bb} related terms are very small causing little difference of σ_h. However, as shown in the figure, when the flow responses vary rapidly, the partial differential terms with regard to space and time become more and more critical, and therefore the influence of C_{bb} becomes significant, leading to a clear decrease in the uncertainty growth.

Finally, as the mainstream flooding wave passed, the partial differential terms (gradient terms) get small again, and therefore the influence of channel width uncertainty on system responses becomes less significant again. In conclusion, channel width uncertainty may decrease the growth ratio of flow uncertainties because of its detention effect on the upstream waves (which is similar to a flow routing process of deterministic wave propagation process), resulting in a relatively longer period for uncertainty propagation process than deterministic channel condition. Moreover, such detention effect of channel width uncertainty increases with the uncertainty extent (σ_B).

4.5 Stochastic Influence of Random Manning's *n*

In this section, the impacts of Manning's coefficient (*n*) are considered to investigate how the uncertainty of the roughness along the channel affects the unsteady flow response in the channel. As stated in section 4.1, the exponential distribution function of Manning's n is defined by:

$$C_{nn}(x;\chi) = \sigma_n^2 * \exp(-|x-\chi|/\lambda_n T_0) \qquad [4.6]$$

in which x and χ are two specific location considered, σ_n is the standard deviation of Manning's n, and λ_n is the correlation length of this exponential distribution.

For numerical tests, a mean value of Manning's n = 0.03 (reference), together with two different standard deviations of σ_n = 1/3μ_n and σ_n = 1/6μ_n (reference)and two different correlation lengths of λ_n = 0.27 and λ_n = 2.7 are applied for investigation in this section. Though for side inflow of mountain rivers the value of Manning's n could be larger and also the uncertainty magnitude, the main channel roughness and slope are rather mild. With the prior concerning of main channel in this study, the roughness and slope are assumed to be small in present study. And the base flow condition is the same as stated in section 4.3.1.

The computation results are plotted in Figure 4.8. It can be seen that under the correlation length λ_n = 0.27, the impacts of different value of σ_n on flow uncertainty are hard to distinguish. The reason is that a weak correlation of roughness in space will have impacts in mainly a small interval of distance, leading to very minor influence on the flow uncertainty in the whole flow domain (with relatively long period). However, when the correlation length value of λ_n is increased from 0.27 to 2.7, which imposes a stronger correlation of roughness in space, the results indicate clearly that the influence of this factor on the flow uncertainty

becomes more significant. It is also observed that with higher correlation length λ_n, the covariance of Manning's *n* along the whole flow domain grows, and therefore the uncertainty level is weakened at first though it still has the same propagation speed.

Over time, the effect of this larger uncertainty of roughness becomes gradually important, resulting in higher uncertainty at final steady state. As for the influence of the uncertainty of roughness, namely the standard deviation of Manning's *n*, both the cases under correlation $\lambda_n = 0.27$ and $\sigma_n = 0.01$ (or $\sigma_n = 0.005$) are plotted in the figure as well for comparison. With higher standard deviation of roughness, the rising of σ_h becomes slower with the same reason that the larger uncertainty of roughness may weaken the uncertainty level of the wave at first, but with time goes, the final steady σ_h value is larger under higher uncertainty of roughness though it takes a relatively longer period to reach the final state. It is also noticed that at the flow domain close to upstream (e.g., at node point 11 in the figure), the curves under high roughness uncertainty have lower growth rates, but as it goes to the downstream (at node point 31), the uncertainty effects will accumulate with time so that the curve growth rates overtake the curves under lower roughness uncertainty. On this point, it can be concluded that the influence of uncertainty of channel roughness is historically dependent (larger time scale or longer period), which becomes more important and thus should be paid more attention during uncertainty analysis for a relatively long channel flow process.

(a)

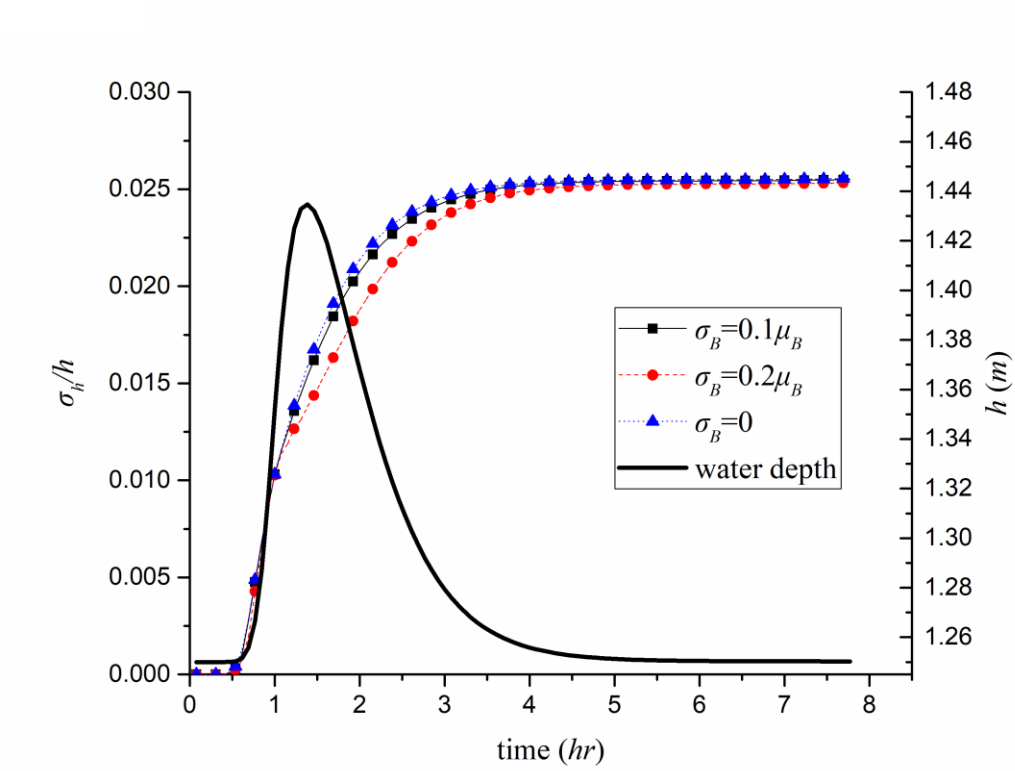
0.030
0.025
0.020
0.015
0.010
0.005
0.000
σ_h/h
1.48
1.46
1.44
1.42
1.40
1.38
1.36
1.34
1.32
1.30
1.28
1.26
h (m)
σ_B=0.1μ_B
σ_B=0.2μ_B
σ_B=0
water depth
0
1
2
3
4
5
6
7
8
time (hr)

(b)

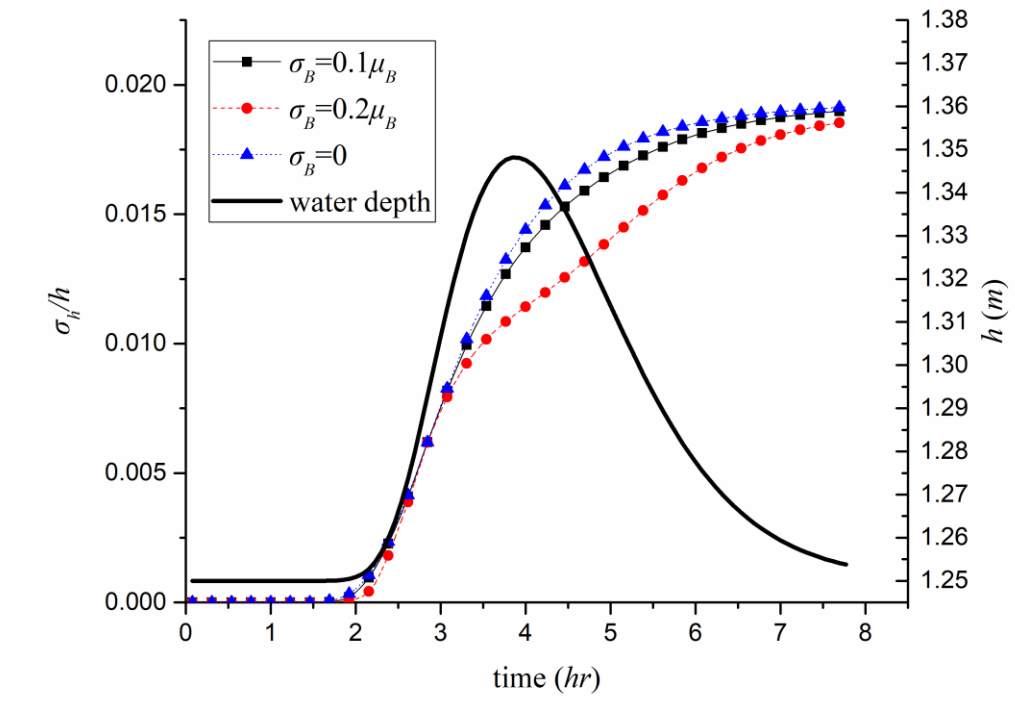
0.020
0.015
0.010
0.005
0.000
σ_h/h
1.38
1.37
1.36
1.35
1.34
1.33
1.32
1.31
1.30
1.29
1.28
1.27
1.26
1.25
h (m)
σ_B=0.1μ_B
σ_B=0.2μ_B
σ_B=0
water depth
0
1
2
3
4
5
6
7
8
time (hr)

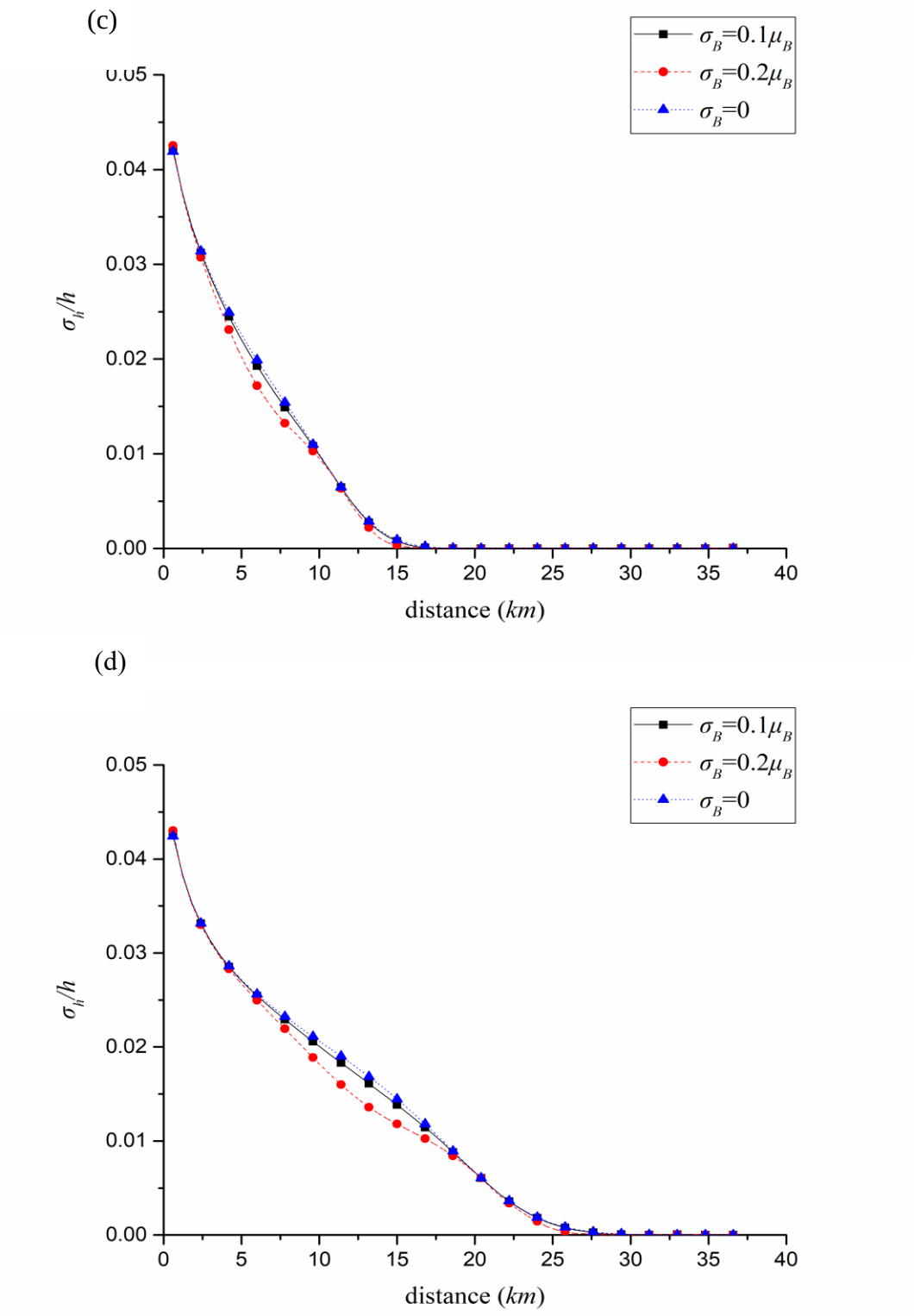

Figure 4.7 (a) Time variation of σ_h and water depth at node 11 under different σ_B; (b) time variation of σ_h and water depth at node 31 under different σ_B; (c) spatial profile of σ_h at time 20 under different σ_B; (d) spatial profile of σ_h at time 40 under different σ_B

(a)

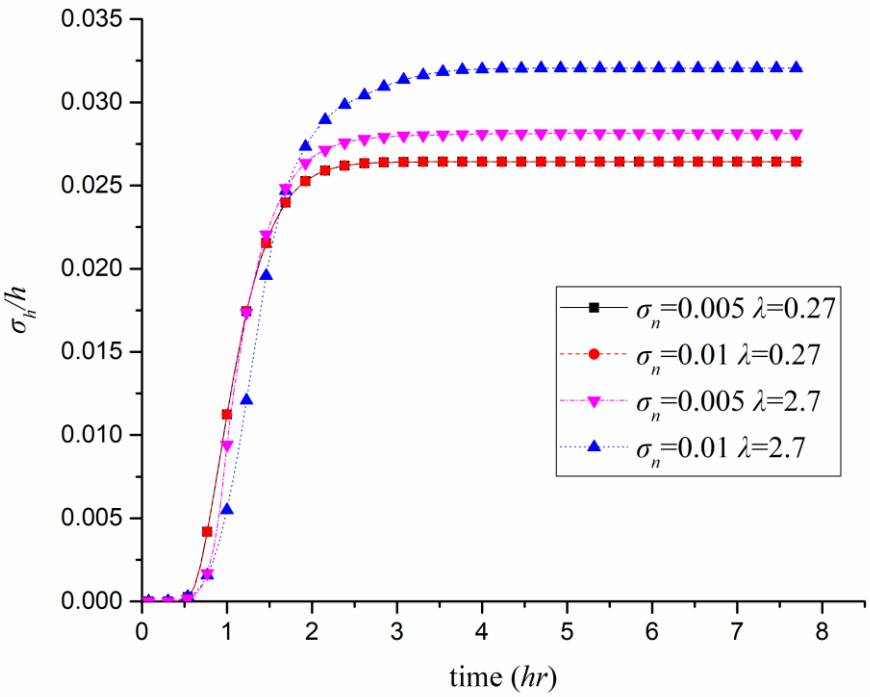
0.035
0.030
0.025
0.020
0.015
0.010
0.005
0.000
σ_h/h
0
1
2
3
4
5
6
7
8
time (*hr*)
σ_n=0.005 λ=0.27
σ_n=0.01 λ=0.27
σ_n=0.005 λ=2.7
σ_n=0.01 λ=2.7

(b)

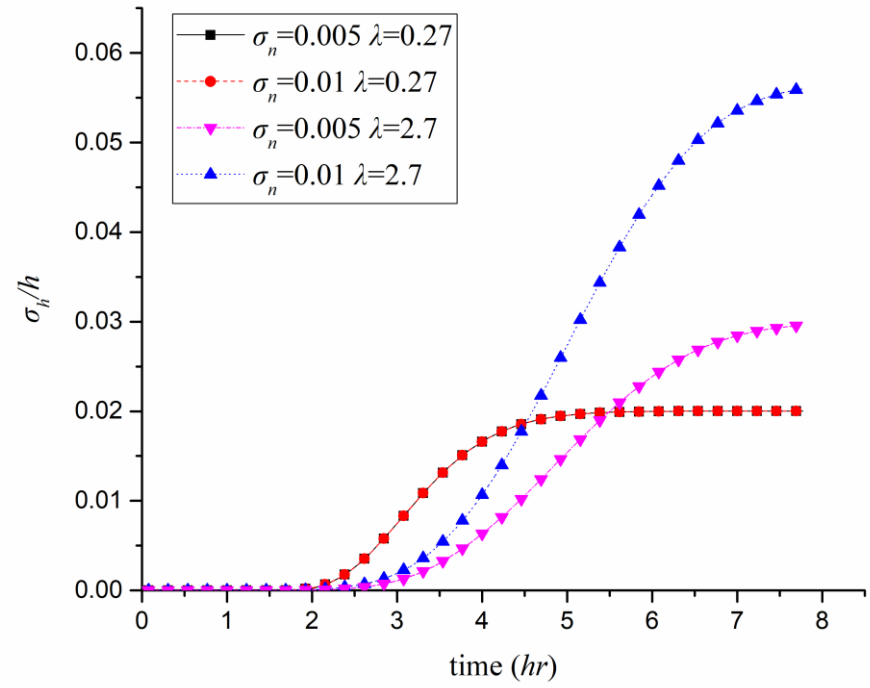
0.06
0.05
0.04
0.03
0.02
0.01
0.00
σ_h/h
0
1
2
3
4
5
6
7
8
time (*hr*)
σ_n=0.005 λ=0.27
σ_n=0.01 λ=0.27
σ_n=0.005 λ=2.7
σ_n=0.01 λ=2.7

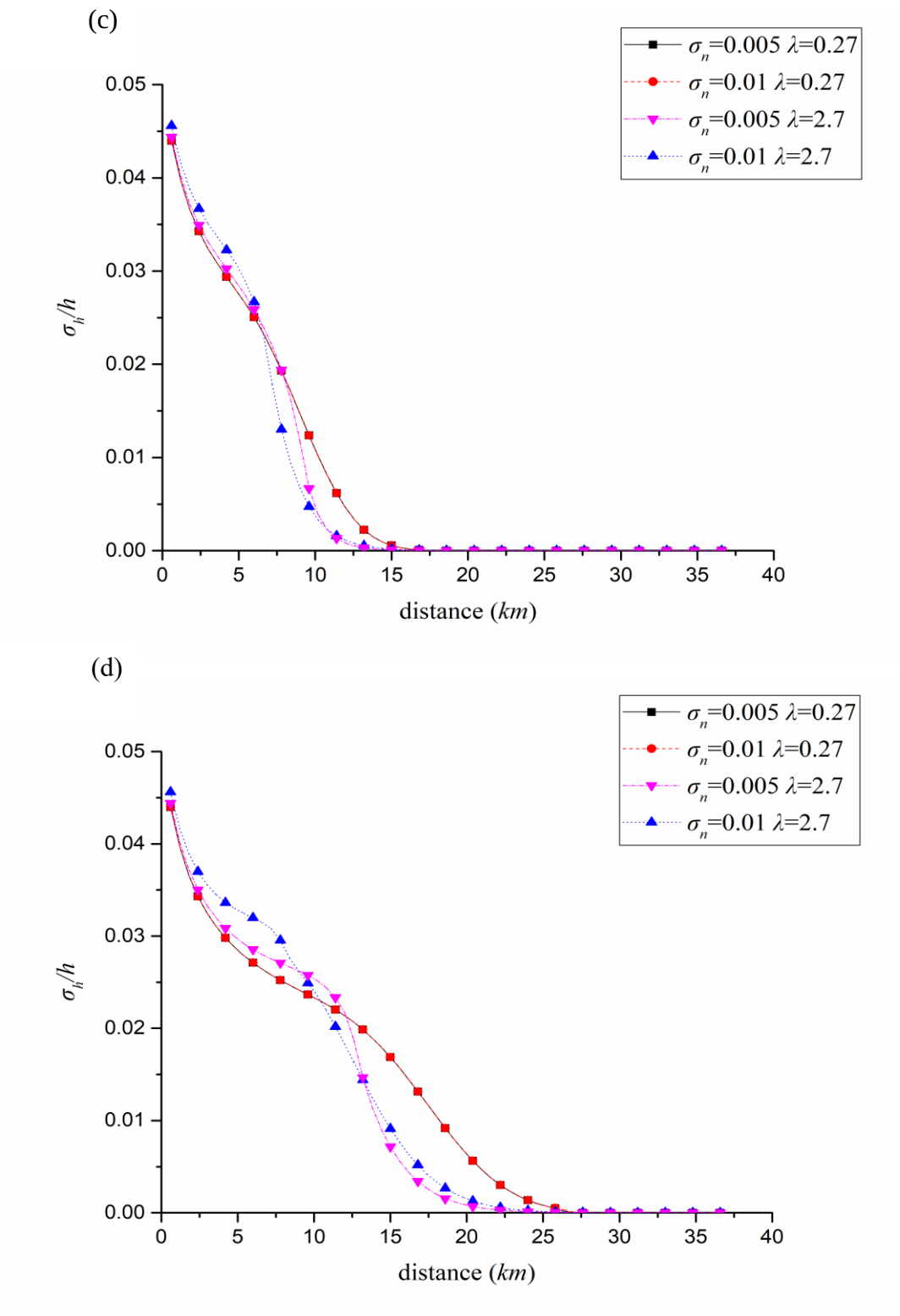

Figure 4.8 (a) Time variation of σ_h and water depth at node 11 under different $\sigma_n.\lambda_n$; (b) time variation of σ_h and water depth at node 31 under different $\sigma_n.\lambda_n$; (c) spatial profile of σ_h at time 20 under different $\sigma_n.\lambda_n$; (d) spatial profile of σ_h at time 40 under different $\sigma_n.\lambda_n$

4.6 Stochastic Influence of Random Bed Slope S_0

In this section, the influence of random channel bed slope S_0 is investigated, in order to examine the sensitivity of the stochastic unsteady flow responses to the uncertainty of bed slope. As defined in the model assumptions in Chapter 3, the bed slope is relatively mild and uniform, which means the variation of the bed slope is supposed to be within a relatively small range. For analysis in this research, the stochastic distribution function describing the uncertainty of bed slope is given by:

$$C_{ss}(x,\chi) = \sigma_s^2 * \exp(-|x-\chi|/\lambda_s T_0) \quad [4.7]$$

in which σ_s is the standard deviation of the bed slope of the hypothetical channel and stay steady everywhere along the channel, λ_s is the correlation length in space, x and χ are two independent location considered. Since the bed slope is uniform, the space correlation goes to infinity ($\lambda_s = \infty$), and the function becomes the form below:

$$C_{ss}(x,\chi) = \sigma_s^2 \quad [4.8]$$

For illustration, two different standard deviation values of $\sigma_s = 0.1\mu_s$ and $\sigma_s = 0.2\mu_s$ are applied to numerical tests in this section, where μ_s is the mean of bed slope. Base flow condition is set to be the same uniform condition as section 4.3.1.

Figure 4.9 presents the results of unsteady flow responses (by taking water depth for demonstration) are obtained under different uncertainty conditions of the bed slope (including also the deterministic condition with $\sigma_s = 0$). The overall results show clearly that the uncertainty of bed slope may have significant influence on the unsteady flow response variability in the channel. Specifically, the flow response grows with relatively slower speed for the bed slope with uncertainty. The reason might be attributed to the negative correlation between bed slope uncertainty and the

inflow uncertainty, and therefore the uncertainty wave is weakened in the early times after its arrival. However, over the time, the bed slope uncertainty begins to become dominant gradually, until the growth rate becomes higher, leading to higher uncertainty at final stage. As a result, the duration of flow uncertainty propagation and evolution becomes relatively longer for the uncertainty cases. However, from these figures, the similar time arrivals of upstream wave/flow uncertainty for different uncertainties of bed slope (at both node 11 and node 31) indicate that the uncertainty of bed slope has little influence on flooding wave speed propagation in the channel.

Furthermore, the comparative results in both temporal and spatial domains in Fig. 4.9 demonstrate clearly that the influence of the uncertainty of the bed slope is increasing with the uncertainty extent of the slope. Specifically, the flow response variability for the case of $\sigma_s = 0.2\mu_s$ is much larger than that for the case of $\sigma_s = 0.1\mu_s$ in the whole inspection domain of interest in this research. Meanwhile, with larger bed slope uncertainty, it takes more time for the flow response variability to attain the final steady state of variation (node 11), which means that larger uncertainty of bed slope may present relatively longer-period influence on the unsteady flow response variation. In conclusion, the bed slope uncertainty may have a significant influence on the flow response variation though it neutralizes the upstream inflow uncertainty at first, but it finally leads to much higher flow uncertainty at the downstream in the channel. The results and analysis of this section, indicate obviously the importance of considering and including the uncertainty of bed slopes in stochastic open channel flow analysis, especially in many practical natural/mountainous river channels which subject to various uncertainties.

(a)

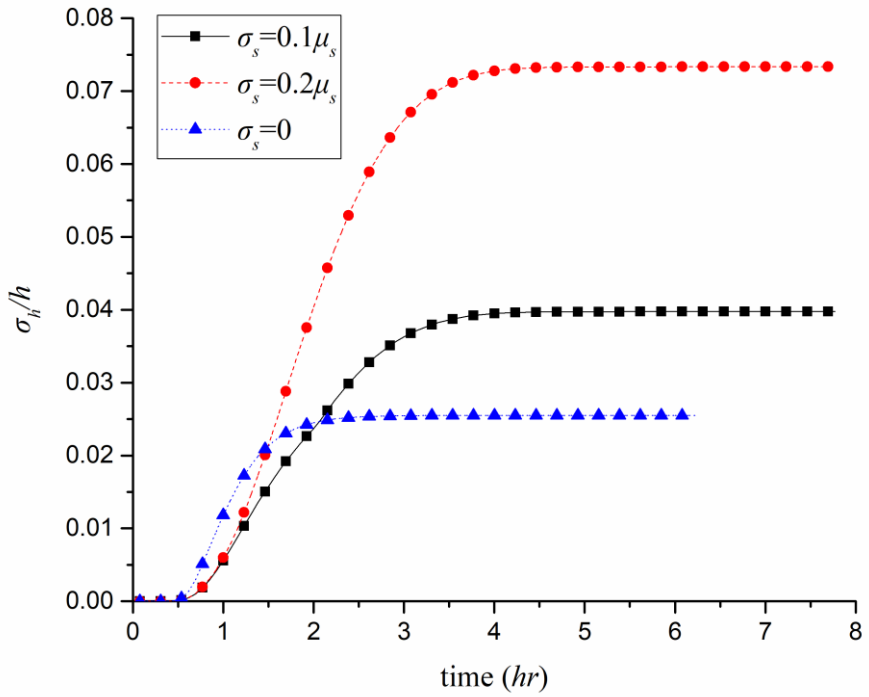
σ_s=0.1μ_s
σ_s=0.2μ_s
σ_s=0
σ_h/h
time (*hr*)
0.00
0.01
0.02
0.03
0.04
0.05
0.06
0.07
0.08
0
1
2
3
4
5
6
7
8

(b)

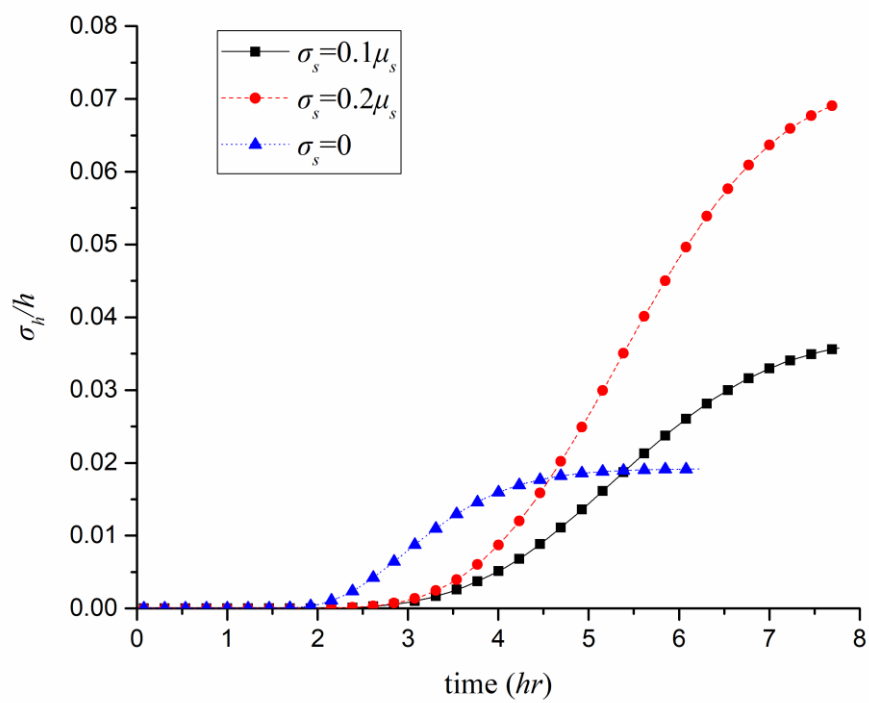
σ_s=0.1μ_s
σ_s=0.2μ_s
σ_s=0
σ_h/h
time (*hr*)
0.00
0.01
0.02
0.03
0.04
0.05
0.06
0.07
0.08
0
1
2
3
4
5
6
7
8

(c)

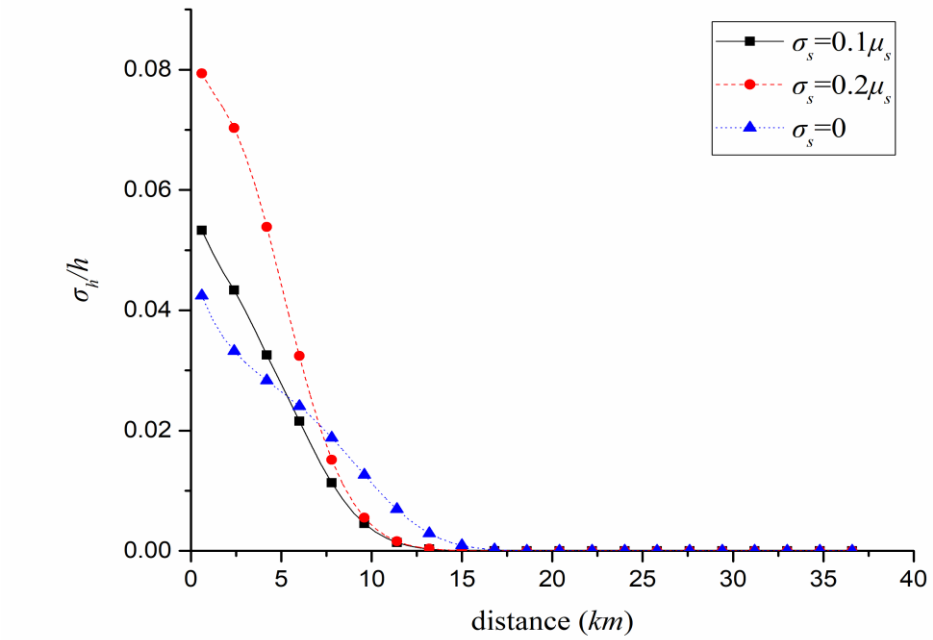

(d)

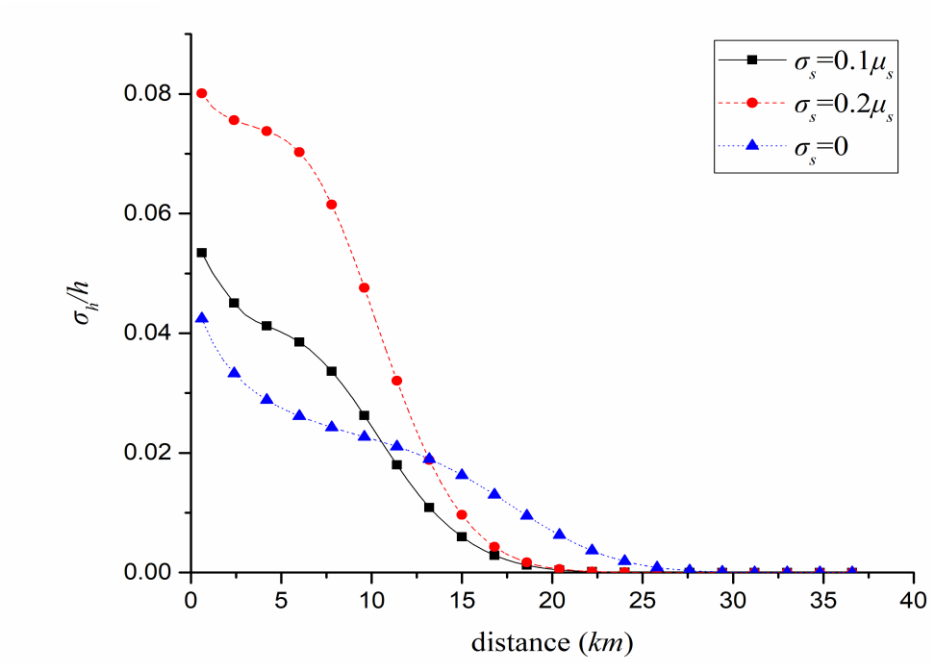

Figure 4.9 (a) Time variation of σ_h and water depth at node 11 under different σ_s; (b) time variation of σ_h and water depth at node 31 under different σ_s; (c) spatial profile of σ_h at time 20 under different σ_s; (d) spatial profile of σ_h at time 40 under different σ_s

4.7 Stochastic Influence of Lateral Inflows

In complex open channel systems, especially in mountainous region, side lateral inflows commonly occur along the flow channel. This section is conducted to analyze the effects of different lateral inflows along the channel on the upstream uncertainty wave propagation. For tests, the upstream flow uncertainty ($\sigma_{qu} = 0.1Q_{u,}$ $\sigma_{qu} = 0.2Q_u$) are the same as the former section, while three different base flow cases are considered and studied for comparative analysis in this section (i.e., no lateral flow, lateral flows at first 10 space steps and at second 10 space steps, respectively; for simplicity, termed as base flow cases 1, 2 and 3 hereafter). The obtained results are shown in Figure 4.10 below. Note that due to the lateral inflow (with sum up to $10m^3/s$), which is assumed to uniformly distribute along the lateral inflow section, the total base flow becomes finally $30m^3/s$ in the downstream of the channel for both base flow cases 2 and 3.

The overall results in Figure 4.10 show that, compared to original case 1 without lateral flow, the lateral flow (cases 2 and 3) may have significant influence on the uncertainty level and propagation in the unsteady open channel flows. Specifically, at the node 11, the standard deviation σ_h of case 2 becomes much smaller than it under the other base flow cases. This is mainly because that the lateral inflow located upstream to the node 11 which has increased the whole base flow discharge in the channel, and thus weakens the uncertainty level (uncertainty relative to base flow) from the random upstream inflow. This similar influence has been shown for the node 31 under the lateral inflow cases 2 and 3, where the lateral flows are located at the upstream of this node. But the comparative results also show that, at this node 31, the uncertainty growth rate for the base flow case 3 becomes slower

than that for base flow 2, which indicates the lateral inflow may cause more attenuation with distance in addition to the original base flow from upstream end.

The horizontal profiles of standard deviation σ_h at time points 20 and 40 in Figure 4.10 demonstrate almost the same findings that the lateral flow along the channel has obvious influence on the flow uncertainty at the downstream of the lateral flow location, and at the same time, the influence decreases along the flow direction. It is learned as well that the lateral inflow in base flow case 3 has slight effects on the flow uncertainty in the nearby upstream flow area where the uncertainty level is less than that for base flow case 1, and this difference grows over time. By inspection, this phenomenon is mainly due to the subcritical flow condition where the wave speed exceeds the water velocity in the channel, so that the uncertainty level of the flooding wave is able to propagate upstream continuously under this base flow condition. These results also demonstrate that the lateral flows (cases 2 and 3) have little impact on the uncertainty (also wave) propagation speed since the arrival time moments of the uncertainty at the same location are exactly same for different base flow conditions.

(a)

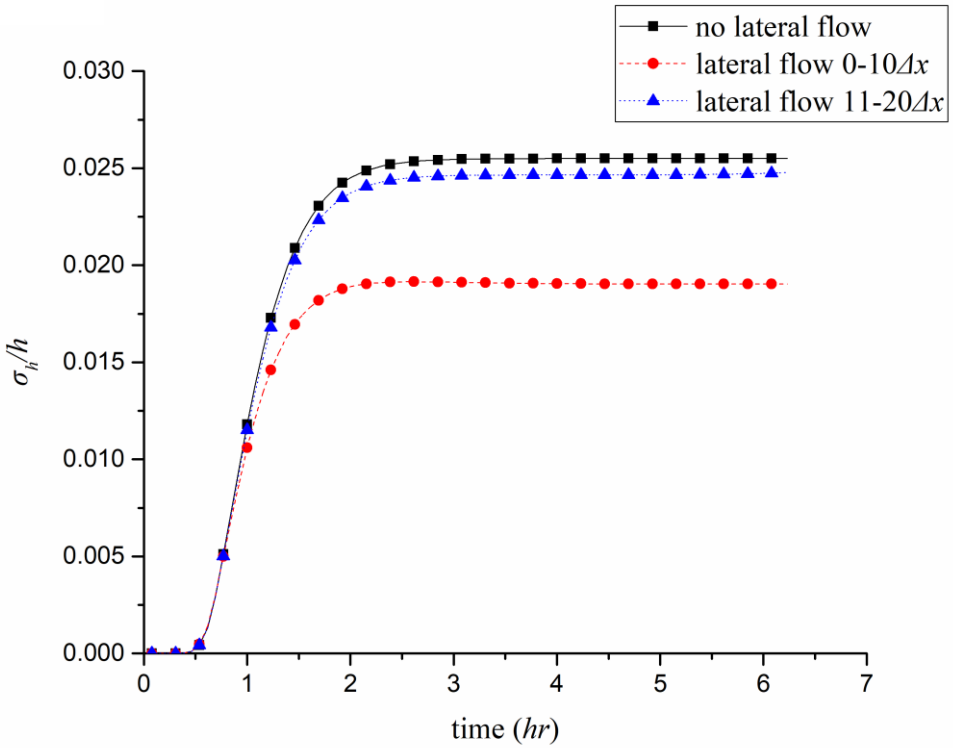
no lateral flow
lateral flow 0-10Δx
lateral flow 11-20Δx
σ_h/h
time (hr)
0.000
0.005
0.010
0.015
0.020
0.025
0.030
0
1
2
3
4
5
6
7

(b)

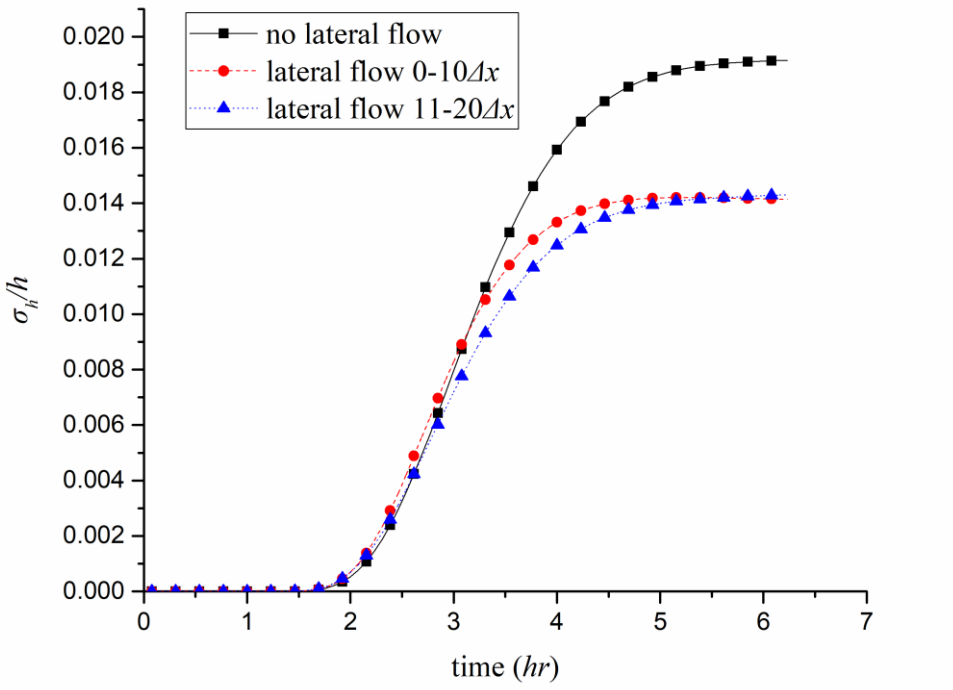
no lateral flow
lateral flow 0-10Δx
lateral flow 11-20Δx
σ_h/h
time (hr)
0.000
0.002
0.004
0.006
0.008
0.010
0.012
0.014
0.016
0.018
0.020
0
1
2
3
4
5
6
7

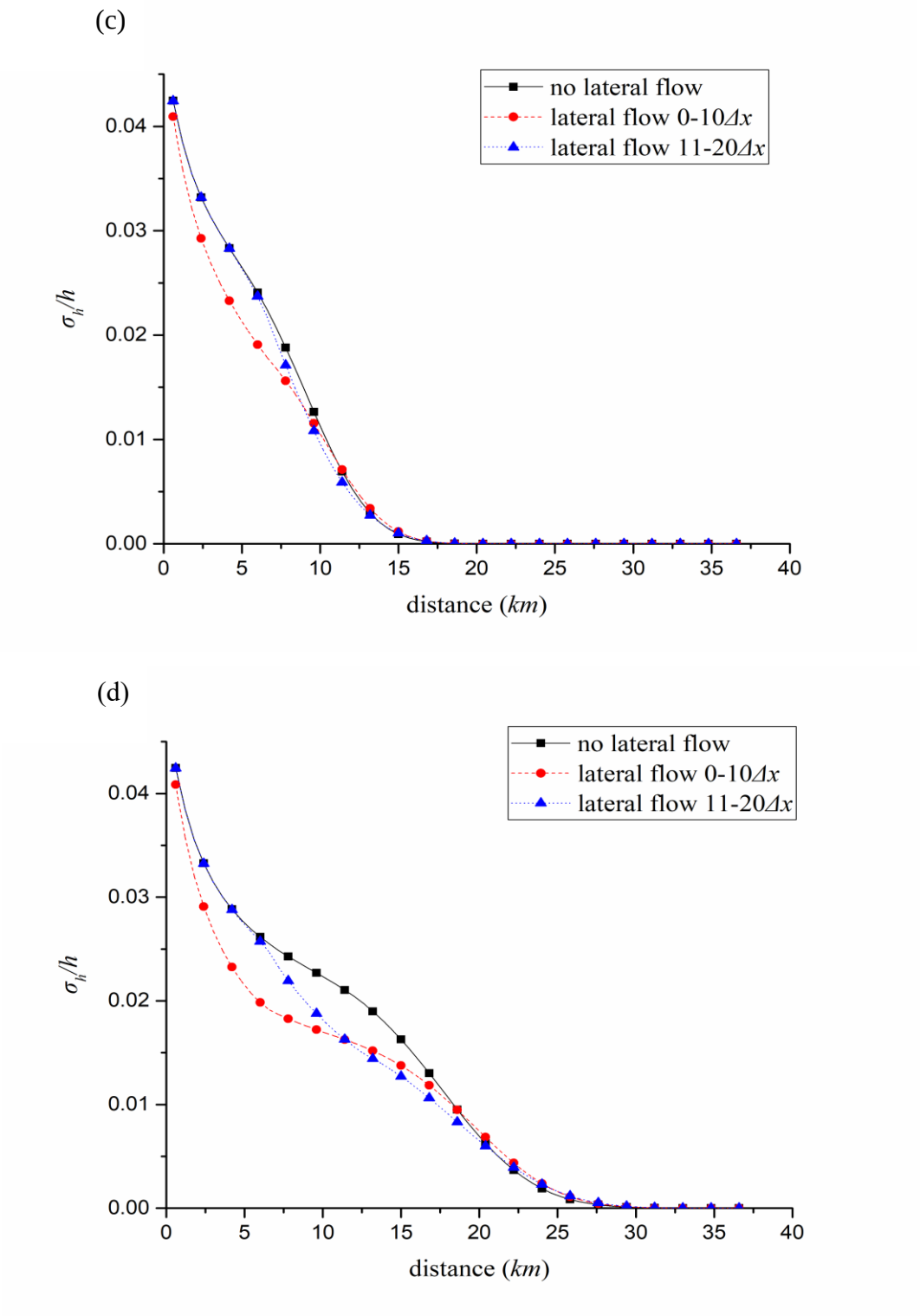

Figure 4.10 While $\sigma_{qu} = 0.1Q_u$ (a) time variation of σ_h and water depth at node 11 under different lateral flow; (b) time variation of σ_h and water depth at node 31 lateral flow; (c) spatial profile of σ_h at time 20 under different lateral flow; (d) spatial profile of σ_h at time 40 under different lateral flow

4.8 Combined Influence of Different Uncertainties

The individual influence of different uncertainties on the open channel flow responses have been examined above, with results indicating the potential and significant impact of each uncertainty factor. In this section, the combined influence with existence of all above uncertainty factors on the unsteady flow responses is further investigated in this section by the developed stochastic model and numerical scheme in Chapter 3 in this thesis work. For demonstration, the upstream boundary inflow properties are the same as presented in section 4.3.4, with other uncertainty factors as follows: uncertainty of channel width is set to be $\sigma_B = 0.2\mu_B$, roughness uncertainty is $\sigma_n = 1/3\mu_n$, and bed slope uncertainty is $\sigma_s = 0.1\mu_s$. For comparison, the results of combined and individual influences of these uncertainty factors are obtained and plotted in Fig. 4.11 for comparative analysis, with the results in the temporal domain for nodes 11 and 31 shown in Figure 4.11(a) and Figure 4.11(b), and the results in the spatial domain along the channel given in Figure 4.11(c) and Figure 4.11(d), respectively.

From Figure 4.11(a), which is for the time variation result of water depth response (σ_h) at node 11, it can be observed that the influence of roughness and channel width is much less important than that of bed slope effect in this upstream location, and therefore the curve of combined result coincides with the bed slope result through the whole process (i.e., dominated mainly by bed slope influence). In Figure 4.11(b), which plots the σ_h variation at node 31, it is found that the influence of the bed slope uncertainty still dominates the system response uncertainty behavior, however, compared with above upstream node 11, the influence of the uncertainty of the roughness starts to play more important role (although it is still much smaller than that of bed slope) because of the longer propagation distance of the wave

uncertainty in the channel, such that σ_h under combined uncertainty condition becomes relatively larger than that under random bed slope only. In conclusion, under the analysis conditions given in this study, the flow uncertainty in the channel is mainly dominated by the randomness of channel bed slope, and the random roughness effects become more obvious during the uncertainty wave propagation process towards downstream. Note that these observation and results are analyzed and summarized only for the cases of interest herein, which are mainly aimed to demonstrate the validity and feasibility of the developed 1D stochastic model and numerical solution scheme in this research. More other practical cases can be investigated with the aid of this developed model and method for the in-depth understanding of the influence of uncertainties on unsteady open channel flows and also the better design and management of the practical engineering systems.

(a)

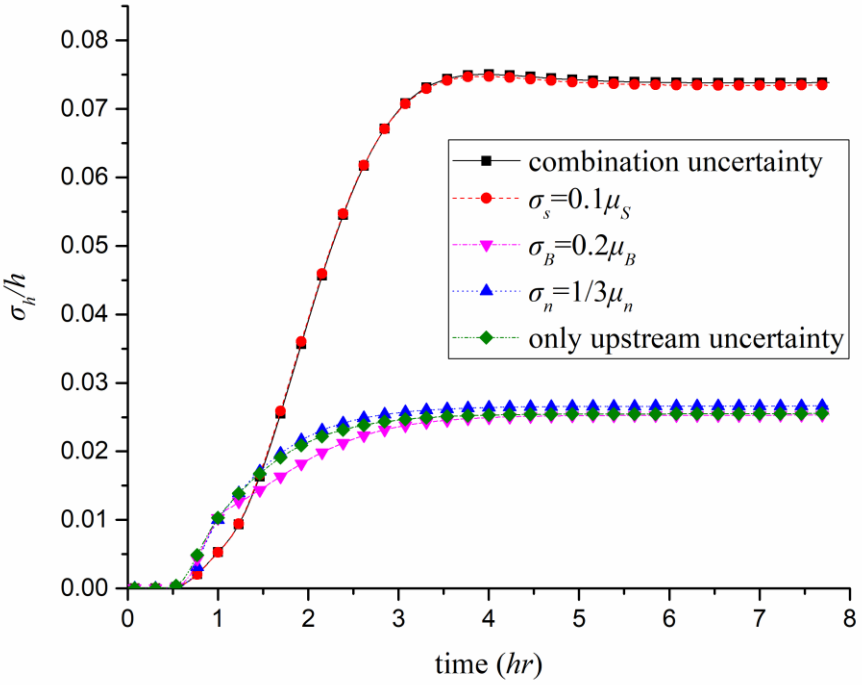
combination uncertainty
σ_s=0.1μ_S
σ_B=0.2μ_B
σ_n=1/3μ_n
only upstream uncertainty
σ_h/h
time (*hr*)

(b)

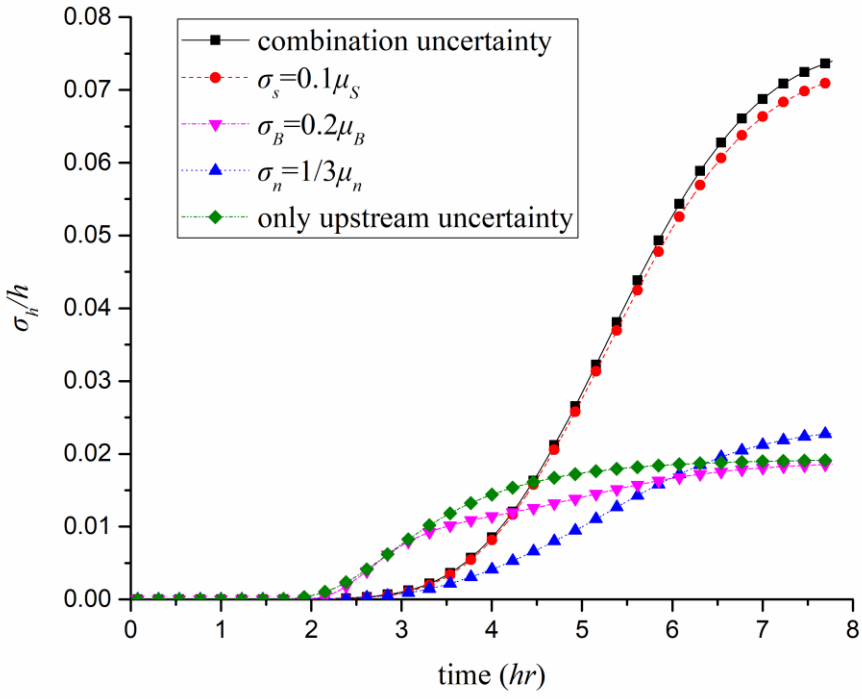
combination uncertainty
σ_s=0.1μ_S
σ_B=0.2μ_B
σ_n=1/3μ_n
only upstream uncertainty
σ_h/h
time (*hr*)

(c)

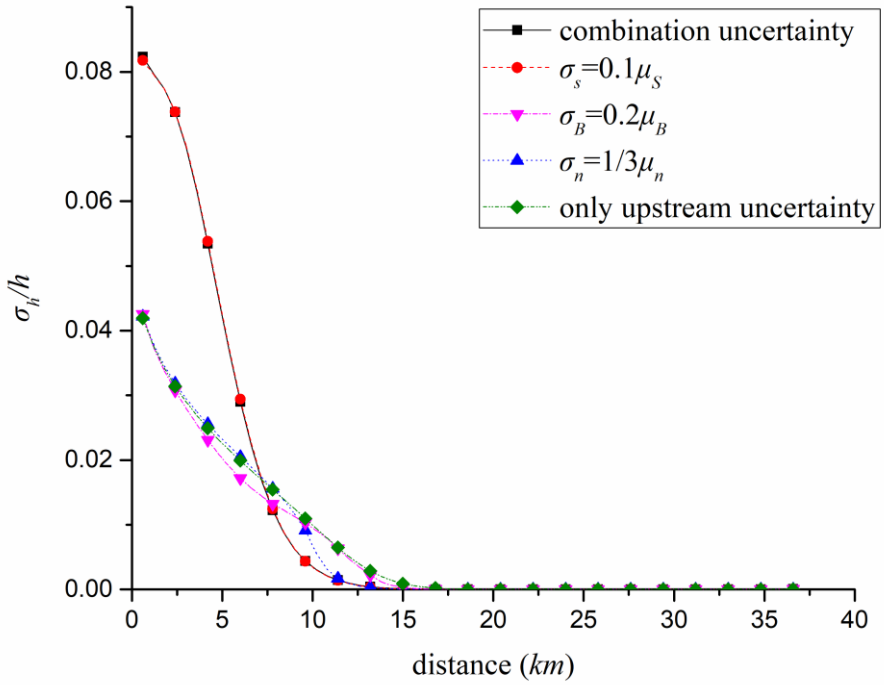

(d)

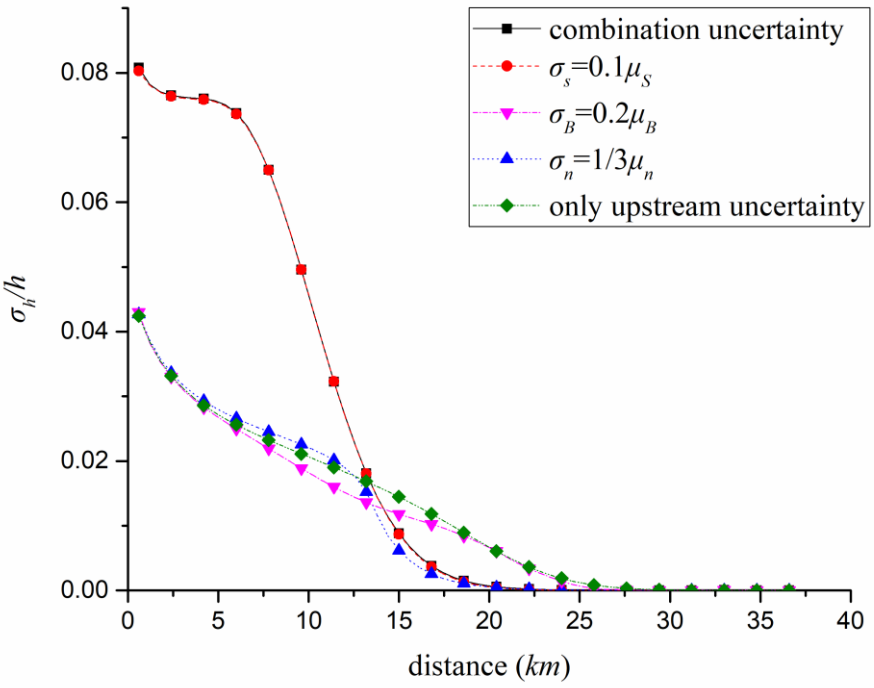

Figure 4.11 Time variation of σ_h under different condition at (a) node 11; (b) node 31; spatial profile of $\sigma_h$at (c) time 20; (d) time 40

4.9 Summary and Discussion

4.9.1 Summary of this chapter

In this chapter, the stochastic model is applied through extensive numerical applications to investigate the influences of different uncertainty factors in the open channel system on the variability and uncertainty propagation of system responses. The factors of upstream inflows (stationary and non-stationary base flows), Manning's *n*, and lateral flows are investigated for the uncertainty analysis by the developed model and method in this research.

Based on the model application and results analysis, the characteristics of the uncertainty propagation in the unsteady open channel flows have been discussed in detail under the influences of different model input variables. Furthermore, the results indicate that the uncertainty of the Manning's *n* presents a historical (long time period) dependence on affecting the stochastic features of system responses, and the location of the lateral flows along the channel may have important influence on the uncertainty propagation in the system. Meanwhile, the developed model and method may provide quantified evaluations on the influence of different uncertainty factors on the variability of the system responses such as water depth and flowrate, as well as the stochastic characteristic of unsteady open channel flows.

Consequently, the case applications and results analysis demonstrate that the developed model and method of this thesis research can provide an essential extension for the theoretical development of open channel flows as well as a useful tool for practical engineering design and management.

4.9.2 Computational efficiency of this model

The computation effort needed for the 1D stochastic model developed in this study mainly subjects to the computation grid size, and the number of random input variables (uncertainty factors) as well. With a flow domain discretized into grids of N_x nodes in space and N_t nodes in time, namely a grid size of $N_x \times N_t$, the total nodes number in computation for solution of standard deviation σ_h are:

$$N_\sigma = (aN_x + bN_t + N_x \times N_t) \times N_x \times N_t \qquad [4.9]$$

where a is the number of spatial random variables (e.g. Manning's n), and b is the number of temporal random variables (e.g. the boundary inflow Q_u) respectively. It is clear that the total number of computation nodes is dependent on the degree of discretization. The computation effort could be unsatisfying when the flow domain and the flow duration are long, which leads to large number in N_x and N_t. However, compared with other stochastic analysis methods (such as Monte-Carlo Simulation), the time required for the computation and analysis by this developed method becomes much less, and thus this method will be more practical to use for solving engineering problems.

Particularly, if only part of the flow domain rather than the whole channel, or a certain period of time rather than the whole process are of interest, which is reasonable for open channel engineering practices, the computation nodes number would be:

$$N_\sigma = (aN_x + bN_t + cN_x + dN_t) \times N_x \times N_t \qquad [4.10]$$

where c and d are the nodes number in time and space respectively of interest. Therefore, the number of nodes required for computation is reduced greatly if only

part of the whole process is under consideration, which promises a reasonable number of times in computation.

In addition, all the equations derived for the 1D stochastic analysis in Chapter 3 are linear equations, which makes it much easier with less effort for numerical solution. In fact, it takes only about 0.015 seconds for each time-step computation for the cases of interest above in this research, and therefore only less than 1000 seconds computation time have been taken for each of the cases applied in this study. While for Monte Carlo simulation, tens of thousands of simulations will be required for obtaining accurate and convergent results in problems with many uncertainty variables (Tung et al. 2006), and thus by estimation, it would take more than 10 times of the computation time for the simple application cases of this study than the analysis method developed in this research.

Consequently, the developed stochastic model and method of this thesis work could provide very efficient and feasible analysis for the uncertainty evaluation of unsteady open channel flows, which may become a useful tool for the future practical applications.

CHAPTER 5 SUMMARY AND CONCLUSIONS

5.1 Summary of This Thesis Research

Flow behaviors in open channel systems are closely related to human civilization and social development. Human has taken advantages of rivers and excavate canals for agricultural and industrial purposes, but suffered from the disasters such as flood and mudslide as well. Therefore, the understanding of open channel flow process is vital, and to this end, many research projects in this field were conducted in past decades. A thorough literature review in this thesis research has indicated that these past and current researches are largely conducted, either for simple open channel systems that was aimed to develop theory and model, or for deterministic situations of the system operation that was targeted to solve problems under specific conditions encountered in practice. However, open channel systems can be highly complex, especially for mountainous rivers, including not only their configurations and topologies but also the inside flow and operation conditions that usually subject to various uncertainties in both temporal and spatial domains. As a result, the flow process in such open channel system may become random and stochastic, so that the design, operation and management of the open channel flows are very difficult to deal with (i.e., time and space dependent variation for the dynamic flow process). However, the past studies on open channel uncertainty either considering only single/independent parameters, or the models and solution methods are very complex with difficulty in practical application, which has motivated this thesis research.

The research work conducted in this thesis presents a general 1D stochastic model and solution method as well as analysis framework for unsteady complex

open channel flows with different uncertainties. This model takes most common variables of unsteady flow process in complex open channel systems into consideration including channel width, channel bed slope, roughness, boundary inflow discharge, and lateral inflow along the channel, providing an approach to solve the first two statistical moments of stochastic flow process. Specifically, the proposed solution methods for these stochastic results are demonstrated through various applications in this research, in which the software EPA SWMM is employed for the zeroth-order solution and a combination of Preissmann four-point scheme and Gaussian elimination for solving numerically the first-order linear partial differential covariance equations. This means this study provides a general 1D stochastic model considering uncertainty of all important parameters of open channel flow both temporally and spatially with an efficient solution method

The developed 1D stochastic model and solution method is then primarily validated and verified by the comparison with the results from a previous research, and the result shows good agreement in the prediction of uncertainty propagation behaviors. Afterwards, the validated model is applied to study further the unsteady open channel flow systems under different uncertainty conditions. Overall results and analysis demonstrate that the variabilities of unsteady flow responses (such as water depth and discharge/velocity) can be affected in both temporal and spatial domains by different random factors with different extents during the unsteady flow process. Particularly, not only the amplitude but also the propagation speed of the uncertainty may be affected during the unsteady flow process. The main results are summarized as below.

(1) The uncertainty of the upstream inflow (σ_{qu} and λ_{qu}) is found to have great influence on the variability of the unsteady flow responses along the open

channel. Specifically, the system response is almost changing linearly to the inflow variance, as indicated in the derived results in Chapter 3. However, the inflow uncertainty has little influence on the uncertainty propagation speed in the whole domain of the application results. That is, the speed of uncertainty propagation is the same as the mainstream flooding wave speed of the base flow, confirming the same characteristic paths of zeroth-order and first-order equations implicated in the stochastic model.

(2) The uncertainty of open channel width is assumed to have the same variation at all location (i.e., fully spatial correlated) in this thesis. As indicated in the first-order covariance equations in Chapter 3, C_{bb} related term values are sensitive to the partial differential values of water depth h and velocity v in both time and space. Thus, the channel width uncertainty effects only become obvious when h and v varies rapidly in time or space, and it is found that the occurrence of channel width can decrease the growth rate of σ_h. However, its influence on the final values at steady stage is little, which means a longer flow uncertainty grow process.

(3) In this study, the channel bed roughness is represented by Mannings's coefficient n, which has been included in the model development in Chapter 3. The application results and analysis indicate that the randomness of Manning's n provides clear influence on the unsteady flow behavior. Especially when the correlation length λ_n of random roughness along the channel becomes larger, which indicates stronger spatial correlation of roughness, the influence on the uncertainty of flow response becomes more significant. Moreover, the uncertainty of channel roughness

may weaken the wave variability during the initial stage, while gradually increase the wave changes when the uncertainty of flow response (water depth σ_h) grows to a certain gradient during the later stage of the unsteady open channel flows.

(4) Bed slope uncertainty with infinite spatial correlation (i.e., fully correlated) is then investigated for different flow situations. The results show that the variability of water depth (σ_h) grows slower at the early stage with the presence of bed slope uncertainty, but with time goes, σ_h grows faster and finally reaches a relatively larger value. This indicates the slope uncertainty might have a negative correlation with the upstream inflow, which results in that the response uncertainty is mainly governed by the inflow variability, while with the time goes, the slope uncertainty becomes more and more dominant to the variability of system responses (e.g., downstream of the channel).

(5) The lateral inflow along the channel at different location is investigated to explore its effects on uncertainty wave propagation towards downstream. Note that the lateral flow along the channel may increase the base flow discharge, and thus can actually weaken the relative uncertainty level of system response with time. Especially, under the subcritical flow condition, the uncertainty wave may propagate to upstream as well, and therefore, the lateral flow can suppress the upstream flow uncertainty with time. However, the results also reveal that the lateral flow has little influence on the uncertainty wave propagation speed.

(6) Finally, the influence of the combination of different uncertainty factors on the system flow response is examined by the developed model. The results

show that the uncertainty of channel bed slope dominants the variation tendency of flow property uncertainties, while the roughness effects are found to be more obvious with distance from upstream increase. As for uncertainty of channel width, its influence is relatively insignificant compare to bed slope and roughness on the uncertainty factors combination condition.

5.2 Contributions of This Thesis Work and Recommendations for Future Research

This research aims to study the stochastic characteristics of complex open channel flows through the establishment of one-dimensional (1D) stochastic model and the systematic analysis of different factors affecting the uncertainty evolution based on the developed model. The originality and main contributions of this thesis research include:

(1) Developing the 1D stochastic model of unsteady open channel flows for the first two statistic moments;

(2) Analyzing the uncertainty propagation and sensitivity of unsteady open channel flows to the different random inputs and parameters as well as system conditions based on the developed 1D stochastic model; and

(3) Understanding the stochastic characteristics of unsteady open channel flows by examining the influence ranges and relative importance of different uncertainty factors to the open channel flow responses (water depth and flowrate/velocity) under different system and flow conditions.

The achievements and results of the research in this thesis, including the developed 1D stochastic model, the numerical simulation data and the sensitivity analysis results, are expected to be useful for: (1) understanding the complex hydraulic process and stochastic evolution mechanism of open channel flow systems; and (2) providing useful tools for the engineering practice of hydraulic structure design and open channel flow management.

Despite that the above-mentioned contributions of this research, the applications of the developed model and method as well as the study of practical open channel flow systems may still encounter many potential difficulties. On the basis of the results and achievements of current research work, more future work will be required to improve and enhance the study of unsteady open channel flows, with some recommendations (also the limitations of current work) as follows:

(1) The developed stochastic model in this study is based on 1D averaged flow characteristics in the system, and the open channel is assumed to be rectangular prismatic throughout the analytical derivation and application process in this research. For open channels in engineering practice, however, the flow conditions and channel configurations could very complicated, such that the 1D stochastic model should be extended to more general situations;

(2) Only subcritical flow situations are considered and applied in the cases study of this research, and more supercritical flow cases are required to generalize the results and findings of this thesis;

(3) For simplicity of analysis and unavailability of supporting data, all uncertainty parameters of interest in this research are assumed to follow the stationary Gaussian distribution and exponentially distributed in both

temporal and spatial domains. In the future, it is necessary to examine the validity of such assumptions, and if possible, to obtain and apply the exact distributions of these random factors from enough measurement dataset by experimental tests. Also, by conducting the study on influence range of different parameter uncertainty, the importance of their effects can be obtained. Therefore, with better understanding of the stochastic flow process, the model can be slightly modified in specific cases application and the input data would be more accurate, so that the developed model and method would be more useful and applicable to practical engineering problems.

REFERENCE

Afzal, B., Faruque, M.A. and Balachandar, R. (2009) Effect of Reynolds number, near-wall perturbation and turbulence on smooth open-channel flows. Journal of hydraulic research 47(1), 66-81.

Alcrudo, F. and Garcia ‐ Navarro, P. (1993) A high ‐ resolution Godunov ‐ type scheme in finite volumes for the 2D shallow ‐ water equations. International Journal for Numerical Methods in Fluids 16(6), 489-505.

Alias, N.A., Liang, Q. and Kesserwani, G. (2011) A Godunov-type scheme for modelling 1D channel flow with varying width and topography. Computers & fluids 46(1), 88-93.

Amiri, S., Talebbeydokhti, N. and Baghlani, A. (2013) A two-dimensional well-balanced numerical model for shallow water equations. Scientia Iranica 20(1), 97-107.

Anastasiou, K. and Chan, C. (1997) Solution of the 2D shallow water equations using the finite volume method on unstructured triangular meshes. International Journal for Numerical Methods in Fluids 24(11), 1225-1245.

Andersson, J. and Shapiro, A.M. (1983) Stochastic analysis of one ‐ dimensional steady state unsaturated flow: A Comparison of Monte Carlo and Perturbation Methods. Water resources research 19(1), 121-133.

Audusse, E. (2005) A multilayer Saint-Venant model: derivation and numerical validation. Discrete & Continuous Dynamical Systems-B 5(2), 189-214.

Bakr, A.A., Gelhar, L.W., Gutjahr, A.L. and MacMillan, J.R. (1978) Stochastic analysis of spatial variability in subsurface flows: 1. Comparison of one ‐ and three ‐ dimensional flows. Water resources research 14(2), 263-271.

Bates, P.D. and De Roo, A. (2000) A simple raster-based model for flood inundation simulation. Journal of Hydrology 236(1-2), 54-77.

Bates, P.D., Horritt, M.S. and Fewtrell, T.J. (2010) A simple inertial formulation of the shallow water equations for efficient two-dimensional flood inundation modelling. Journal of Hydrology 387(1-2), 33-45.

Benkhaldoun, F. and Seaïd, M. (2010) A simple finite volume method for the shallow water equations. Journal of computational and applied mathematics 234(1), 58-72.

Bermúdez, A., Rodríguez, C. and Vilar, M. (1991) Solving shallow water equations by a mixed implicit finite element method. IMA journal of numerical analysis 11(1), 79-97.

BHA (2018) Safety Tips for Times of Flooding and Other Severe Weather Situations.

Bhatia, R. and Riley, T. (2016) India crippled by extreme weather as 100 million exposed to floods. https://www.theguardian.com/sustainable-business/2016/apr/21/india-drought-flooding-natural-disasters-risk-population-economy-insurance.

Bloom, D., Dewan, A., Deaton, J. and Castillo, M. (2017) More than 250 dead in Colombia mudslides. https://edition.cnn.com/2017/04/03/americas/colombia-mudslide/index.html.

Bradford, S.F. and Sanders, B.F. (2002) Finite-volume model for shallow-water flooding of arbitrary topography. Journal of Hydraulic Engineering 128(3), 289-298.

Cao, R.R., Wang, H. and Pope, S.B. (2007) The effect of mixing models in PDF calculations of piloted jet flames. Proceedings of the combustion institute 31(1), 1543-1550.

Chanson, H. (2004) Hydraulics of open channel flow, Butterworth-Heinemann.

Chau, K., Wu, C. and Li, Y. (2005) Comparison of several flood forecasting models in Yangtze River. Journal of Hydrologic Engineering 10(6), 485-491.

Chau, K.W. and Yang, W.-W. (1992) A knowledge-based expert system for unsteady open channel flow. Engineering Applications of Artificial Intelligence 5(5), 425-430.

Chen, J., Li, Q., Niu, J. and Sun, L. (2011) Regional climate change and local urbanization effects on weather variables in Southeast China. Stochastic Environmental Research and Risk Assessment 25(4), 555-565.

Chen, K., Duan, H., Yan, X., Wang, X. and Liu, X. (2017) On the influence of lateral flows on the uncertainty of unsteady open channel flows in mountainous rivers. 37th IAHR World Congress, Kuala Lumpur, Malaysia 13-18 August, 2017.

Chen, M., Keller, A.A., Zhang, D., Lu, Z. and Zyvoloski, G.A. (2006) A stochastic analysis of transient two‐phase flow in heterogeneous porous media. Water resources research 42(3).

Chen, M., Zhang, D., Keller, A.A. and Lu, Z. (2005) A stochastic analysis of steady state two‐phase flow in heterogeneous media. Water resources research 41(1).

Cheng, N.-S. (2014) Resistance coefficients for artificial and natural coarse-bed channels: Alternative approach for large-scale roughness. Journal of Hydraulic Engineering 141(2), 04014072.

Cheng, N.-S., Nguyen, H.T., Zhao, K. and Tang, X. (2010) Evaluation of flow resistance in smooth rectangular open channels with modified Prandtl friction law. Journal of Hydraulic Engineering 137(4), 441-450.

Comiti, F., Andreoli, A., Lenzi, M. and Mao, L. (2006) Spatial density and characteristics of woody debris in five mountain rivers of the Dolomites (Italian Alps). Geomorphology 78(1), 44-63.

Delbari, M., Afrasiab, P. and Loiskandl, W. (2009) Using sequential Gaussian simulation to assess the field-scale spatial uncertainty of soil water content. Catena 79(2), 163-169.

Dettinger, M.D. and Wilson, J.L. (1981) First order analysis of uncertainty in numerical models of groundwater flow part: 1. Mathematical development. Water resources research 17(1), 149-161.

Di Liberto, M. and Ciofalo, M. (2011) Unsteady turbulence in plane channel flow. Computers & fluids 49(1), 258-275.

Dikow, E. (1988) Stochastic analysis of groundwater flow in a bounded domain by spectral methods. Transport in porous media 3(2), 173-184.

Dooge, J.C., Kundzewicz, Z.W. and Napiorkowski, J.J. (1983) On backwater effects in linear diffusion flood routing. Hydrological Sciences Journal 28(3), 391-402.

Doucet, A., De Freitas, N. and Gordon, N. (2001) Sequential Monte Carlo methods in practice, pp. 3-14, Springer.

EPA (2017) Urban Runoff: Low Impact Development. https://www.epa.gov/nps/urban-runoff-low-impact-development.

Fagherazzi, S., Furbish, D.J., Rasetarinera, P. and Hussaini, M.Y. (2004) Application of the discontinuous spectral Galerkin method to groundwater flow. Advances in Water Resources 27(2), 129-140.

Fischer-Antze, T., Stoesser, T., Bates, P. and Olsen, N. (2001) 3D numerical modelling of open-channel flow with submerged vegetation. Journal of hydraulic research 39(3), 303-310.

Fread, D. (1974a) Implicit dynamic routing of floods and surges in the Lower Mississippi.

Fread, D.L. (1974b) Numerical properties of implicit four-point finite difference equations of unsteady flow.

Fuentes-Mariles, Ó.A., Domínguez-Mora, R., Arganis-Juárez, M.L., Herrera-Alanís, J.L., Carrizosa-Elizondo, E. and Sánchez-Cruz, J.A. (2015) Estimate of design hydrographs for the Angostura Dam, Sonora, using statistical and spectral methods. Water Resources Management 29(11), 4021-4043.

Fujihara, M. and Borthwick, A.G. (2000) Godunov-type solution of curvilinear shallow-water equations. Journal of Hydraulic Engineering 126(11), 827-836.

Gambolati, G. (1993) On time integration of groundwater flow equations by spectral methods. Water resources research 29(4), 1257-1267.

Garcia, A.G. (2000) Orthogonal sampling formulas: a unified approach. SIAM review 42(3), 499-512.

Gates, T.K. and Al-Zahrani, M.A. (1996) Spatiotemporal stochastic open-channel flow. I: Model and its parameter data. Journal of Hydraulic Engineering 122(11), 641-651.

Ge, L. and Cheung, K.F. (2010) Spectral sampling method for uncertainty propagation in long-wave runup modeling. Journal of Hydraulic Engineering 137(3), 277-288.

Gelhar, L.W., Gutjahr, A.L. and Naff, R.L. (1979) Stochastic analysis of macrodispersion in a stratified aquifer. Water resources research 15(6), 1387-1397.

Ghanbari, R.N. and Bravo, H.R. (2011) Evaluation of correlations between precipitation, groundwater fluctuations, and lake level fluctuations using spectral methods (Wisconsin, USA). Hydrogeology Journal 19(4), 801-810.

Golden, L.A. and Springer, G.S. (2006) Channel geometry, median grain size, and stream power in small mountain streams. Geomorphology 78(1), 64-76.

Graham, W. and McLaughlin, D. (1989) Stochastic analysis of nonstationary subsurface solute transport: 2. Conditional moments. Water resources research 25(11), 2331-2355.

Guganesharajah, K., Lyons, D., Parsons, S. and Lloyd, B. (2006) Influence of uncertainties in the estimation procedure of floodwater level. Journal of Hydraulic Engineering 132(10), 1052-1060.

Harris, M. (2015) China's sponge cities: soaking up water to reduce flood risks. https://www.theguardian.com/sustainable-business/2015/oct/01/china-sponge-cities-los-angeles-water-urban-design-drought-floods-urbanisation-rooftop-gardens.

Harten, A., Lax, P.D. and Leer, B.v. (1983) On upstream differencing and Godunov-type schemes for hyperbolic conservation laws. SIAM review 25(1), 35-61.

Hattermann, F., Huang, S., Burghoff, O., Hoffmann, P. and Kundzewicz, Z. (2015) Brief Communication: An update of the article “Modeling flood damages under climate change conditions–a case study for Germany”. Natural Hazards and Earth System Sciences Discussions 3, 7231-7245.

Haworth, D. (2010) Progress in probability density function methods for turbulent reacting flows. Progress in Energy and Combustion Science 36(2), 168-259.

He, H., Zhou, J., Peart, M.R., Chen, J. and Zhang, Q. (2012) Sensitivity of hydrogeomorphological hazards in the Qinling Mountains, China. Quaternary International 282, 37-47.

Heggen, R. (1991) Critical depth, velocity profile, and channel shape. Journal of Irrigation and Drainage Engineering 117(3), 442-448.

Hicks, F. and Steffler, P. (1995) Comparison of finite element methods for the St. Venant equations. International Journal for Numerical Methods in Fluids 20(2), 99-113.

Horritt, M. (2002) Stochastic modelling of 1-D shallow water flows over uncertain topography. Journal of Computational Physics 180(1), 327-338.

Horritt, M. and Bates, P. (2002) Evaluation of 1D and 2D numerical models for predicting river flood inundation. Journal of Hydrology 268(1-4), 87-99.

Hougardy, S. and Vygen, J. (2016) Algorithmic Mathematics, Springer.

IFS (2012) Three Gorges driftsätter IFS Applications. http://news.cision.com/se/ifs/i/three-gorges-dam-small,c1262559.

Keller, R. and Rodi, W. (1988) Prediction of flow characteristics in main channel/flood plain flows. Journal of hydraulic research 26(4), 425-441.

Kirkpatrick, D.D. (2015) New Suez Canal Expansions. https://cn.nytimes.com/world/20150807/cc07egypt/zh-hant/.

Klimenko, A.Y. and Pope, S. (2003) The modeling of turbulent reactive flows based on multiple mapping conditioning. Physics of Fluids (1994-present) 15(7), 1907-1925.

Knight, D.W. and Demetriou, J.D. (1983) Flood plain and main channel flow interaction. Journal of Hydraulic Engineering 109(8), 1073-1092.

Knio, O. and Le Maitre, O. (2006) Uncertainty propagation in CFD using polynomial chaos decomposition. Fluid Dynamics Research 38(9), 616-640.

Lambrechtsen, F.J. (2013) Second-Order Perturbation Analysis of the St. Venant Equations in Relation to Bed-Load Transport and Equilibrium Scour Hole Development.

Le Maıtre, O., Knio, O., Najm, H. and Ghanem, R. (2004) Uncertainty propagation using Wiener–Haar expansions. Journal of Computational Physics 197(1), 28-57.

Leach, A. (2016) Soak it up: China's ambitious plan to solve urban flooding with 'sponge cities' https://www.theguardian.com/public-leaders-network/2016/oct/03/china-government-solve-urban-planning-flooding-sponge-cities.

Li, C.W. and Zeng, C. (2009) 3D Numerical modelling of flow divisions at open channel junctions with or without vegetation. Advances in Water Resources 32(1), 49-60.

Li, C.W. and Zhang, M.L. (2010) 3D modelling of hydrodynamics and mixing in a vegetation field under waves. Computers & fluids 39(4), 604-614.

Li, J.-x. and Liu, S.-x. (2015) Focused wave properties based on a high order spectral method with a non-periodic boundary. China Ocean Engineering 29(1), 1-16.

Li, S.G. and McLaughlin, D. (1991) A nonstationary spectral method for solving stochastic groundwater problems: Unconditional analysis. Water resources research 27(7), 1589-1605.

Liang, Q. (2010) Flood simulation using a well-balanced shallow flow model. Journal of Hydraulic Engineering 136(9), 669-675.

Liggett, J. (1993) Critical depth, velocity profiles, and averaging. Journal of Irrigation and Drainage Engineering 119(2), 416-422.

Lin, C.-P., Ni, C.-F., Li, I.-H. and Lu, C.-H. (2015) Stochastic delineation of well capture zones in aquifers of Choushui River alluvial fan in central Taiwan, pp. 427-432, IEEE.

Lin, J. and Soong, H. (1979) Junction losses in open channel flows. Water resources research 15(2), 414-418.

Liu, G., Zhang, D. and Lu, Z. (2006) Stochastic uncertainty analysis for unconfined flow systems. Water resources research 42(9).

Liu, Q., Qin, Y., Zhang, Y. and Li, Z. (2015a) A coupled 1D–2D hydrodynamic model for flood simulation in flood detention basin. Natural hazards 75(2), 1303-1325.

Liu, X. (2014) Modern Water Resources Engineering, pp. 127-158, Springer.

Liu, X., Infante Sedano, J.Á. and Mohammadian, A. (2015b) A coupled two-dimensional numerical model for rapidly varying flow, sediment transport and bed morphology. Journal of hydraulic research 53(5), 609-621.

Lu, Z. (2008) Stochastic Modeling of Unsteady Open Channels and Reliability Analysis, the Hong Kong University of Science and Technology, Hong Kong.

Ma, F., Wei, M.S. and Mills, W.H. (1987) Correlation structuring and the statistical analysis of steady-state groundwater flow. SIAM Journal on Scientific and Statistical Computing 8(5), 848-867.

MacKay, D.J. (1998) Learning in graphical models, pp. 175-204, Springer.

Mantoglou, A. and Wilson, J.L. (1982) The turning bands method for simulation of random fields using line generation by a spectral method. Water resources research 18(5), 1379-1394.

Marzouk, Y.M., Najm, H.N. and Rahn, L.A. (2007) Stochastic spectral methods for efficient Bayesian solution of inverse problems. Journal of Computational Physics 224(2), 560-586.

McAnally, M.J., Richard (2016) Waterwindow Amplifying The Conversation On Flood Resilience. http://www.globalresiliencepartnership.org/news/2016/04/13/waterwindow-amplifying-the-conversation-on-flood-resilience/.

McKay, M.D., Beckman, R.J. and Conover, W.J. (2000) A comparison of three methods for selecting values of input variables in the analysis of output from a computer code. Technometrics 42(1), 55-61.

Merz, B. and Thieken, A.H. (2005) Separating natural and epistemic uncertainty in flood frequency analysis. Journal of Hydrology 309(1-4), 114-132.

Myers, W. (1978) Momentum transfer in a compound channel. Journal of hydraulic research 16(2), 139-150.

Myers, W. and Brennan, E. (1990) Flow resistance in compound channels. Journal of hydraulic research 28(2), 141-155.

Napiorkowski, J.J. and Dooge, J.C. (1988) Analytical solution of channel flow model with downstream control. Hydrological Sciences Journal 33(3), 269-287.

Nash, D. (2017) World Water Day: Why tackling flooding remains a sustainability priority. http://www.globalresiliencepartnership.org/news/2017/03/22/world-water-day/.

Ni, C.-F., Lin, C.-P., Li, S.-G. and Liu, C.-J. (2011) Efficient approximate spectral method to delineate stochastic well capture zones in nonstationary groundwater flow systems. Journal of Hydrology 407(1-4), 184-195.

Pironneau, O. (1989) Finite element methods for fluids, Wiley Chichester.

Pope, S. (1994) Lagrangian PDF methods for turbulent flows. Annual review of fluid mechanics 26(1), 23-63.

Pope, S.B. (1985) PDF methods for turbulent reactive flows. Progress in Energy and Combustion Science 11(2), 119-192.

Reagana, M.T., Najm, H.N., Ghanem, R.G. and Knio, O.M. (2003) Uncertainty quantification in reacting-flow simulations through non-intrusive spectral projection. Combustion and Flame 132(3), 545-555.

Roe, P.L. (1981) Approximate Riemann solvers, parameter vectors, and difference schemes. Journal of Computational Physics 43(2), 357-372.

Rouse, H. (1965) Critical analysis of open-channel resistance. Journal of the Hydraulics division 91(4), 1-23.

Salway, M. (2009) Incredible Photos of the Dorrigo Mountain Road Flood. http://www.mikesalway.com.au/incredible-photos-of-the-dorrigo-mountain-road-flood/.

Schaffranek, R.W. (1987) Flow model for open-channel reach or network.

Schneider, W.J., Rickert, D.A. and Spieker, A.M. (1973) Role of water in urban planning and management, US Geological Survey.

Sett, K., Jeremić, B. and Kavvas, M.L. (2007) Probabilistic elasto-plasticity: solution and verification in 1D. Acta Geotechnica 2(3), 211-220.

Si, B.C. (2008) Spatial scaling analyses of soil physical properties: A review of spectral and wavelet methods. Vadose zone journal 7(2), 547-562.

Sinha, J., Eswaran, V. and Bhallamudi, S.M. (1995) Comparison of spectral and finite-difference methods for flood routing. Journal of Hydraulic Engineering 121(2), 108-117.

Smith, J.D. and McLean, S. (1984) A model for flow in meandering streams. Water resources research 20(9), 1301-1315.

Smith, L. and Freeze, R.A. (1979) Stochastic analysis of steady state groundwater flow in a bounded domain: 1. One-dimensional simulations. Water resources research 15(3), 521-528.

Sturm, T.W. (2010) Open channel hydraulics, McGraw-Hill New York.

Tayfur, G., Kavvas, M.L., Govindaraju, R.S. and Storm, D.E. (1993) Applicability of St. Venant equations for two-dimensional overland flows over rough infiltrating surfaces. Journal of Hydraulic Engineering 119(1), 51-63.

Teng, J., Jakeman, A., Vaze, J., Croke, B.F., Dutta, D. and Kim, S. (2017) Flood inundation modelling: A review of methods, recent advances and uncertainty analysis. Environmental Modelling & Software 90, 201-216.

Tung, Y.-K., Yen, B.C. and Melching, C.S. (2006) Hydrosystems engineering reliability assessment and risk analysis, McGraw-Hill New York.

Tung, Y.K. and Mays, L.W. (1981) Risk models for flood levee design. Water resources research 17(4), 833-841.

Vereecken, H., Kasteel, R., Vanderborght, J. and Harter, T. (2007) Upscaling Hydraulic Properties and Soil Water Flow Processes in Heterogeneous Soils. Vadose zone journal 2007 v.6 no.1(no. 1), pp. 1-28.

Vila, J.P., Chazel, F. and Noble, P. (2017) 2D versus 1D models for Shallow Water Equations. Procedia IUTAM 20, 167-174.

Wagner, J.M., Shamir, U. and Marks, D.H. (1988) Water distribution reliability: simulation methods. Journal of water resources planning and management 114(3), 276-294.

Willis, R., Finney, B.A., McKee, M. and Militello, A. (1989) Stochastic analysis of estuarine hydraulics. Stochastic Hydrology and Hydraulics 3(2), 71-84.

Wohl, E. (2013) Mountain rivers revisited, John Wiley & Sons.

Wohl, E., Kuzma, J.N. and Brown, N.E. (2004) Reach ‐ scale channel geometry of a mountain river. Earth Surface Processes and Landforms 29(8), 969-981.

Wood, E. (1977) An analysis of flood levee reliability. Water resources research 13(3), 665-671.

Wood, E.F. and Rodríguez-Iturbe, I. (1975) A Bayesian approach to analyzing uncertainty among flood frequency models. Water resources research 11(6), 839-843.

Xiu, D. (2009) Fast numerical methods for stochastic computations: a review. Communications in computational physics 5(2-4), 242-272.

Xiu, D. and Karniadakis, G.E. (2002) The Wiener--Askey polynomial chaos for stochastic differential equations. SIAM journal on scientific computing 24(2), 619-644.

Xiu, D. and Karniadakis, G.E. (2003) Modeling uncertainty in flow simulations via generalized polynomial chaos. Journal of Computational Physics 187(1), 137-167.

Xiu, D., Lucor, D., Su, C.-H. and Karniadakis, G.E. (2002) Stochastic modeling of flow-structure interactions using generalized polynomial chaos. Journal of Fluids Engineering 124(1), 51-59.

Yen, B.C. (1971) Spatially varied open-channel flow equations.

Yen, B.C. (2002) Open channel flow resistance. Journal of Hydraulic Engineering 128(1), 20-39.

Yen, B.C. and Tung, Y.-K. (1993) Some recent progress in reliability analysis for hydraulic design. Reliability and uncertainty analysis in hydraulic design, BC Yen and YK Tung, eds., ASCE, Reston, VA, 35-79.

Ying, X., Khan, A.A. and Wang, S.S. (2004) Upwind conservative scheme for the Saint Venant equations. Journal of Hydraulic Engineering 130(10), 977-987.

Yoon, J. and Kavvas, M.L. (2003) Probabilistic solution to stochastic overland flow equation. Journal of Hydrologic Engineering 8(2), 54-63.

Zhang, D. and Lu, Z. (2004) An efficient, high-order perturbation approach for flow in random porous media via Karhunen–Loeve and polynomial expansions. Journal of Computational Physics 194(2), 773-794.